THROMBOXANE RECEPTOR SIGNALLING AND REGULATION IN THE PERINATAL PULMONARY CIRCUIT

BY

MARTHA HINTON

A THESIS SUBMITTED TO THE FACULTY OF GRADUATE STUDIES
OF

THE UNIVERSITY OF MANITOBA

IN PARTIAL FULFILMENT OF THE REQUIREMENTS OF THE DEGREE
OF

MASTER OF SCIENCE

DEPARTMENT OF PHYSIOLOGY

UNIVERSITY OF MANITOBA

WINNIPEG

THE UNIVERSITY OF MANITOBA

FACULTY OF GRADUATE STUDIES

*****

COPYRIGHT PERMISSION

Thromboxane Receptor Signalling and Regulation in the Perinatal Pulmonary Circuit

BY

Martha Hinton

A Thesis/Practicum submitted to the Faculty of Graduate Studies of The University of Manitoba in partial fulfillment of the requirement of the degree

Of

MASTER OF SCIENCE

ACKNOWLEDGMENTS

I would like to extend my gratitude to my supervisor, Dr. Shyamala Dakshinamurti, whose encouragement and enthusiasm has been invaluable in the completion of this project. Her drive and commitment is greatly appreciated. I also would like to thank to Lynne Mellow, Alex Gutsol and Gerald Stelmack who helped me in the lab and taught me all of the techniques I needed to complete my research.

My committee members, who have provided me with incredible support, are greatly thanked. I thank Dr. Halayko for his confidence in my research abilities, constant encouragement and collaboration. I thank Dr. Stephens for always being ready for a discussion and showing me that research can become a life-fulfilling, exciting endeavour. I also thank Dr. Bose for her support and words of encouragement.

For their financial support I thank the Canadian Institute for Health Research, the University of Manitoba and the Manitoba Institute of Child Health (Biology of Breathing Group).

Most of all, I would like to thank my family and friends. Your support and belief in me has meant the world, and I couldn't have done this without you.

TABLE OF CONTENTS

ACKNOWLEDGMENTS ii

LIST OF TABLES v

LIST OF FIGURES vi

LIST OF ABBREVIATIONS vii

I. ABSTRACT p. 1

II. OBJECTIVES AND RATIONALE p. 3

III. LITERATURE REVIEW

III.1. PERINATAL PULMONARY CIRCULATORY TRANSITION p. 4

III.2. PERSISTENT PULMONARY HYPERTENSION OF THE NEWBORN p. 6
III.2.1. ANIMAL MODELS OF PPHN p. 8

III.3. HYPOXIA p. 10
III.3.1. HYPOXIC PULMONARY VASOCONSTRICTION p. 10
III.3.2. CELLULAR OXYGEN-SENSING p. 12
III.3.3. OXIDATIVE STRESS AND SMOOTH MUSCLE p. 13

III.4. ARACHIDONIC ACID METABOLISM p. 14
III.4.1. REGULATION OF THROMBOXANE PRODUCTION p. 16

III.5. THROMBOXANE RECEPTOR p. 17
III.5.1. G-PROTEIN COUPLED RECEPTORS p. 17
III.5.2. THROMBOXANE RECEPTOR CHARACTERISTICS p. 19
III.5.3. SECOND MESSENGER SIGNALLING p. 21

III.6. SMOOTH MUSCLE CELL CONTRACTION p. 22
III.6.1. CALCIUM-DEPENDENT SMOOTH MUSCLE CONTRACTION p. 23
III.6.1.1. MECHANISMS TO INCREASE INTRACELLULAR CALCIUM p. 23

IV. HYPOTHESES AND SPECIFIC AIMS p. 26

V. MANUSCRIPT I-

M. Hinton, L. Mellow, A.J. Halayko, A. Gutsol and S. Dakshinamurti. **HYPOXIA INDUCES HYPERSENSITIVITY AND HYPERREACTIVITY TO THROMBOXANE RECEPTOR AGONIST IN NEONATAL PULMONARY ARTERIAL MYOCYTES.** Am J Physiol Lung Cell Mol Physiol 290: L375-L384, 2006. p. 29

VI. MANUSCRIPT II-

M. Hinton, A. Gutsol and S. Dakshinamurti. **THROMBOXANE HYPERSENSITIVITY IN HYPOXIC PULMONARY ARTERY MYOCYTES: ALTERED TP RECEPTOR LOCALIZATION AND KINETICS.** Am J Physiol Lung Cell Mol Physiol epub before print (Nov 3, 2006).doi:10.1152/ ajplung.00229.2006. p. 66

VII. SUMMARY p. 106

VIII. FUTURE DIRECTIONS p. 108

IX. REFERENCES p. 114

LIST OF TABLES

TABLE II.1. Thromboxane receptor saturation binding kinetics. p. 84

LIST OF FIGURES

FIGURE 1.	Arachidonic acid metabolism.	p. 15
FIGURE I.1.	*In vivo* and *in vitro* hypoxic exposure protocol.	p. 36
FIGURE I.2.	Hypoxic pulmonary hypertension diagnosed by relative increase in right to left ventricular weight ratio.	p. 42
FIGURE I.3.	Myocyte Ca^{2+} mobilization response to U46619.	p. 44
FIGURE I.4.	Time to peak Ca^{2+} mobilization response after agonist addition.	p. 46
FIGURE I.5.	Dose response curves for peak Ca^{2+} mobilization to KCl and U46619.	p. 47
FIGURE I.6.	Pathway of hypoxic myocyte hyperreactivity to U46619 determined by serial calcium channel blockade.	p. 48
FIGURE I.7.	Thromboxane receptor-independent calcium pool mobilization from intracellular SR stores.	p. 50
FIGURE I.8.	Thromboxane receptor localization is altered by hypoxic exposure.	p. 51
FIGURE II.1.	Thromboxane receptor expression in large and small arteries.	p. 80
FIGURE II.2.	Subcellular thromboxane receptor localization.	p. 82
FIGURE II.3.	Thromboxane receptor expression.	p. 83
FIGURE II.4.	Competitive binding kinetics.	p. 85
FIGURE II.5.	Thromboxane receptor co-immunoprecipitation.	p. 87
FIGURE II.6.	Maximal G-protein activation, PKC and PKA regulation of thromboxane receptor.	p. 88
FIGURE 2.	GPCR cross-talk and regulation of IP-R signalling in hypoxia.	p. 110
FIGURE 3.	Extinction of hypoxic effects on TP-R responsiveness.	p. 112
FIGURE 4.	TP-R signalling and PASMC contraction.	p. 113

LIST OF ABBREVIATIONS

ATP	adenosine triphosphate
Bmax	maximal binding
BSA	bovine serum albumin
CO_2	carbon dioxide
COX	cyclooxygenase
CPI-17-	protein kinase C-potentiated myosin phosphatase inhibitor 17kDa
DAG	diacyl glycerol
DNA	deoxyribonucleic acid
EC50	effective concentration for 50% response
ECMO	extracorpeal membrane oxygenation
eNOS	endothlial nitric oxide synthase
ER	endoplasmic reticulum
ET_A	endothelin-1 receptor (type A)
ET-1	endothelin-1
F_{IO2}	fraction of inspired oxygen
GPCR	G protein coupled receptor
HBS	HEPES buffered saline solution
HBSS	Hanks' Balanced Salt Solution
HEK	human embryonic kidney cell
HIF-1α	hypoxia inducible factor-alpha
HPV	hypoxic pulmonary vasoconstriction
HRE	hypoxic response element

IL-1	interleukin-1
IP3	inositol triphosphate
IP-R	prostacyclin receptor
Kd	dissociation constant
Kv	voltage-sensitive potassium channel
LPS	lippopoylsaccharide
MLCK	myosin light chain kinase
MLCP	myosin light chain phosphatase
NADPH	nicotinamide adenine dinucleotide phosphate
NO	nitric oxide
O_2	oxygen
PA	pulmonary artery
P_{ACO2}	alveolar partial pressure of CO_2
P_{AO2}	alveolar partial pressure of O_2
PASMC	pulmonary artery smooth muscle cell
PKA	protein kinase A
P_b	barometric pressure
PDI	protein disulphide isomerase
PGI_2	prostacyclin
P_{H2O}	water vapour pressure
PIP2	phosphatidylinositol biphosphate
PKA	protein kinase A
PKC	protein kinase C

PKG	protein kinase G
PLC	phospholipase C
PMA	phorbol 12-myristate 13-acetate
PP1	protein phosphatase 1
PP2A	protein phosphatase 2A
PPHN	persistent pulmonary hypertension of the newborn
PVR	pulmonary vascular resistance
R	respiratory quotient
ROS	reactive oxygen species
RT-PCR	reverse transcriptase polymerase chain reaction
SR	sarcoplasmic reticulum
TNFα	tumour necrosis factor α
TP-R	thromboxane receptor
TxA	thromboxane
U46619	((1,5,5,)-hydroxy-11 alpha,9 alpha-epoxymethano)prosta 5Z, 13E-dienoic acid
VOCC-	voltage-gated calcium channel

I. ABSTRACT

INTRODUCTION: Hypoxia can cause neonatal pulmonary hypertension (PPHN) which is characterized by vasospasm and increased thromboxane (TxA) production. We studied changes in TxA responsiveness and TxA receptor (TP-R) expression and regulation in pulmonary artery (PA) myocytes following hypoxia.

METHODS: Myocytes from 3rd-6th generation PA of newborn piglets were cultured and exposed to 10 % O_2 for 3 days *in vivo* or *in vitro*; controls were normoxic myocytes from age-matched animals. TxA-induced Ca^{2+} responses were measured using fura-2AM. TP-R was studied by immunocytochemistry, western blot, RT-PCR, immunohistology, immunoprecipitation, and Scatchard analysis.

RESULTS: Myocytes exposed to hypoxia became hyper-responsive and hyper–sensitive to TxA; this persisted long after removal from hypoxia. Total TP-R gene expression and protein abundance was unaltered. In hypoxia, cell surface TP-R decreased while affinity increased. Smaller caliber arteries expressed TP-R in pigs with PPHN. The hypoxia-induced decrease in TP-R Kd correlated with decreased TP-R phosphorylation on serine residues and increased Gαq coupling. Diminished normoxic TP-R responsiveness could be mimicked by activation of PKA.

CONCLUSIONS: The normoxic TP-R is relatively desensitized, likely achieved by PKA-dependent phosphorylation. Hypoxia re-sensitizes the TP-R and induces TP-R expression in smaller arteries, therefore increasing TxA responsiveness and contributing to increased vasospasm, a characteristic of PPHN. Identification of the mode of hypoxia-induced sensitization of these PASMCs to TxA may reveal a mechanism by which this

sensitization may be reversed. This in turn may improve the response to current available therapies for PPHN.

II. Objectives and Rationale

Persistent pulmonary hypertension of the newborn (PPHN) has an incidence in Canada of up to 6.8 in every 1000 live births, and up to one third of patients do not respond to current therapies. The rapid and largely unpredictable progression of PPHN from sustained vasoconstriction to irreversible vascular remodelling often becomes fatal in otherwise healthy infants. PPHN can develop due to a number of insults, such as meconium aspiration, hypoxia and sepsis; as a result, many mechanisms underlie the disease. We are focusing on thromboxane (TxA) and its role in the development of PPHN. TxA is a potent vasoconstrictor whose production has been shown to be increased in a piglet model of hypoxia-induced PPHN. We aim to study the alteration in responsiveness to TxA in cultured neonatal pulmonary artery smooth muscle cells from resistance vessels exposed to moderate hypoxia *in vivo* or *in vitro*, as well as the longevity and mechanisms behind such changes.

III. Literature Review

III.1. Perinatal Pulmonary Circulatory Transition

The lung develops in five distinct stages; embryonic, pseudoglandular, canalicular, saccular and alveolar stages (17). Imperative to proper lung development is the coordination between airway and vascular branching and growth. Angiogenesis of pulmonary arteries follows developing airways, therefore ensuring that capillaries are situated in close proximity to alveoli to allow efficient gas exchange (17).

Fetal circulation differs from *ex utero* circulation because of the inclusion of the low resistance placental vascular bed and the high resistance conditions in the pulmonary circuit. The human fetal blood volume is approximately 10 to 12% of body weight, with the majority of that volume pooling in the low resistance placental vascular bed (24). Blood pressure at 19-21 weeks gestation is normally about 15mmHg (24).

Shunts and Fetal Blood Flow. In general, circulation is unique in the fetus because of different conduits available to distribute oxygenated blood to the organs and to transfer oxygen-depleted blood to the placenta. In the fetus, the flow of blood to the lung is approximately 8% of the total cardiac output, while the placenta receives about 40% (30). The three shunts available for cardiac output in fetal circulation are the ductus venosus, ductus arteriosus, and the foramen ovale (24). Right ventricular output shunted across the ductus arteriosus may travel to the placenta via the umbilical circulation (16). In normal fetal circulation, right ventricular output, which is approximately two thirds of total cardiac output, mainly goes to the placenta, allowing blood to become oxygenated (16). Oxygenated blood leaves the placenta via the umbilical vein and flows into the right atrium through the ductus venosus (36). Blood from the lower body returns to the

right atrium by the inferior vena cava (36). The open foramen ovale, situated between the right and left atria, allows some of the oxygenated blood returning from the placenta into the left atrium to be distributed to vascular beds supplied by the aorta. The blood shunted into the left atria moves to the left ventricle and is then pumped to the head and upper extremities (36). At birth, pulmonary flow increases from less than 10% of right ventricular output to the entire cardiac output (17).

High Pulmonary Vascular Resistance. Maintenance of high pulmonary vascular resistance (PVR) in fetal circulation is achieved in part by active tone due to agonists such as thromboxane, leukotrienes and endothelin (10). PVR is O_2-sensitive, and resistance decreases in the presence of high oxygen. Shear stress and vasodilators such as prostacyclin and nitric oxide increase blood flow (16). These mediators are all decreased in the fetal circulation, contributing to increased PVR. In the fetus, resistance in the pulmonary vessels is also elevated because there are a reduced number of pulmonary arteries and the alveoli are filled with fluid, which causes an increased surrounding pressure on the vessel wall, tending to restrict open-probability (10, 16). These conditions, in conjunction with a patent ductus arteriosus, force blood leaving the right ventricle to shunt right to left through the open ductus arteriosus, allowing it to preferentially flow through the lower resistance, systemic vascular bed (10).

Normal Circulatory Transition. Normal circulatory transition occurs at the onset of ventilation and delivery of oxygen to the lung (44). To ensure adequate oxygen acquisition at birth, the majority of cardiac output must shift from the placenta to the lung; uterine contraction assists in this by increasing surrounding pressure on the placenta, therefore restricting blood flow through its vessels (30). The normally rapid

decrease in pulmonary vascular resistance at the time of birth occurs as a result of ventilation, increased oxygen, and increased shear stress which contributes to the rise in NO (nitric oxide), bradykinin and PGI_2 (prostacyclin) production (17). PVR also decreases as alveoli expand with gas, resulting in the un-kinking of vessels which tethers the alveoli open (46). By 12 to 24 hours of life, the pulmonary vascular resistance decreases to 80% of that which it was *in utero* and continues to fall progressively, reaching an adult value at one month age (46).

III.2. Persistent Pulmonary Hypertension of the Newborn

Persistent pulmonary hypertension of the newborn (PPHN) is a disease that begins essentially as the persistence of fetal circulation after birth (46). PPHN occurs 1.9 times for every 1000 live births in Canada (46). Pulmonary circuit pressure in conditions of pulmonary hypertension exceed 25mmHg (17).

Causes of PPHN vary and often manifest in conjunction with additional respiratory or cardiovascular complications. In general, causes of PPHN fall within three categories; (*i*) underdevelopment, (*ii*) maldevelopment and, (*iii*) maladaptaion.

(i) Underdevelopment, or prematurity, can lead to the development of PPHN because the gas exchange surface of the lung simply isn't sufficiently developed to handle the task of acquiring oxygen for the rest of the body (46). Underdevelopment implies hypoplasia of lungs, which can be due to underinflation in oligohydramnious, or due to space-occupying lesions such as congenital diaphragmatic hernia. Decreased circuit capacity results in increased right to left shunting through the foramen ovale or ductus arteriosus (50).

(ii) Maldevelopment, defined as developmental aberration in structure or function, can cause PPHN following premature closure of the ductuc arteriousus. This can be mimicked in a lamb model by *in utero* ductal ligation causing increased shear stress and blood flow through the high resistance fetal pulmonary circuit (50).

*(iii)*PPHN can also occur due to a perinatal stressor in otherwise healthy infants (46). PPHN due to maladaptation occurs when there is normal anatomy, but fetal circulation persists due to pulmonary vasospasm resulting from perinatal stress such as; acidosis, hypothermia, hypoglycemia, hypercarbia, hypoxia, aspiration, sepsis, surfactant deficiency, pneumonia or haemorrhage (50).

Characteristics of PPHN include maintenance of high pulmonary arterial tone, hypoxemia and right-to left shunting of blood between the atria in the heart as well as via the ductus arteriosus and intrapulmonary arterio-venous connections (44). PPHN leads to vascular remodelling, in the form of smooth muscle cell hypertrophy and hyperplasia, extension of smooth muscle into smaller vessels, and adventitial thickening (55). In a post-mortem study, small pulmonary arteries (<75μM in diameter) were shown to increase their medial thickness 4 fold, and there was an increase in adventitial thickness around arteries ranging from 75 to 500μM in diameter (55). Fetal pulmonary arterial smooth muscle exhibits high proliferation while neonatal pulmonary artery smooth muscle proliferation is relatively decreased. However, neonatal pulmonary artery smooth muscle from bovine with hypoxia-induced PPHN proliferates to the same extent as that seen in the fetus (52). The pulmonary artery medial layer is composed of phenotypically different smooth muscle cells with diverse morphology, immunobiochemistry, patterns of

arrangement, orientation and expression of protein (52). Production of molecules affecting smooth muscle tone have been shown to be altered in various models of PPHN, with the balance skewed away from dilators towards constrictors. For example, the endothelin (ET-1)– NO axis was demonstrated to favour ET-1 in PPHN. Endothelin receptor, ET_A, blockade inhibited vasoconstriction in a model of hypoxia-induced PPHN (36). The endothelial-derived relaxing factor, later discovered to be NO, results in dilatation of pulmonary arteries by activation of the soluble guanylate cyclase pathway, and this has been shown to be decreased in PPHN (23). The PGI_2 – TxA axis also shifts towards the constrictor, TxA, in a model of PPHN (8). The role of prostanoids has not been as extensively examined as NO and ET-1 with regards to PPHN development and management.

Current therapies for PPHN include surfactant, phosphodiesterase inhibitors, endothelin antagonists, calcium channel blockers, $MgSO_4$, and tolazoline (a vasodilator that also increases cardiac output that may act through histamine, cholinergic and adrenergic receptors) (50). The most common treatments for PPHN include inhaled NO, ECMO, and aerosolized PGI_2 (46).

III.2.1. Animal Models of PPHN

Neonatal pulmonary hypertension can be studied in a variety of animal models, with many irritants causing the initiation of disease development. Because PPHN can develop for many reasons and in combination with other disease states, many animal models correlate only with specific cases.

One of the more recent models for PPHN is the endothelial nitric oxide synthase (eNOS) deficient mouse, which universally develops fatal pulmonary hypertension due to

the disregulation of angiogenesis (14). These mice don't have a mature or developed pulmonary vascular bed, and therefore cannot survive due to inadequate ventilation-perfusion matching.

Other classical models of PPHN include acute and chronic hypobaric or normobaric neonatal hypoxia (6). PPHN can be caused by perinatal hypoxia, therefore this animal model is warranted, however hypoxia induced in hypobaric conditions may introduce an additional variable to disease development. Limitations of this type of animal model include the timing of onset of hypoxia; in human cases, brief hypoxia at the onset of perinatal circulatory transition may have different pathophysiology than moderate or severe hypoxia initiated long after successful lung ventilation. Also, the pulmonary circuit in different animals may exhibit varying degrees of sensitivity to acute hypoxia. For example, in the newborn mouse, chronic hypoxia must be used to observe PPHN-like symptoms (1).

In utero ductal ligation in the lamb is another popular model of PPHN which creates a condition of pulmonary overflow in the fetal circuit (6). Etiology of PPHN in this context may include a myogenic response to vascular wall strain, as the conditions of high flow in the normally constricted pulmonary circuit during lung development would compound the detrimental pathology.

There are also animal models that utilize meconium aspiration and endotoxemia to induce PPHN development (6). These models focus on the hypertensive effects of pulmonary or systemic inflammation.

III.3. HYPOXIA

Varying degrees of tissue hypoxia are considered in human pathophysiology, ranging from virtual anoxia in tumours, to states of oxygen debt seen in over-worked skeletal muscle. The lung, in particular, does not become completely oxygen starved unless breathing is obstructed, and is in a position to receive the highest level of oxygenation. Therefore, the level of hypoxia discussed in the context of pulmonary hypertension is considered moderate (8-12% O_2). Physiologically, hypoxia occurs at approximately 20 to 60mmHg pO_2 (47). Moderate hypoxia has not been shown to alter cellular energy production, in the form of ATP, although it can change the behaviour of some cell types, including smooth muscle (47).

The alveolar gas equation is;

$$P_{AO2} = (P_b - P_{H2O}) \times F_{IO2} - \frac{P_{ACO2}}{R}$$

Where, P_{AO2} is alveolar partial pressure of O_2 is equal to the difference between barometric pressure (P_b) and water vapour pressure (P_{H2O}) multiplied by the fraction of inspired O_2 (F_{IO2}), corrected for the alveolar CO_2 partial pressure (P_{ACO2}) and the respiratory quotient (R). At sea level, the P_b is normally around 760 mmHg, P_{H2O} at 37 °C is 47 mmHg, P_{ACO2} is 40 mmHg and R is 0.8. With everything else held constant, changing F_{IO2} from 21% to 10% would make the P_{AO2} 21.3 mmHg instead of 99.73 mmHg.

III.3.1. HYPOXIC PULMONARY VASOCONSTRICTION

Hypoxia-induced vasoconstriction is unique to the pulmonary circuit. Low O_2 tension in other organs such as the brain or over-exerted muscles, results in vasodilation.

However, in the lung, hypoxic pulmonary vasoconstriction (HPV) is a physiologically advantageous phenomenon that serves to match perfusion to ventilation (40). Therefore, pulmonary blood vessels in close proximity to air-expanded alveoli will be relatively dilated to allow maximum blood flow and therefore maximize O_2 uptake. An example of an instance when HPV is advantageous is in fetal pulmonary circulation, where high pulmonary vascular resistance is maintained in part by HPV resulting from low pO_2, approximately 20 Torr (33). Following respiration at the time of birth, PVR decreases in part due to an acute increase in pO_2 (38).

In vivo, HPV begins at a pO_2 of 60 to 80 Torr, a threshold that alters with age (40). HPV occurs within minutes of hypoxic exposure and can cause an increase in PVR of 50 to 300% (33). The mechanism by which HPV occurs is not completely understood, however it is known that a decrease in O_2 concentration, as is seen in hypoxia, may lead to an alteration in K^+, Ca^{2+}, and H^+ ion concentrations in a manner that would enhance smooth muscle cell contraction by regulating several ion channels (38). Ca^{2+} entry through voltage operated Ca^{2+} channels as well as release from the ryanodine-sensitive intracellular stores are required for the development of HPV (47). It is also known that the hypoxic vasoconstrictor response requires an intact endothelium to be maximal, can be suppressed by cooling and Ca^{2+} channel inhibition, and is not affected by cyclooxygenase (COX) inhibition (40). While HPV is advantageous in some cases and leads to more efficient O_2 acquisition, in some disease states, it even further hinders oxygenation. For instance, in PPHN, if an infant experiences a hypoxic episode, HPV would occur therefore decreasing perfusion to match the compromised ventilation. This would further interrupt normal pulmonary circulatory transition and the entire lung would

remain vasospastic. Also, in animal models of hypoxic-PPHN where inhaled O_2 is held at a controlled concentration, for example 10% O_2 instead of the normal 21%, would cause HPV that would even further decrease O_2 uptake due to global pulmonary vasoconstriction.

III.3.2. Cellular Oxygen-Sensing

Glomus cells in the carotid body sense hypoxia by Kv (voltage-sensitive potassium channel) associated membrane depolarization, which starts a cascade that induces an increase in lung ventilation (18). Low oxygen tension has been shown to inhibit Kv channels, resulting in membrane depolarization (8, 47). There is also a genomic component to cellular hypoxia sensing which involves the transcription factor, hypoxia-inducible factor, HIF-1α (18).

A universal cellular oxygen *sensor* is unknown, however there are 2 popular hypotheses; the redox hypothesis and the heme-protein hypothesis (18). The heme protein hypothesis suggests that hypoxia interferes with heme breakdown, and this sets off a cascade leading to membrane depolarization (18). The redox hypothesis suggests that a change in oxygen tension alters reactive oxygen species (ROS) generated by the mitochondria NADPH oxidase system. In normoxia, the ROS generated by the mitochondria lead to oxidation of the Kv channel which activates a Kv current, allowing the cell to maintain resting membrane potential. However, in hypoxic conditions, it is thought that the mitochondria would produce less ROS which would lead to a decrease in K_V channel function, resulting in plasma membrane depolarization (47). This would then lead to the inhibition of Ca^{2+} activated K^+ channels, which open in response to an increase in intracellular Ca^{2+} concentration (18).

Still debatable is the correlation between increased or decreased ROS production and hypoxic conditions, probably due to unavailability of robust ROS measurement techniques. Cells can also mount a response to hypoxia by altering specific gene expression. HIF-1 is a transcription factor that binds to DNA in the promoter region of genes that contain a hypoxia response element (HRE) during periods of low O_2 (41). HIF-1 is a heterodimer, composed of the constitutively expressed HIF-1β, and the low oxygen-regulated HIF-1α (42). HIF-1α can only bind HIF-1β after specific proline residues have been hydroxylated (42). The helix-loop-helix transcription factor is important in times of hypoxic stress because it regulates the expression of over 100 genes, some of which are include glycolytic pathway enzymes, vascular growth factors, and proteins that contribute to maintenance of vascular tone (41). In short, there must be a cellular oxygen sensor to induce increased HIF-1α expression, and the resulting regulation of gene expression leads to an increased expression of proteins that allow regulated use of energy, leading to HPV in pulmonary arteries.

III.3.3. Oxidative Stress and Smooth Muscle

In the vasculature, the endothelium is first to mount a response to hypoxia by increasing expression of vasoconstrictors and growth factors while also decreasing expression of proliferative inhibitors and nitric oxide production (25). In vessels, oxidative stress can be generated by a change in O_2 tension, nitric oxide synthases, cytochrome P450, xanthine oxidase, NAD(P)H oxidases and COX (53).

A decrease in pO_2 can lead to an increase in intracellular Ca^{2+} concentration in many cell types, including smooth muscle (47). An increase in oxygen concentration

leads to an increase in PKG activity by changing cGMP binding, dissociation rate of cGMP, autophosphorylation of PKG and subcellular localization of PKG (38).

III.4. Arachidonic Acid Metabolism

Phospholipase A_2 is the main enzyme that regulates and catalyzes the production of arachidonic acid (AA), achieved by hydrolysis of membrane phospholipids (2). Arachidonic acid synthesis is stimulated by mechanical, hormonal and nervous mechanisms which activate phospholipases (11). AA is a 20-carbon essential fatty acid which is the precursor for the eicosanoids, which include prostaglandins, prostacyclin, thromboxane and leukotrienes (2). Subsequent to AA production, it can be metabolized by either lipoxygenase to produce leukotrienes or cyclooxygenase (COX) to generate prostaglandins as is shown in Figure 1 (11). Both leukotrienes and prostaglandins are thought to mediate the inflammatory response mainly because their administration can mimic inflammatory symptoms, they are increased in areas of inflammation and become decreased after the use of anti-inflammatory treatment (11). There are 2 isoforms of COX expressed in vascular smooth muscle, COX-1 and COX-2, both of which lead to the formation of prostaglandins (32). The difference between the enzymes is their expression patterns; COX-1 is constitutively expressed while COX-2 is an inducible isoform (32). Increased COX-2 expression has been shown to be involved in both acute and chronic inflammation (26). Endothelial expression of COX-2 is up-regulated following cellular stimulation with cytokines, growth factors, hypoxia, oncogenes and mitogens such as TNFα (tumor necrosis factor α), LPS (lippopoylsaccharide), IL-1 (interleukin-1) (26). Once COX catalyzes the reaction of AA to PGH_2, the prostanoid produced depends on what enzymes are present in higher abundance. For example, in platelets, the main

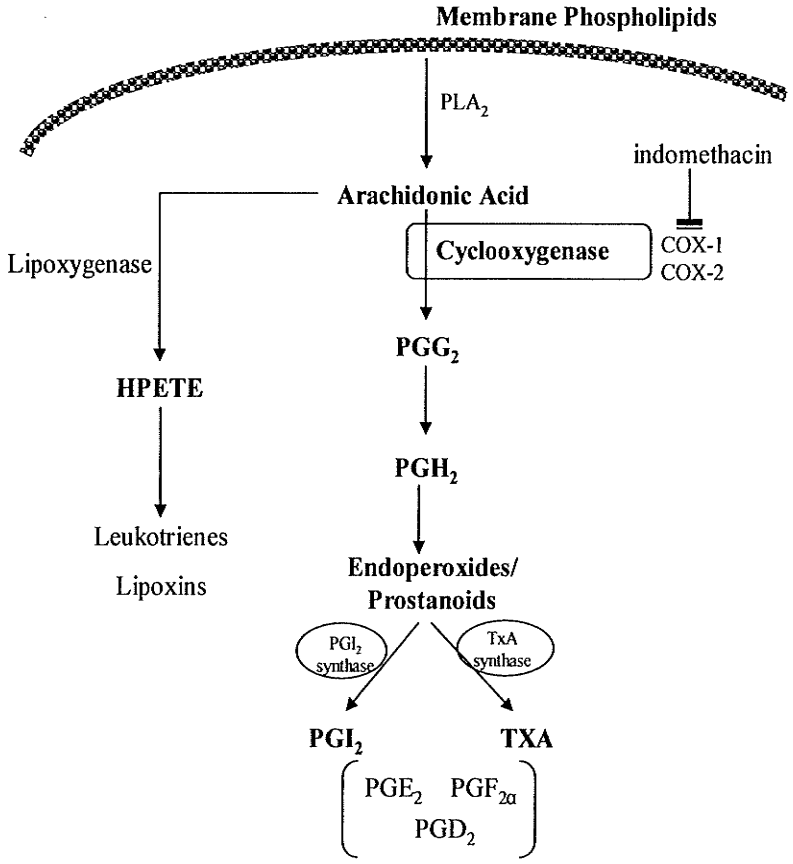

Figure 1. Arachidonic acid metabolism.

Membrane phospholipids are metabolized by phospholipase A_2 (PLA) into aracidonic acid. Arachidonic acid can be further metabolized by either lipoxygenase (to form leukotriene or lipoxin end products), or by cyclooxygenenase (COX-1 or COX-2 isoforms) to form prostanoids. The prostanoids produced depend on the relative abundance and activity of enzymes such as prostacyclin (PGI_2) synthase and thromboxane (TxA) synthase, that result in production of PGI_2 and TxA, respectively.

enzyme is thromboxane synthase, while in endothelial cells, the main enzyme present is prostacyclin synthase (26). There are 5 naturally occurring prostanoids produced by vascular smooth muscle; PGD_2, PGE_2, $PGF_{2\alpha}$, PGI_2, and TxA (15).

III.4.1. Regulation of Thromboxane Production

All prostanoids have extremely short half-lives, and therefore act in an autocrine or a paracrine fashion (32). Thromboxane (TxA) is a constrictor prostanoid (35), with a half life of about 30 seconds (22). Prostacyclin is a vasodilator prostanoid that has a relatively longer half life of about 3 min (26). TxA is mainly produced by platelets and activated macrophages and can lead to platelet shape change, adhesion, dense granule secretion and aggregation (39). Other actions of TxA include; vascular smooth muscle constriction, endothelium prostacyclin release, smooth muscle hypertrophy (22). Thromboxane, especially that produced by COX-2, has been implicated in endothelial cell migration and angiogenesis (19).

In vascular smooth muscle, TxA has been shown to induce smooth muscle contraction in a Ca^{2+}-independent manner, and can maintain elevated tone even in the presence of the nitric oxide donor, sodium nitroprusside (35). In rat caudal arterial smooth muscle, TxA mimetic U46619 causes Ca^{2+} entry through L-type Ca^{2+} channels, and this entry is required for force development (51). In rat caudal artery, a thromboxane agonist results in Ca^{2+}-sensitization via a Rho kinase dependent mechanism, but independent of PKC as CPI-17 phosphorylation state was not altered following stimulation (20).

Thromboxane has clinical implications in diseases such as asthma and hypertension (19). In a piglet model of hypoxia-induced PPHN, acute exposure to

hypoxia (3 days) leads to an increase in TxA and a decrease in prostacyclin in serum (8). Pulmonary vessels at basal tone respond to arachidonic acid by dilation in normoxic neonatal arteries; arteries from pigs with hypoxia-induced PPHN contract in response to exogenous addition of arachidonic acid, likely due to altered thromboxane synthase activity (8).

III.5. Thromboxane Receptor

The thromboxane receptor (TP-R) is a member of the 7-transmembrane G protein coupled receptor superfamily. There is one gene for the TP-R; in the human, it is located on chromosome 19p13.3 (22). From this one gene, two isoforms of TP-R, α and β, are produced by alternative splicing (22). TP-Rα and TP-Rβ have identical N-terminal domains and differ exclusively at the C-terminal tail with the β isoform having the extended tail (22). The C-terminal tail determines G protein coupling specificity. Both isoforms of TP-R have identical affinities for ligand and are expressed in most cell types (39). Human vascular smooth muscle has both TP-Rα and TP-Rβ (3) while platelets express mostly TP-Rα (19).

III.5.1. G-protein Coupled Receptors

Signals from the extracellular space must be specifically detected and translated into the cell by receptors that link to various signal transduction cascades, to result in a change in cell function or state. One specific family of receptors are proteins composed of seven transmembrane domains and coupled to a transducer protein on the intracellular side of the membrane; they are known as G-protein coupled receptors (GPCR). GPCRs have 7 hydrophobic domains (12). Receptor-ligand interaction occurs at a specific binding pocket on an extracellular domain of a GPCR and leads to stabilization of the

receptor in a new, activated conformation (13). The activated conformation enhances coupling of the intracellular domain of the receptor to a heterotrimeric G protein. The signal transduction cascade that a particular GPCR couples to is determined by the C-terminal tail of the receptor, which will couple to a specific isoform of G protein. Each intracellular G protein has an α- β- and γ- subunit, all of which can exist in a number of isoforms. In mammalian cells, there are 15 known Gα subunit isoforms and it is the α-subunit that is most responsible for signal transduction cascade specificity (12). The α-subunits can be categorized into four families; Gs, Gi/Go, G12 and Gq, each having a tendency to couple to specific signalling cascades (34).

A GPCR coupled to a G protein is stabilized in an open conformation, allowing it to bind to its specific ligand. When a GPCR binds its specific agonist, the receptor changes its conformation, causing the α-subunit of the intracellular G protein to exchange a GDP for a GTP. The GTP-α-subunit dissociates from the βγ-subunits and translocates to the effector enzyme, which then activates or inhibits a signal transduction cascade. Some examples of effector proteins are; adenylate cyclase and phospholipase C (12). When the GTP on the α-subunit is hydrolyzed to GDP, this enhances the tendency for the whole G protein to re-associate and interact with the GPCR, therefore completing the cycle. GPCRs can undergo post-translational modification which can alter distribution and function (12). For example, glycosylation regulates receptor distribution while palmitoylation alters receptor-ligand interaction. Gα subunits may undergo post-translational modification in the form of reversible palmitoylation or irreversible N-myristoylation which will differentially target them to the plasma membrane (5). Gγ

subunits can undergo prenylation (5). Phosphorylation of serine, threonine or histidine residues of G-subunits can alter signal peak and duration (5).

III.5.2. THROMBOXANE RECEPTOR CHARACTERISTICS

The TP-R has been described in most organs, including spleen, heart, brain, lung, liver, eye, placenta, intestine, kidney, uterus and thymus (19). The TP-R has been described in most cells as well, such as; platelets, smooth muscle, endothelial cells, epithelial cells, cardiac muscle cells, astrocytes and schwann cells (19). The binding characteristics of the TP-R have been described for various tissues. The rat vascular smooth muscle thromboxane receptor can exist in a high- and low-affinity state, while platelets from rats have a single binding class (15). In human platelets, the TP-R has 2 binding sites; a high affinity low capacity site, and a low affinity high capacity site (27). Density of the TP-R in vascular smooth muscle is less than in platelet membranes (31). TP-R affinity is approximately 10 fold lower than for many other high affinity receptors (31). The TP-R Kd for U46619 in pig aorta smooth muscle membrane is 68nM (31). In human platelets, the Kd for U46619 is 47nM and the Kd for SQ29548, a TP-R antagonist, is 10nM (27). An increase in Ca^{2+} concentration in a lysed membrane preparation increases U46619 binding, but has no effect on total receptor abundance (31). Because the two isoforms have identical binding pockets, different binding characteristics does not necessarily imply that there is isoform switching.

Desensitization is a means by which a system can regulate signalling in a negative feedback mechanism, mostly achieved by sequestration, but also by covalent modification. The TP-R, in particular, can be modified by covalent and non-covalent mechanisms such as phosphorylation, proteolysis and disulphide bond formation (7).

Desensitization is a common occurrence with GPCRs (39). β_2- receptors are known to become desensitized due to phosphorylation on serine and threonine residues by PKA, PKC and GRKs; resensitization involves dephosphorylation (43). The TP-R becomes transiently desensitized after long-term presence of agonist (43). Along with receptor internalization, the TP-R can also become desensitized by phosphorylation on specific residues. The phosphorylation site involved in TP-R desensitization is located within the C-terminal tail, and deletion of that site inhibits desensitization (43). There is one known PKA phosphorylation site and 4 known PKC phosphorylation sites on the TP-R (19). Phosphorylation of GPCRs often leads to arrestin binding, which leads to internalization and sequestration of receptors following activation (43). TP-Rα is subject to prostacyclin-induced desensitization by phosphorylation of the receptor on serine 329 by PKA, or by phosphorylation on serine 331 by NO-induced activation of PKG in a transfected HEK cell system (39). TP-Rβ internalizes after long-term agonist exposure in a negative feedback mechanism (39). If phosphorylation causes desensitization, then dephosphorylation should cause resensitization. In fact, inhibition of the PP1 and PP2A with calyculin maintains the TP-R in a desensitized state (43).

Cellular redox state influences receptor sensitivity; in human platelet membranes, incubation with reducing agents leads to a decrease in Bmax and an increase in Kd of the remaining TP-R, while incubation with oxidizing agents leads to an increase in Bmax without altering affinity (7). TP-R primarily couples to Gαq (39). TP-R signalling through tyrosine kinase, PKC, Rho kinase and IP3 (inositol triphosphate) leads to smooth muscle cell contraction (19). H_2O_2-induced oxidative stress can alter regulation of many cellular processes and lead to post-translational modification of many proteins including

the thromboxane receptor (45). In a transfected cell system, oxidative stress caused a shift in intracellular TP-R localization from the ER (endoplasmic reticulum) to the golgi apparatus, and stabilized already produced receptor, possibly via the unfolded protein response mechanism (45). An increase in oxidation state in whole cells led to an increase in membrane-bound TP-R, but did not change receptor affinity (45).

III.5.3. Second Messenger Signalling

Signalling cascades downstream of the TP-R induce changes in ion concentrations, contraction, cytoskeletal arrangement, cell adhesion, motility, gene transcription, proliferation and cell survival and programmed cell death by coupling to signalling cascades such as IP3, DAG (diacycl glycerol), cAMP, Ras, Rho, PI3 kinase, PKC and PKA (19). TP-R is known to regulate the ERK and MAPK pathways in vascular smooth muscle, and therefore is mitogenic (19). In human vascular smooth muscle, Gα13 signalling from TP-Rα or TP-Rβ leads to an increase in Na^+/H^+ exchange (3). Cotransfection of COS-7 cells with TP-Rα and Gα13 or Gαq increases I-BOP affinity (3). Both TP-R isoforms couple to Gαq. The Gαq-subunit couples the receptor to the effector protein, phospholipase C (PLC). PLC is an enzyme that converts phosphatidylinositol biphosphate (PIP2) into IP3 and DAG (12). DAG is one of the known activators of PKC, which has been shown to reduce relaxation by phosphorylation of MLCP (myosin light chain phosphatase), which decreases phosphatase specific activity. The main downstream effect of IP3 second messenger signalling is Ca^{2+} mobilization from intracellular IP3-gated stores, which enhances smooth muscle contraction. IP3 binds to its receptor on the SR membrane, leading to Ca^{2+} release. Ca^{2+} release from this store produces Ca^{2+} waves or oscillations in the smooth muscle

cytoplasm. The frequency of these oscillations correlates with development of force and maintenance of muscle tone. Through generation of IP3, TP-R coupled to Gαq results in Ca^{2+}-dependent smooth muscle contraction (9).

III.6. Smooth Muscle Cell Contraction

The main function of muscle is contraction. Conserved within all muscle cells, cardiac, skeletal and smooth muscle contraction requires interaction between myosin and actin filaments in the form of cross-bridges. A cross-bridge forms when a myosin head binds to a neighbouring actin filament. This interaction leads to the development of force when the myosin head undergoes a conformational change, forming a power stroke that results in the pulling of actin filaments towards the myosin molecule center (48). Actin filaments are attached to other structural elements in the cell, such as integrins and dense plaques. Therefore, movement of actin filaments is transmitted throughout the cell and results in a change in cell length and increases force development.

Although cross-bridges are required for all muscle contraction, the regulation of cross-bridge formation differs between cell types. In skeletal muscle, much of the regulation involves the thin filament, actin. In smooth muscle, contraction is controlled by the thick filament, myosin. Myosin control of smooth muscle contraction combines signals from multiple transduction pathways. Briefly, in smooth muscle, regulatory light chains on myosin must become phosphorylated in order for the protein to become activated and allow it to interact with actin. Overall levels of activated myosin are determined by the balance in activities of myosin light chain kinase (MLCK) and myosin light chain phosphatase (MLCP) which phosphorylate and de-phosphorylate the myosin light chain respectively (37).

III.6.1. Calcium-Dependent Smooth Muscle Contraction

Calcium is a tightly regulated ion in all cell types, including smooth muscle. In a resting smooth muscle cell, intracellular unbound Ca^{2+} exists in the nanamolar range, while concentrations in the extracellular space and levels stored within the SR are approximately 10,000 times higher (29). This huge differential in distribution is established and maintained by the specific receptors and ion channels embedded within the SR membrane and plasma membrane as well as Ca^{2+}-binding proteins that buffer intracellular Ca^{2+} concentration (21). Cytoplasmic free Ca^{2+} levels must be strictly controlled because the ion modulates many signal transduction pathways including; programmed cell death (apoptosis), proliferation, transcriptional activation, adherence, migration, and secretion. Perhaps the cell function most associated with intracellular Ca^{2+} levels is muscle contraction. Calcium regulates smooth muscle contraction by 4 ions binding to calmodulin which then activates MLCK via the formation of a ternary complex, resulting in myosin light chain phosphorylation, cross-bridge formation and subsequent contraction.

III.6.2. Mechanisms to Increase Intracellular Calcium

Because Ca^{2+} is involved in so many signalling pathways, many stimuli are able to augment intracellular Ca^{2+} concentrations. Mechanisms that can raise Ca^{2+} levels in smooth muscle include; (a) stretching the cell or (b) electrical stimulation which leads to membrane depolarization and Ca^{2+} influx, and nervous or hormonal production of molecules that (c) open ion channels on the cell membrane or (d) interact with G-protein coupled receptors (49).

Extracellular Calcium Entry. Ca^{2+} can enter the cell by flowing through ion channels located in the plasma membrane. Voltage-gated calcium channel (VOCC) open when the smooth muscle membrane becomes depolarized by either electrical stimulation or altered ionic concentrations. Open VOCC, also known as L-type Ca^{2+} channel, are the major source of Ca^{2+} for contraction. Ligand-gated Ca^{2+} channels open after binding to a specific ligand (for example; the purinoreceptor, P2X opening after binding ATP). Both voltage-gated and ligand-operated Ca^{2+} channels allow movement of the ion down its electrochemical gradient, into the cell (49).

Intracellular Calcium Mobilization. The main storage space for Ca^{2+} is the SR. The SR takes up approximately 6% of smooth muscle cell volume and can be found superficially or deep within the cytoplasm (54). It contains the Ca^{2+}-binding proteins calsequestrin and calreticulin that help to buffer and concentrate Ca^{2+} in the SR (49). The SR contains two functionally and spatially separate Ca^{2+} pools; the ryanodine-sensitive and the IP3-gated Ca^{2+} pools (20).

The ryanodine-sensitive Ca^{2+} pool releases Ca^{2+} in response to a localized increase in Ca^{2+}, in a mechanism termed Ca^{2+}-induced Ca^{2+} release. Ryanodine receptors are the main intracellular calcium release channel in striated muscle, while their expression is relatively low in vascular smooth muscle (28). Ca^{2+} release from ryanodine-sensitive stores is most commonly accessed after VOCC opening in response to membrane depolarization, forming what is called a Ca^{2+} spark (54).

The IP3-gated Ca^{2+} pool is accessed when cytosolic IP3 levels increase, most commonly after G-protein coupled receptor activation. Ca^{2+} release from this store is known as a Ca^{2+} puff (54). Ca^{2+} puffs have been shown to correlate with formation of

Ca^{2+} waves which lead to smooth muscle contraction as they provide Ca^{2+} deep within the cell to calmodulin, the activator of MLCK. Ca^{2+} release from this store has been shown to also affect release from ryanodine-sensitive stores, demonstrating that in some cases, the ryanodine-sensitive and IP3-gated Ca^{2+} pools do not always act as separate entities (54). Of current interest are Ca^{2+} waves, which are spatial and temporal patterns that propagate throughout a cell by a positive feedback mechanism (4).

Mitochondria can act as a Ca^{2+} sink when intracellular Ca^{2+} concentration is high. Because mitochondria can sequester Ca^{2+}, it is suggested that it can also participate in Ca^{2+} signalling through the permeability transition pore being triggered by ryanodine-sensitive Ca^{2+} release. However, Ca^{2+} extrusion from the mitochondria is most commonly associated with apoptosis and probably is not a very influential source of Ca^{2+} for smooth muscle contraction.

IV. HYPOTHESES AND SPECIFIC AIMS

Neonatal persistent pulmonary hypertension (PPHN) can be caused by hypoxic exposure. Vasospasm is characteristic of early stage PPHN. In a piglet model of hypoxia-induced PPHN, altered COX activity leads to an increased thromboxane: prostacyclin ratio, potentiating vasospasm.

- **HYPOTHESIS 1:** Moderate hypoxia causes increased thromboxane sensitivity in neonatal pulmonary arterial smooth muscle cells.
- **HYPOTHESIS 2:** Altered myocytes agonist sensitivity in animals with hypoxic PPHN can persist during cell growth in normoxia.

Ca^{2+} responsiveness to TxA mimetic, U46619, of control or hypoxic PASMC will be measured using live cell Ca^{2+} imaging with the fluorescent, ratiometric dye fura-2AM. Peak Ca^{2+} response will determine maximal response while analysis of U46619 dose response curves will determine sensitivity. Persistence of hypoxia-induced effects of TxA responsiveness will be determined by exposing PASMCs to 10% O_2 in vivo and then culturing the cells in normoxia, comparing responsiveness to myocytes obtained from normal age-matched animals.

Hypoxia can cause phenotypic modulation in cultured pulmonary artery smooth muscle cells. Hypoxia causes membrane depolarization in smooth muscle. IP3-gated and ryanodine-sensitive SR Ca^{2+} channels may access separate intracellular Ca^{2+} pools. In vascular smooth muscle cells, intracellular Ca^{2+} pools may alter with phenotype, thereby altering pathway of Ca^{2+} mobilization.

- **HYPOTHESIS 3:** Elevated TxA-induced Ca^{2+} response in hypoxia is due to increased intracellular SR Ca^{2+} stores, specifically the IP3-gated Ca^{2+} pool.

PASMCs (control or hypoxic) will be stimulated with agonists that initiate Ca^{2+} release from internal stores in a thromboxane-receptor independent manner. IP3-gated Ca^{2+} pools will be accessed by stimulating PASMC with ATP in a Ca^{2+}-free environment to activate the P2Y receptor which mobilizes Ca^{2+} by generation of IP3. The ryanodine-sensitive Ca^{2+} pools will be accessed by direct stimulation, using caffeine or low doses of ryanodine. Peak Ca^{2+} response to these agonists will be measured using the florescent calciometric dye, fura-2AM, to determine if responsiveness is altered by hypoxia.

The thromboxane receptor (TP-R) is a G-protein coupled receptor. Availability of receptor can regulate responsiveness to agonists. In hypoxia, responsiveness to TxA is increased.

- **HYPOTHESIS 4:** Cell surface TP-R is increased following moderate hypoxic exposure.

TP-R gene expression will be assessed by RT-PCR and protein abundance will be measured in whole cells by western blot. Fractionated whole cell lysates (membranous and cytosolic fractions) will be studied by western blot. PASMCs will also be permeabilized by fixation with paraformaldehyde or preserved with the membrane intact by fixation with methanol to study intracellular and cell-surface TP-R localization. As well, radioligand binding will be measured under saturating conditions to measure maximal TP-R ligand binding in normoxic and hypoxic myocyte membrane fractions.

TxA responsiveness is increased in myocytes exposed to hypoxia, however cell surface TP-R abundance is decreased.

- **HYPOTHESIS 5:** TP-R affinity is increased in hypoxic smooth muscle cells.

Scatchard analysis of [H^3]-SQ29548 binding will be measured in membranous fraction of normoxic or hypoxic PASMC. To study agonist binding, competitive binding kinetics will be studied using unlabeled U46619 to displace [H^3]-SQ29548.

Normoxic neonatal myocytes are hyposensitive to TxA; the TP-R is abundant on the cell surface but has a decreased affinity. Many GPCRs are phosphorylated to regulate activity. Phosphorylation of serine residues on the TP-R results in desensitization.

- **HYPOTHESIS 6:** Normoxic TP-R is more phosphorylated than hypoxic TP-R, and this decreases coupling to Gαq.

Whole PASMC lysate will be incubated with TP-R antibody to immunoprecipitate the TP-R. The resulting protein will be separated by SDS-PAGE and probed for serine phosphorylation or Gαq.

V. MANUSCRIPT I

HYPOXIA INDUCES HYPERSENSITIVITY AND HYPERREACTIVITY TO THROMBOXANE RECEPTOR AGONIST IN NEONATAL PULMONARY ARTERIAL MYOCYTES

M. Hinton [1,3], L. Mellow [3], A.J. Halayko [1,2,3], A. Gutsol [3], S. Dakshinamurti [1,2,3]

Departments of Physiology [1] and Pediatrics [2], University of Manitoba

Biology of Breathing Group [3], Manitoba Institute of Child Health

715 McDermott Ave, Winnipeg, Canada R3E3P4

Am J Physiol Lung Cell Mol Physiol 290: L375-L384, 2006.

ABSTRACT

Neonatal persistent pulmonary hypertension (PPHN), caused by perinatal hypoxia or inflammation, is characterized by an increased thromboxane:prostacyclin ratio and pulmonary vasoconstriction. We examined effects of hypoxia on myocyte thromboxane responsiveness.

Myocytes from 3rd-6th generation pulmonary arteries of newborn piglets were grown to confluence and synchronized in contractile phenotype by serum deprivation. On the final 3 days of culture, myocytes were exposed to 10% O_2 for 3 days; control myocytes from normoxic piglets were cultured in 21% O_2. PPHN was induced in newborn piglets by 3 day hypoxic exposure (FiO_2 0.10); pulmonary arterial myocytes from these animals were maintained in normoxia. Ca^{2+} mobilization to thromboxane mimetic U46619 and ATP was quantified using fura-2AM.

Three day hypoxic exposure in vitro results in increased basal $[Ca^{2+}]i$, faster and heightened peak Ca^{2+} response, and decreased U46619 EC50. These functional changes persist in myocytes exposed to hypoxia in vivo but cultured in 21% O_2. Blockade of Ca^{2+} entry and store refilling do not alter peak U46619 Ca^{2+} responses in either hypoxic or normoxic myocytes. Blockade of ryanodine-sensitive or IP3-gated intracellular Ca^{2+} channels inhibits hypoxic augmentation of peak U46619 response. Ca^{2+} response to ryanodine alone is undetectable; ATP-induced Ca^{2+} mobilization is unaltered by hypoxia, suggesting no independent increase in ryanodine-sensitive or IP3-linked intracellular Ca^{2+} pool mobilization. We conclude hypoxia has a priming effect on neonatal pulmonary arterial myocytes, resulting in increased resting Ca^{2+}, thromboxane hypersensitivity and hyperreactivity. We postulate that hypoxia increases agonist-induced

TP-R-linked IP3 pathway activation. Myocyte thromboxane hyperresponsiveness persists in culture after removal from the initiating hypoxic stimulus, suggesting altered gene expression.

INTRODUCTION

Persistent pulmonary hypertension of the newborn (PPHN), defined as a failure of the normal fall in pulmonary vascular resistance at or shortly after birth (36), has an incidence of between 0.4 to 6.8 per 1000 live births (57). It represents a common pathway of injury response following a multiplicity of perinatal stresses, including hypoxia, inflammation and direct lung injury such as meconium aspiration (9). The initial clinical picture of PPHN is of dynamic pulmonary vasospasm, with labile flow through the pulmonary circuit and right to left shunting of blood across the ductus arteriosus. Vasodilator response progressively diminishes (18), giving way to increased extracellular matrix deposition, medial smooth muscle proliferation (39) and impaired vascular distensibility (54), resulting in an increase in pulmonary vascular resistance no longer amenable to therapeutic intervention. While the primary defect in PPHN has been held to be of endothelial origin, up to one third of patients treated with exogenous nitric oxide do not respond (23), suggesting a downstream alteration in pulmonary vascular smooth muscle function.

In neonatal sepsis or direct lung injury, an immediate increase in circulating inflammatory cytokines, including TNF-α, IL-1B, IL-6 and IL-10 (11, 37, 49) triggers second messenger pathways favouring contraction and smooth muscle proliferation (8). Cyclooxygenase (COX) pathway metabolites are implicated in increased pulmonary vascular tone. Arachidonic acid metabolites contribute to the early pulmonary hypertensive response in meconium aspiration (51) and sepsis (27). Thromboxane A_2, a prostanoid with potent vasoconstrictive and mitogenic properties, contracts pulmonary vascular smooth muscle by binding to $G_{q/11}$ coupled sarcolemmal receptors, leading to

increased intracellular [Ca^{2+}], force generation, and sensitization of the contractile apparatus to Ca^{2+} (7). Thromboxane is known to be crucial in mediating septic pulmonary hypertension in the neonate (16, 27). Thromboxane also underlies the pulmonary arterial constrictor response to acetylcholine in hypoxic neonatal piglets; early development of thromboxane-mediated constriction contributes to the pathogenesis of chronic hypoxic pulmonary hypertension in newborns (20). Moreover, in an animal model of perinatal hypoxia, diminished cyclooxygenase-1 and prostacyclin synthase activity are shown to cause a shift in production of arachidonic acid metabolites toward an increased thromboxane to prostacyclin ratio; the relative increase in thromboxane may contribute to development of increased pulmonary arterial tone in hypoxic pulmonary hypertension (19). Acutely altered arachidonic acid metabolism in the hypoxic pulmonary circuit is localized to the arterial endothelium and adventitia, with smooth muscle acting as the effector (2). In infants with congenital diaphragmatic hernia, postductal hypoxemia and alveolar to arterial oxygen ratio are inversely correlated with thromboxane to prostacyclin metabolite ratio, suggesting an increased influence of thromboxane (42).

Hypoxia is known to alter perinatal pulmonary vascular agonist responses, blunting acetylcholine-mediated vasorelaxation, while engendering a constrictor response to cholinergic stimulation, mediated by thromboxane (19). The early development of thromboxane-mediated constriction is postulated to contribute to the pathogenesis of PPHN. The roles of hypoxia in potentiating the prostanoid vasoconstrictor response in neonatal pulmonary artery, and the effects of hypoxia on myocyte thromboxane sensitivity, have not been elucidated to date. In this study, we examine pathways of thromboxane-induced calcium mobilization in primary cultured neonatal pulmonary

arterial myocytes, following *in vivo* and *in vitro* exposures to moderate hypoxia; our hypotheses were that the calcium response of hypoxic myocytes to thromboxane would be enhanced, and that *in vivo* hypoxic thromboxane sensitization would not be extinguished by subsequent normoxic cell culture.

MATERIALS AND METHODS

Induction of Hypoxic PPHN

Animals were housed in a thermoregulated isolette with appropriate diurnal cycling, in accordance with CCAC guidelines. Newborn piglets (< 24hours old; N=10) were sacrificed on the day of arrival from a pathogen-free farm-supplier. For the *in vivo* hypoxic model, newborn piglets (N=4) were placed in a normobaric hypoxic chamber (FiO_2 0.10, achieved by a mixture of room air with N_2) for 3 days. The chamber was opened for no more than 1 hour a day for feeding and cleaning; this protocol has been rationalized by other groups (20). Age-matched control piglets were also obtained at 3 days of age (N=10). All piglets were euthanized by pentobarbital overdose and exsanguination. Heart and lungs were removed en bloc and placed in oxygenated cold (4°C) Ca^{2+}-free Krebs-Henseleit physiological buffer (containing in mM: 112.6 NaCl, 25 $NaHCO_3$, 1.38 NaH_2PO_4, 4.7 KCl, 2.46 $MgSO_4 \cdot 7H_2O$, 5.56 Dextrose; pH 7.4). Relative cardiac weight ratio (blotted tissue weight, right ventricle to left ventricle plus septum) was measured to establish the diagnosis of PPHN by estimating right ventricular afterloading.

Primary Pulmonary Arterial Smooth Muscle (PASMC) Culture

Pulmonary arteries were cultured by a dispersed cell method selective for myocytes (50). Briefly, 2nd to 6th generation pulmonary arteries were obtained by microdissection into Ca^{2+}- free Krebs-Henseleit physiological buffer. Arteries were allowed to recover in cold HEPES-buffered saline solution (HBS; composition in mM: 130 NaCl, 5 KCl, 1.2 $MgCl_2$, 1.5 $CaCl_2$, 10 HEPES, 10 glucose; pH 7.4) supplemented with an antibiotic/antimycotic mixture and gentamicin. Arteries were then washed twice with Ca^{2+}-reduced HBS (20μM $CaCl_2$), and finely minced. Arterial tissue was transferred to a digestion medium containing Ca^{2+}-reduced HBS, type I collagenase (1750 U/ml), dithiothreitol (1mM), bovine serum albumin (BSA; 2mg/ml), and papain (9.5 U/ml) for 15 min at 37°C with gentle agitation. Dispersed PASMC were collected by centrifugation at 1200 RPM for 5min, washed in Ca^{2+}-free HBS to remove digestion solution, and then re-suspended in culture medium. The cells were plated on 4-chambered coverglass plates at a density of 4.4 x 10^4 cells/cm^2, in Hams F-12 medium with L-glutamine supplemented with 10% fetal calf serum, 1% penicillin, and 1% streptomycin.

Once cells were grown to confluence in 21% O_2 (approximately 10 days), they were serum-deprived for 2 days (in Hams F-12 medium with L-glutamine/penicillin/streptomycin and 1% insulin-transferrin-selenium) in order to synchronize in a contractile phenotype. Hypoxic cultures were then maintained serum-free in a sealed hypoxic environment (10% O_2, 5% CO_2) for 3 days (equivalent to the exposure time for *in vivo* hypoxia); control cultures were maintained serum-free in normoxia (21% O_2, 5% CO_2). PASMCs from hypoxic piglets and from their age-

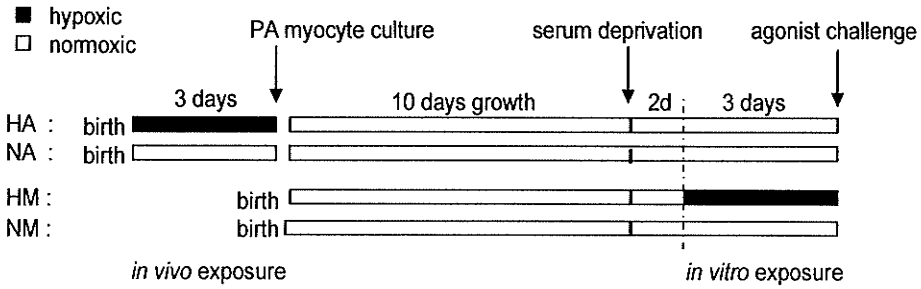

(HA = hypoxic animal; NA = normoxic animal; HM = hypoxic myocyte; NM = normoxic myocyte)

Figure I.1 ***In vivo*** **and** ***in vitro*** **hypoxic exposure protocol**

Treatment groups consist of: pulmonary arterial myocytes from piglets exposed to in vivo hypoxia for the first 3 days of life (hypoxic animals, HA); myocytes from age-matched normoxic control piglets at 3 days age (normoxic animals, NA); myocytes from newborn (<24 hour age) piglets cultured in in vitro hypoxia for 3 days (hypoxic myocytes, HM) or cultured in normoxia (normoxic myocytes, NM). All cells are synchronized in contractile phenotype by serum deprivation for a total of 5 days prior to agonist challenge.

matched controls were also grown to confluence in normoxia. The four treatment groups are delineated in Fig I.1.

Calcium Imaging

Cells were rinsed free of media in Hanks' Balanced Salt Solution (HBSS; containing in mM: 1.26 $CaCl_2$, 0.493 $MgCl_2$-$6H_2O$, 0.407 $MgSO_4$-$7H_2O$, 5.33 KCl, 0.441 KH_2PO_4, 4.17 $NaHCO_3$, 137.93 NaCl, 0.338 $NaHPO_2$) with 0.1% BSA. Myocytes were loaded with the Ca^{2+}-sensitive fluorescent dye fura 2-acetoxymethyl ester (fura- 2AM) dissolved in DMSO, as 5μM in an HBSS/0.1% BSA solution, with 1.0 μg/ml pluronic acid (used for AM ester solubilization), for 1 hour at 37°C. Extracellular fura-2AM was washed off with HBSS/0.1% BSA. The cells were then allowed to recover for 30 minutes at room temperature, allowing for complete cleavage of intracellular AM esters. Incubation and calcium imaging was carried out in 21% O_2. For studies done in a Ca^{2+}-free environment, immediately prior to recording, cells were rinsed twice and then allowed to recover in Ca^{2+}-free HBSS/0.1% BSA, in which $CaCl_2$ was replaced with equimolar $MgCl_2$ for maintenance of cell adherence (17). Ca^{2+}-free HBSS was thereafter used for agonist vehicle and washes. The Ca^{2+}-free studies were utilized for within-treatment group comparisons only, in view of sarcolemmal ion current variables introduced by the difference in external Mg^{2+} concentration.

Coverglass plates were secured on an inverted microscope (Olympus) in room air, and studied at 20x magnification. Real-time ratiometric imaging of intracellular calcium concentration used excitation wavelengths of 340 and 380 nm and an emission wavelength of 510 nm; data was captured via a charge-coupled device camera and Perkin Elmer software.

Responses to U46619 and KCl

Cells were equilibrated in HBSS/0.1% BSA, and a stable 50 sec baseline was recorded at the start of each recording. Agonist stock solutions in HBSS/0.1% BSA were diluted to desired concentration upon addition to the culture well. Thromboxane mimetic U46619 ((1,5,5,)-hydroxy-11 alpha, 9 alpha-epoxymethano) prosta 5Z, 13E-dienoic acid; Sigma, St. Louis, MO) was used in final concentrations ranging between 10^{-10} M and 10^{-4} M (29). KCl concentrations ranged from 25mM to 200mM. A single agonist was added for each culture well. After agonist addition, intracellular calcium concentration was recorded for 150 sec. Agonist was removed by washing twice with 400 µl of HBSS +0.1% BSA. A post-wash stable baseline was also recorded to ensure no shift occurred.

Calcium Channel and Thromboxane Receptor Blockade

Those pathways known to regulate calcium mobilization in response to agonist were examined by incubation of pulmonary arterial myocytes with individual calcium channel blockers for 20 min at room temperature following fura- 2AM loading and prior to addition of U46619. Nifedipine (1µM) was used to selectively block sarcolemmal L-type calcium channels. Ryanodine (100µM) was used to block sarcoplasmic reticulum ryanodine–sensitive channels, and xestospongin (20µM) was used to block IP_3-gated channels (1). Cells were challenged with 10^{-6} M U46619, and calcium mobilization responses recorded. In some experiments, to confirm specificity of receptor activation, the thromboxane A_2 -selective prostanoid receptor (TP-R) was blocked by incubation with 10^{-5} M SQ 29,548 for 20 min at room temperature prior to addition of 10^{-6} M U46619.

Mobilization of Specific Intracellular Calcium Pools

Non-TP-R linked sarcoplasmic reticulum (SR) calcium mobilization was quantified using 20μM ATP to stimulate P2X and P2Y receptors. Maximal calcium mobilization via P2Y was considered an estimate of the SR IP_3-gated calcium pool. P2Y response was isolated by removal of extracellular calcium; P2X response was isolated by blockade of IP_3-gated channels with 20μM xestospongin. The SR ryanodine-sensitive calcium pool was quantified by mobilization with 5μM ryanodine and/or 40mM caffeine.

Calcium Mobilization Data Analysis

Background fluorescence was measured from cell-free areas and subtracted from total fluorescence prior to analysis. No more than 8 equally sized, square regions containing 3-5 cells were selected for the presence of minimal cell-free areas from each microscope field, prior to quantification of calcium responses. Whole cell Ca^{2+} mobilization was analyzed en bloc for each region. Ca^{2+} traces were discarded only if there was not a stable baseline before agonist addition, or if the 340nm excitation value dropped at the same time as the 380nm excitation value, as this would give erroneous peak $[Ca^{2+}]_i$ values with no physiological merit. Peak $[Ca^{2+}]_i$ response was defined as the maximal point of displacement of the rapid calcium transient; as no sustained plateau was apparent in cultured myocyte calcium responses, all subsequent calculations reference peak $[Ca^{2+}]_i$ mobilization. Maximum change in $[Ca^{2+}]_i$ was calculated as the average baseline value subtracted from the peak $[Ca^{2+}]_i$ response to agonist. The time to peak $[Ca^{2+}]_i$ from the point of agonist addition was also documented. The 340/380 nm excitation ratio values were converted to $[Ca^{2+}]_i$ values on a standard curve, generated using calcium standards and calculated by the method of Grynkiewiez (24):

$$[Ca^{2+}]_i = \frac{K_a (R-R_{min}) (F^{380}_{free})}{(R_{max}) (F^{380}_{sat})}$$

Data from individual microscope regions were analyzed using unpaired t-test or one-way ANOVA, with individual comparisons performed by Tukey HSD test. Data are expressed as mean ±SE; $p < 0.05$ was considered significant.

Thromboxane Receptor (TP-R) Localization

PASMCs from newborn piglets were grown to semi-confluence on glass coverslips in 12-well dishes at a density of 4.4 x 10^4 cells/cm^2. Cells were rinsed free of culture media with CB buffer (containing in mM; 10 MES, 150 NaCl, 5 EGTA, 5 $MgCl_2$, 5 glucose) and then fixed with either methanol for 10min to study cell surface TP-R, or 3% paraformaldehyde for 15 minutes at room temperature followed by permeabilization with 0.3% Triton X-100 for 5 min for study of intracellular TP-R. Cells were rinsed twice with CB Buffer and stored in Cyto-TBS (composition in mM; 20 Tris, 154 NaCl, 2 EGTA, 2 $MgCl_2$) at 4°C. Non-specific binding was blocked by incubation with 10% normal donkey serum in Cyto-TBS+1%BSA for 20min at room temperature. PASMCs were then incubated with TP-R rabbit polyclonal antibody (1:50 in Cyto-TBS+1%BSA, Cayman Chemical, MI, USA) overnight at 4°C, followed by incubation with FITC-conjugated donkey anti-rabbit antibody (1:50 in Cyto-TBS+1%BSA, Jackson ImmunoResearch Lab, PA, USA) for 2 hours at room temperature. Nuclei were counterstained with Hoechst 33342. Fluorescence immunocytochemistry images were acquired using an Olympus 1X 70 microscope with wavelengths of 494nm excitation/518nm emission for TP-R, and 346nm excitation /460 nm emission for nuclei. Images were then analyzed with an UltraPix FSI digital camera and UltraView software

(PerkinElmer). Total TP-R protein abundance was also assayed by Western blot in whole cell lysates from confluent myocytes in hypoxic and normoxic culture. Membrane fractions were also obtained by whole cell lysate ultracentrifugation at 150000xg for 30min at 4°C. Samples of 20μg protein separated by SDS-PAGE and blotted onto nitrocellulose membrane were then probed for TP-R. Equality of protein loading was ensured by reprobing blots for β-actin. Visualization of protein bands was by enhanced chemiluminescence (ECL) [Amersham, Piscataway, NJ]. The band representing native TP-R protein was selected on the basis of migrating molecular weight; two additional adjacent bands were selected based on known weights of glycosylated TP-R (25, 52). Data were quantified using a digital imaging densitometer, under non-saturating conditions, with background subtraction achieved by reading the absorbance of an equal sized region directly adjacent to the band. Summated glycosylated and unglycosylated TP-R band densities were normalized to β-actin band density, and represented as ratio of the control value. Data are presented graphically as means ± SEM for a minimum of three replicate samples.

RESULTS

Hypoxic exposure and induction of PPHN

The *in vivo* hypoxic environment for PPHN animals (*HA*) was maintained at FiO_2 9.96 ± 1.37%. Control piglets (*NA*) exhibited a developmentally appropriate decrease in right ventricle to left ventricle plus septum weight ratio over the first three days of life. The development of early pulmonary hypertension in hypoxic piglets was determined by

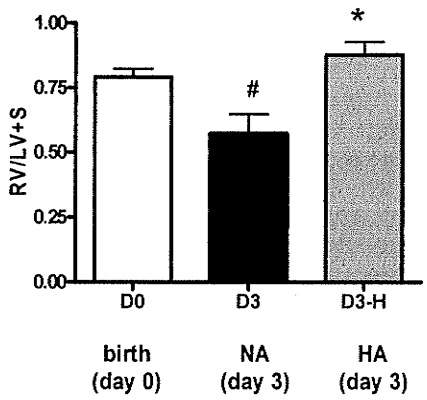

Figure I.2 Hypoxic pulmonary hypertension diagnosed by relative increase in right to left ventricular weight ratio

Pulmonary hypertension is diagnosed by increased cardiac weight ratio of right ventricle to left ventricle plus septum (blotted tissue) following 3 days exposure to moderate normobaric hypoxia, in day 3 hypoxic pigs (*HA*, N=11) compared to day 3 control pigs (*NA*, N=9). Day 0 control pigs (*birth*, N=11) presented as maturational control. (# $p<0.05$ compared to *birth*; * $p<0.05$ compared to *NA*).

an increased right to left cardiac ventricular weight ratio ($p<0.01$), predominantly owing to increased right ventricular weight due to right heart afterloading (Fig I.2).

Calcium Mobilization in Pulmonary Arterial Myocytes to U46619

We used the following four cell culture models: (i) *NA* were PASMCs derived from normal 3 day old pigs, in primary culture at 21% O_2; (ii) *HA* were PASMCs derived from 3 day old piglets with hypoxic PPHN, in primary culture at 21% O_2; (iii) *HM* were PASMCs derived from newborn pigs, in primary culture with incubation in 10.76 ± 0.14% O_2 for the final 3 days of culture; and (iv) *NM* were control PASMCs derived from newborn pigs, in primary culture at 21% O_2.

PASMC basal (unstimulated) intracellular calcium levels were significantly elevated following *in vitro* hypoxic exposures, compared to normoxic controls (Fig I.3A). Intracellular Ca^{2+} levels were increased in myocytes from *NA* and *HA*. Pulmonary arterial myocytes exposed to hypoxic conditions, both *in vivo* (*HA*) and *in vitro* (*HM*), exhibited significantly higher peak Ca^{2+} mobilization response to 10^{-6} M U46619 than did control normoxic myocytes from newborn (*NM*) and 3 day pigs (*NA*) (Fig I.3B, I.3C), despite the very different protocols used for hypoxic exposure *in vivo* compared to *in vitro*. Peak calcium mobilization was enhanced in *HM* cells over a wide range of U46619 doses, compared to *NM* cells (Fig I.3D). The myocyte response to U46619 in all conditions was completely blocked by pre-incubation with the TP receptor inhibitor SQ 29,548 (Fig I.3E), indicating receptor specificity of the U46619 response. The time from agonist addition to peak $[Ca^{2+}]_i$, both in cells exposed to hypoxia *in vitro* or cells cultured from animals exposed to hypoxia *in vivo*, was significantly faster ($p<0.01$) than in their age-matched normoxic control cells at lower doses of U46619 (10^{-7} M) (Fig

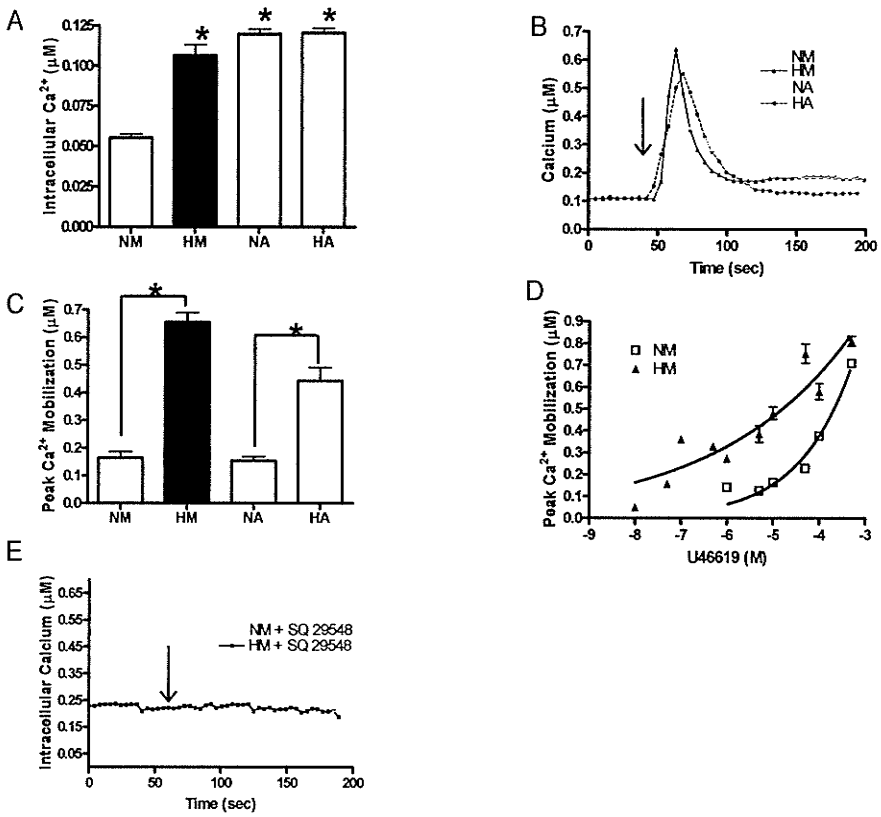

Figure I.3 Myocyte Ca^{2+} mobilization response to U46619

(A) PASMCs exposed to hypoxia for 3 days (*HM*; n=120) have significantly increased resting $[Ca^{2+}]_i$ compared to normoxic controls (*NM*; n=120). Baseline $[Ca^{2+}]_i$ in PASMC from 3 day normoxic pigs (*NA*; n=65) and from animals exposed to 3 day *in vivo* hypoxia (*HA*) are also significantly increased compared to normoxic control (n=120); * $p<0.01$. (B) Representative traces of Ca^{2+} mobilization (in μM) in response to 10^{-6} M U46619 stimulation (arrow) of myocytes derived from neonatal pigs raised in hypoxia for 3 days *in vivo*, and then cultured in normoxia (*HA*), myocytes derived from 3 day normoxic pigs and grown in normoxia (*NA*), myocytes derived from newborn pigs and exposed to *in vitro* hypoxia for 3 days (*HM*) and control myocytes derived from newborn pigs and cultured in normoxia (*NM*). (C) Peak $[Ca^{2+}]_i$ responses of *HA cells* (n=30) and *HM cells* (n=45) to 10^{-6}M U46619 are significantly higher than in *NM cells* (n=37) and *NA* cells (n=41); * $p<0.01$. (D) Peak $[Ca^{2+}]_i$ in *HM* and *NM* myocytes in response to a range of U46619 doses. (E) Representative traces of *NM* and *HM* responses to 10^{-6} M U46619 after pre-incubation with TP receptor inhibitor SQ 29,548 (arrow), demonstrating receptor specificity of agonist. Numerical data quantified in microscopic regions containing 3-5 PASMC loaded with fura-2AM (n=number of microscope regions).

I.4A). However, this difference between treatment groups was not apparent at higher U46619 doses (10^{-6} M), suggesting saturability (Fig I.4B).

Sensitivity of myocyte responsiveness to U46619 was determined by dose response curves normalized to maximal $[Ca^{2+}]_i$ peak within each treatment group. Hypoxia induced sensitization of myocytes to U46619 (Fig I.5A). Dose response curves for U46619 were significantly left shifted in hypoxia, resulting in a lower EC50 for agonist-induced calcium mobilization ($2.1683x10^{-6}\pm0.07751$M in *HM* cells, compared to *NM* cells EC50 of $1.5422x10^{-5}\pm$ 0.06030M; $p<0.0001$). In contrast, the EC50 of calcium mobilization in response to membrane depolarization by KCl was not altered by hypoxic exposure *in vivo* or *in vitro* (Fig I.5B), and peak calcium responses to KCl were not significantly altered.

Pathway of Calcium Mobilization

HM PASMCs incubated in a Ca^{2+}-free environment (Fig I.6A) maintained an increased peak Ca^{2+} response to 10^{-6} M U46619 compared to *NM* PASMCs, as did *HM* PASMCs pre-incubated with nifedipine (Fig I.6B) prior to agonist challenge. However a significant decrease in *HM* peak Ca^{2+} mobilization ($p<0.01$) occurred with both ryanodine (Fig I.6C) and xestospongin (Fig I.6D), dropping the agonist response to a level similar to that of *NM* cells.

Intracellular Calcium Pools in Hypoxia

Ca^{2+} mobilization via ATP-stimulated release from P2Y- IP_3-linked stores was unaltered by *in vitro* hypoxic exposure, suggesting no increase in the intracellular IP_3-gated Ca^{2+} pool (Fig I.7B). Total ATP-induced Ca^{2+} mobilization was also unaltered in

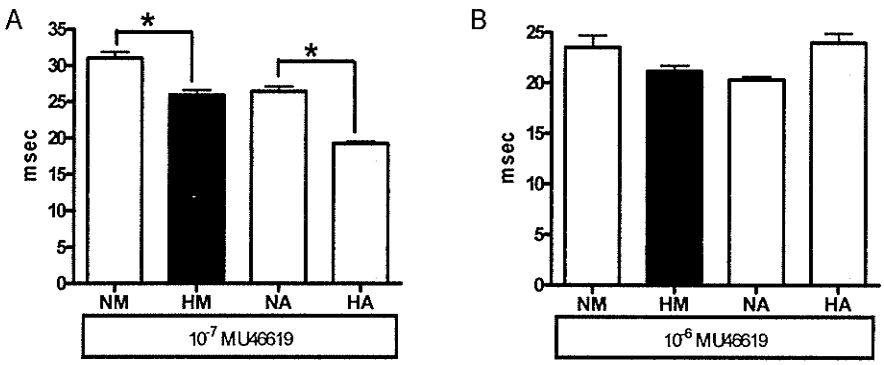

Figure I.4 Time to peak Ca^{2+} mobilization response after agonist addition

(A) Low dose U46619 (10^{-7} M) results in significantly slower peak response time in normoxic control myocytes (*NM*; n=24) compared to myocytes exposed to hypoxia *in vitro* (*HM*; n=24). PASMCs from 3 day normocxic piglets grown in normoxia (*NA*; n=26) also have a significantly slower peak response time than myocytes exposed to hypoxia *in vivo* but cultured in normoxia (*HA*; n=38) (*p<0.01). **(B)** At higher dose (10^{-6}M), no difference in peak U46619 response time between *NM* (n=29), *HM* (n=24), *NA* (n=40) and *HA* (n=32) groups (n=number of microscope regions).

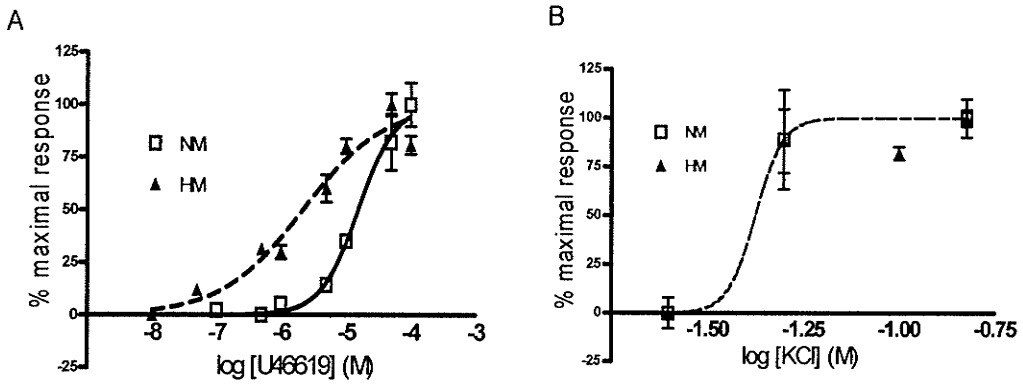

Figure I.5 Dose response curves for peak Ca^{2+} mobilization to KCl and U46619

(A) The U46619 dose response curve for *in vitro* hypoxic myocytes (*HM,* N=3) is significantly left shifted in comparison to the curve for normoxic control cells (*NM,* N=3); $p<0.0001$. Peak Ca^{2+} mobilization is normalized within each group as percent of maximal agonist response. **(B)** KCl dose response curve for *NM* cells (N=3) is not significantly different from the curve for *HM* (N=3), EC50=60.66mM versus 79.23mM, p=NS. (N=number of animals)

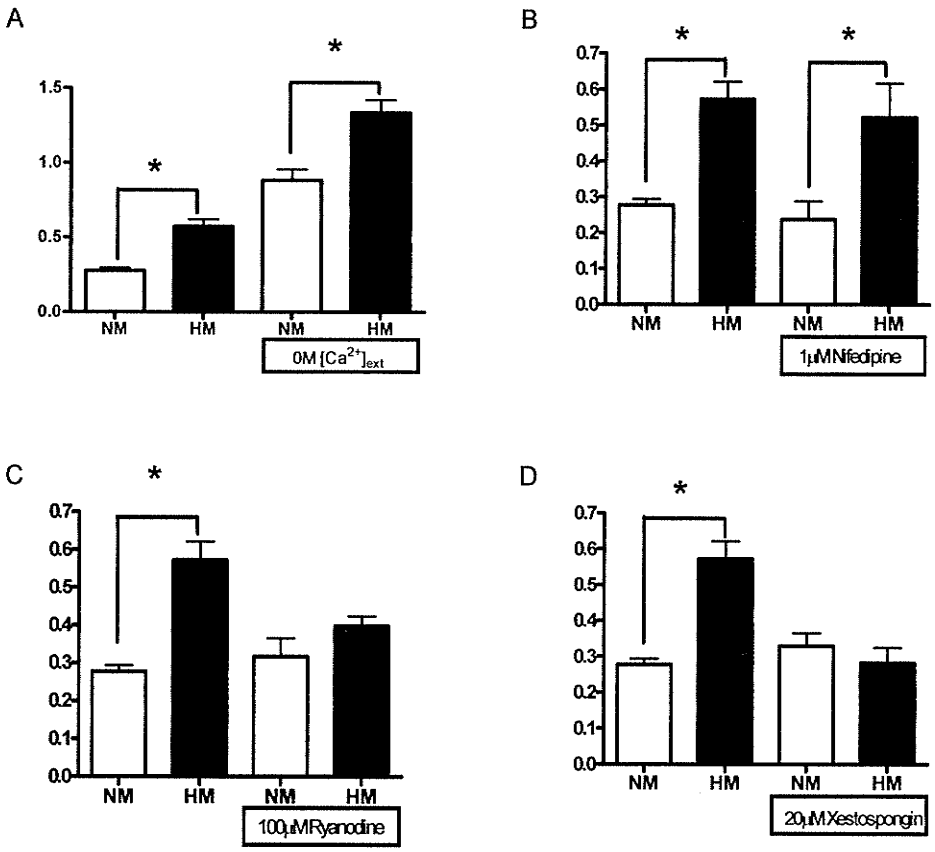

Figure I.6 Pathway of hypoxic myocyte hyperreactivity to U46619 determined by serial calcium channel blockade

Ca^{2+} mobilization responses to 10^{-6} M U46619 in normoxic controls (*NM*; n=84) and in vitro hypoxic myocytes (*HM*; n=62). (A) Stimulation with U46619 after removal of extracellular calcium increases Ca^{2+} mobilization globally, but difference between treatment groups is unaffected (* $p<0.01$); note this histogram has a different Y-axis scale than the ones following. (B) Stimulation with U46619 after pre-incubation with nifedipine (L-type voltage-operated calcium channel blockade) results in unaltered calcium mobilization in hypoxia and normoxia (* $p<0.01$). (C) Stimulation with U46619 after pre-incubation with 100μM ryanodine (blockade of SR ryanodine-sensitive Ca^{2+} channel) decreases Ca^{2+} mobilization in hypoxic myocytes to normoxic levels and obliterates difference between treatment groups. (D) Stimulation with U46619 after pre-incubation with xestospongin (SR IP3-gated channel blockade) also decreases Ca^{2+} mobilization in hypoxic myocytes to normoxic levels, obliterating difference between treatment groups. (n=number of microscope regions).

hypoxic versus normoxic myocytes (Fig I.7A,C). Direct stimulation of Ca^{2+} release from ryanodine-sensitive stores was negligible in cultured PASMC (Fig I.7D).

TP-R Localization

Normoxic myocytes have ample cell surface TP-R (Fig I.8A), as well as internalized TP-R distributed uniformly in the cytoplasm (Fig I.8C). In *HM*, there is a significant decrease in cell surface TP-R signal (Fig I.8B). Permeabilization by PFA fixation reveals decreased TP-R immunostaining, with translocation of the receptor protein to the peri-nuclear region in *HM* (Fig I.8D). Total protein abundance of TP-R is stable in hypoxic whole cell lysates compared to the normoxic group, as demonstrated by Western blot (Fig I.8E). TP-R abundance in the membrane fraction is slightly decreased in HM compared to controls, however this was not statistically significant (Fig I.8F).

DISCUSSION

In this study we examined the distinct phenomena of hypoxia mediated sensitization (lower threshold response to agonist) and hyperreactivity (increased response elicited by a given dose of agonist, or elevation of the plateau or maximal level of response) (21) to thromboxane receptor stimulation. Smooth muscle hyperresponsiveness has been ascribed to altered states of myocyte calcium handling, and our data is consistent with that paradigm (44). Exposure of neonatal pulmonary arterial myocytes to moderate hypoxia for three days *in vitro* results both in sensitization to the thromboxane mimetic U46619, and hyperreactivity as measured by elevated calcium mobilization. We have found: (i) 3 days of hypoxic exposure *in vitro* results in an increased basal Ca^{2+} level, heightened peak Ca^{2+} response, faster peak Ca^{2+} response and

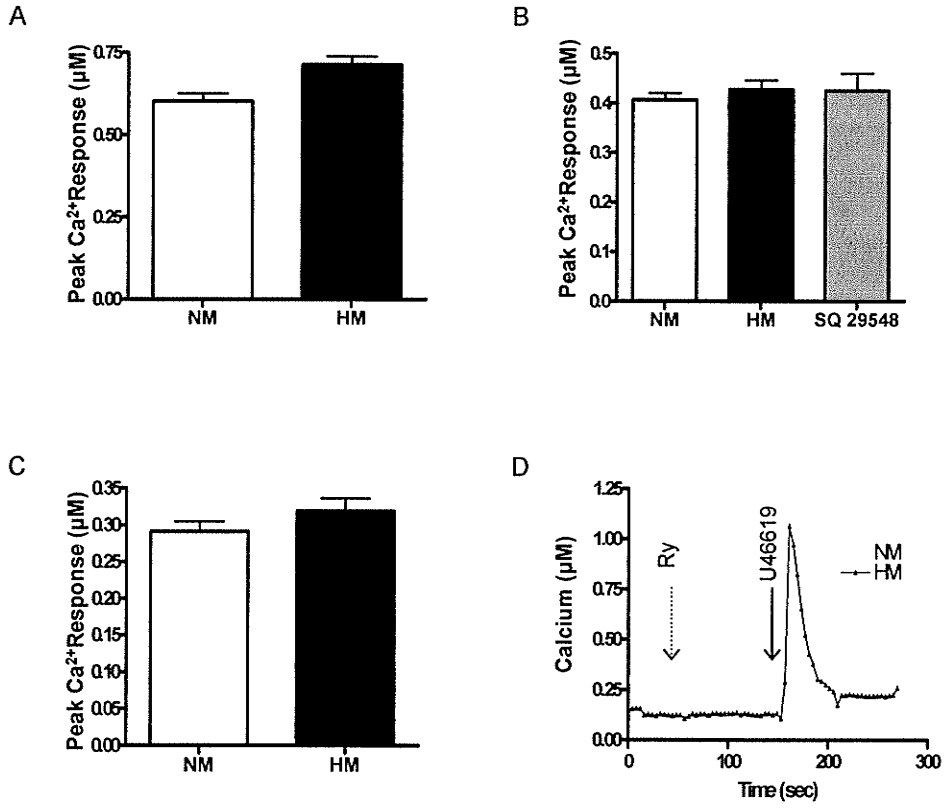

Figure I.7 Thromboxane receptor-independent calcium pool mobilization from intracellular SR stores

Peak Ca^{2+} mobilization responses in normoxic control (*NM*; n=32) and *in vitro* hypoxic PASMC (*HM*; n=40). (A) 20µM ATP stimulation of both P2X and P2Y receptors. (B) ATP stimulation of P2Y receptors alone, achieved by removing extracellular [Ca^{2+}]. (C) ATP stimulation of P2X receptors alone, achieved by pre-incubation with 20µM xestospongin blocking IP3-gated SR channels. No differences in maximal Ca^{2+} release to ATP in *HM* versus *NM*, p=NS. (D) Representative trace: responses to 5µM ryanodine (left arrow) are absent in both *NM* and *HM* myocytes (similar responses obtained to 40µM caffeine, not shown). Subsequent stimulation with 10^{-6}M U46619 (right arrow) confirms viability.

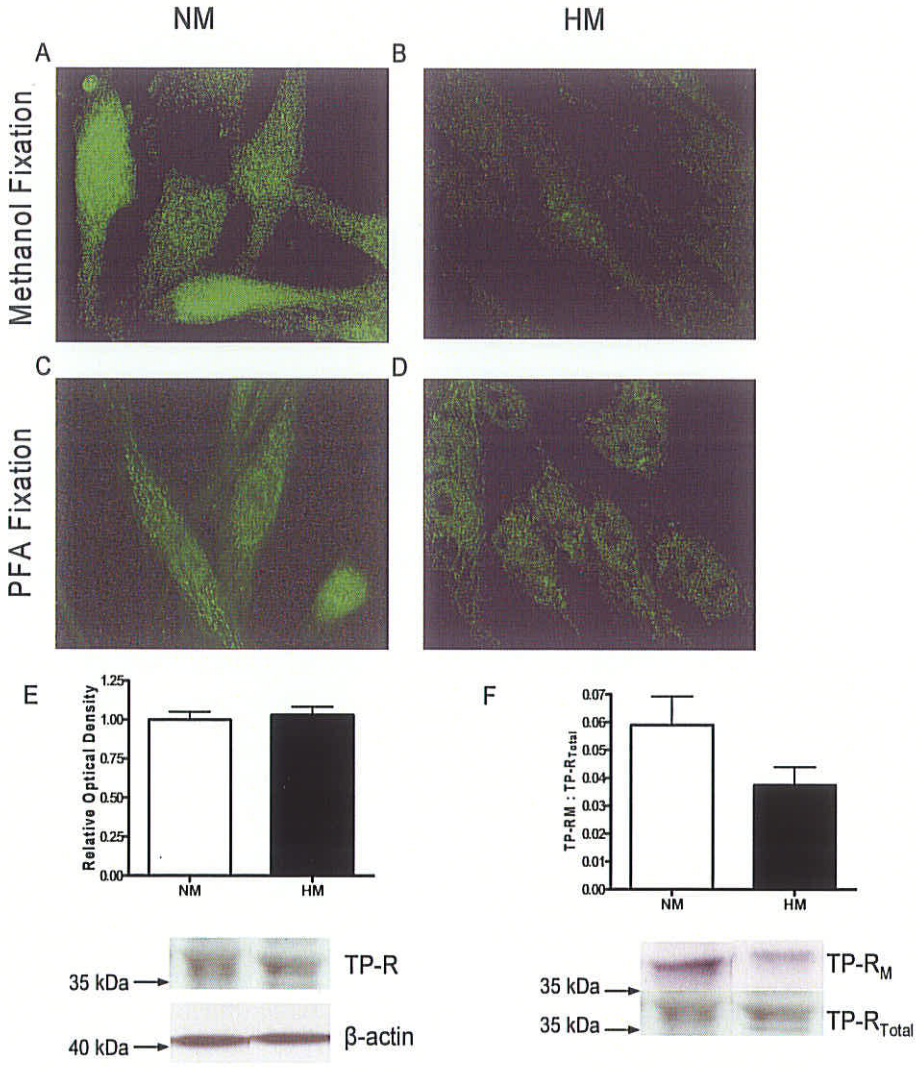

Figure I.8 Thromboxane receptor localization is altered by hypoxic exposure

Representative photomicrographs using a polyclonal thromboxane receptor antibody in *NM* (N=3) and *HM* (N=3) PASMCs. Intact cell immunocytochemistry using methanol fixation reveals cell surface TP-R is more abundant in (A) normoxic myocytes than in hypoxic myocytes (B). Immunostaining after cell permeabilization by PFA fixation indicates cytoplasmic TP-R is widely distributed in normoxic cells (C), while translocating to the perinuclear region in hypoxic PASMCs (D). Total cell TP-R protein abundance, normalized to β-actin remains constant in hypoxia (*HM*; n=9. *NM*; n=9) (E). Membrane TP-R abundance, normalized to whole cell TP-R, shows no significant change between *HM* (n=8) and *NM* (n=8) ((N=number of pigs, n=number of samples)

a decreased EC_{50} for U46619; (ii) these increases persist when PASMCs are exposed to hypoxia *in vivo a*nd then cultured in 21% O_2; (iii) the phenomenon is not ubiquitous, but is specific for thromboxane; and (iv) hypoxia-induced myocyte thromboxane hyperreactivity occurs in the face of decreased cell surface thromboxane receptor expression, suggesting a mechanism of increased receptor sensitivity. Mechanisms of altered calcium mobilization were studied primarily in primary pulmonary arterial myocyte cultures using an *in vitro* environmental manipulation model. An *in vivo* model of hypoxic PPHN followed by myocyte culture in normoxia was also employed to look specifically at extinction of hypoxic alterations in thromboxane response, upon removal of the hypoxic stimulus and proliferation under control conditions. Myocyte monoculture is reliable for study of intracellular calcium mobilization in hypoxia, which correlates with the accrual of early phase tension, and is unaffected by absence of endothelium (48). While others have reported agonist-induced pulmonary arterial calcium mobilization to be diminished following chronic hypoxic exposure of adult rats, it is likely that myocyte agonist insensitivity and loss of calcium oscillations following prolonged hypoxic exposure may relate more to phenotypic alteration associated with pulmonary arterial remodelling (4).

Our data indicate that the elevated peak calcium response in hypoxic pulmonary arterial myocytes is mediated by increased calcium release via SR Ca^{2+} stores (14, 35); other calcium sources may contribute to the overall response, but their relative contribution is not increased in hypoxia, and inhibition of SR calcium mobilization decreases thromboxane-induced calcium transients in hypoxic myocytes to normoxic levels. Thromboxane mimetic U46619-induced calcium response is known to be

redundant, eliciting both intracellular and extracellular calcium mobilization (15, 38, 53). Thromboxane inhibits Kv channel current, leading to myocyte depolarization, activation of L-type Ca^{2+} channels, and vasoconstriction of pulmonary arteries (7); simultaneously, pharmacomechanical coupling occurs via a G-protein coupled mechanism (30), as well as calcium sensitization of smooth muscle mediated by Rho-kinase (22). It is probable that augmented SR Ca^{2+} release is the sole source of the elevated calcium response to U46619 observed in hypoxia. In vascular smooth muscle cells, IP_3-gated and ryanodine-sensitive SR Ca^{2+} channels may access separate intracellular Ca^{2+} pools that alter with phenotype, resulting in altering pathway of Ca^{2+} mobilization with phenotypic modulation (56). Unchanged Ca^{2+} mobilization to ATP in hypoxic myocytes attests that the PASMC IP_3-gated pool is not independently increased in hypoxia. The increased hypoxic PASMC response to U46619 may therefore be due to altered receptor-mediated IP_3 generation upstream. Ryanodine-sensitive Ca^{2+} pools are not amenable to direct stimulation in our model, and therefore likely contribute only to calcium-induced calcium release after primary IP_3-gated channel activation. Enhanced IP_3 generation, reported in hypoxic pulmonary, but not systemic, arterial fibroblasts (45), may contribute toward this mechanism.

A limitation in interpretation of this study may lie in the U46619 EC50 value ranges. The concentrations of U46619 and SQ29548 used in these experiments are derived from dose-response curves cited elsewhere in the literature (34, 41). EC50 data can be dependent upon the preparation type and the specific outcome being measured. U46619 EC50 values in the nanomolar range have been reported in radioligand assays using cell membrane preparations. Much higher values are also reported (in the

micromolar range) for U46619 EC50 when examining contraction of an isolated arterial ring preparation (3), and near micromolar range for myocyte calcium response (7). A low affinity TP-R has been described in cultured vascular myocytes, with EC50 in the micromolar range (34). The dose-response and EC50 values we have reported here are robust with repeated measurement, and we can merely conclude they may be characteristic of our cultured myocyte preparation.

Intracellular calcium measurement is employed in this study as a proxy for myocyte contraction. The relationship has been well established between $[Ca^{2+}]_i$, myosin light chain (LC20) phosphorylation and isometric force development to thromboxane analogue stimulation. In guinea pig aortic strips, steady-state force for contractions stimulated by U46619 assume a similar dependence on LC20 phosphorylation to potassium depolarization, both in the presence and absence of extracellular calcium. A $[Ca^{2+}]_i$ /force relation indicates U46619 stimulates greater isometric force at lower $[Ca^{2+}]_i$ than does KCl depolarization, suggesting increased calcium sensitivity; but the myocyte LC20 phosphorylation/force relationship is unchanged by U46619 in comparison to potassium-induced depolarization (32). As calcium sensitivity as well as muscle preload determine developed force at a given degree of $[Ca^{2+}]_i$ elevation, calcium mobilization responses to U46619 cannot be compared directly to those induced by potassium depolarization (40); however comparisons of myocyte calcium transients generated in response to any one specific agonist may be proportionally related (13, 14).

Of note, pulmonary arterial myocytes in our preparation responded to agonist challenge with a sharp, rapid calcium transient consisting of a peak, a rapidly sloping shoulder without defined plateau, and a clear return to baseline free calcium values within

the 4 to 5 minutes of observation. A more prolonged period of observation did not reveal any alteration in this pattern of response; while the slope of the shoulder occasionally varied, no plateau or sustained calcium elevation was evident, and all traces returned to the pre-agonist baseline. As such, we focused our attention on the peak calcium transient as the primary indicator of myocyte responsiveness as this constituted virtually the entire response. This early calcium spike (<20 sec) is known to correlate with peak myosin phosphorylation, maximal shortening velocity and the majority of isotonic shortening (28), and hence is of physiologic significance for change in vascular diameter. There is reasonable precedent for the measurement of peak calcium mobilization alone in determining pulmonary arterial smooth muscle agonist response (31, 46), and we have analysed our calcium response data accordingly.

We observed elevated resting $[Ca^{2+}]_i$ in hypoxic myocytes, as has been reported by others and ascribed to both sarcoplasmic reticulum release and capacitative calcium entry (12, 33). Altered membrane polarity and voltage-gated calcium channel activity do not contribute to increased calcium mobilization at this oxygen tension, as evidenced by an unchanged EC50 of KCl in agonist-naïve myocytes. These data are consistent with the finding of graded inhibition of outward K^+ current and depolarization of resting membrane potential only at hypoxia below 5% O_2 (43).

We also observed increased sensitivity and reactivity in cells derived from neonatal pigs exposed to hypoxia *in vivo*, but then cultured for 15 days under normoxic conditions, indicating a persistent alteration in myocyte agonist response that is not extinguished after two weeks removal from the sensitizing stimulus. This is in contrast to reports of prompt reversibility of hypoxia-induced alterations in electrophysiological

properties, on return to normoxia (5, 6). The persistence of altered calcium mobilization in cultured myocytes exposed to moderate *in vivo* hypoxia remotely in time, suggests a durable change in thromboxane receptor function and pharmacomechanical coupling that is not extinguished by subsequent normoxic exposure. This finding may carry grave implications for pulmonary circuit responsiveness to inflammatory mediators after the resolution of perinatal hypoxia. Altered gene expression driving persistent functional changes during recovery from hypoxia is not a novel concept. Expression of hypoxia-susceptible genes, including hypoxia-inducible factor, is key to pulmonary vascular remodelling (9, 47). It is known that smooth muscle recovery from hypoxia lags behind endothelial recovery (55), and that pulmonary arterial smooth muscle proliferation, apoptosis and protein synthesis remain altered during recovery from hypoxia (26).

We postulate that hypoxic sensitization to thromboxane agonist occurs at the level of the thromboxane receptor and its associated IP_3 linked pathway, in view of the left-shift in agonist dose response, and the increased rapidity of response at lower agonist doses; the loss of this difference at higher doses may indicate receptor saturability. The data presented here do not yet establish whether altered thromboxane receptor density or avidity may be responsible for the observed myocyte agonist sensitization. However, we demonstrate evidence of thromboxane receptor translocation from the cell surface to a peri-nuclear localization in hypoxia; this may represent a negative-feedback mechanism governing receptor cycling, in the context of agonist hyperreactivity. An increase in receptor-ligand binding, and therefore in receptor avidity, may be implied. It would be pertinent to further evaluate hypoxia-induced sensitization with receptor-binding studies; these fall beyond the scope of this paper.

Hypoxia-induced thromboxane agonist hypersensitivity and hyperreactivity of neonatal pulmonary arterial myocytes may have a synergistic effect on intracellular calcium transients, contributing to the pulmonary vasoconstrictor response to arachidonic acid observed in perinatal hypoxia (20). In addition, we have previously reported calcium sensitization of pulmonary arterial smooth muscle in hypoxic PPHN, due to downregulation of myosin light chain phosphatase activity (10), which would be markedly potentiated by augmented agonist-induced calcium mobilization.

The relationship of hypoxia and inflammation is crucial in the time course and severity of PPHN. We conclude that hypoxia has a priming effect upon the neonatal pulmonary arterial myocyte: hypoxic exposure results in an increased basal Ca^{2+} level, heightened peak Ca^{2+} response, faster peak Ca^{2+} response and a decreased EC_{50} for thromboxane. These increases are mediated by altered pharmacomechanical coupling specific to this agonist, despite a reduction in the cell surface TP-R receptor population. Myocyte thromboxane hyperresponsiveness persists in culture after removal from the initiating hypoxic stimulus, suggesting an alteration at the level of gene expression. We infer that pulmonary thromboxane production, in response hypoxia, or to inflammatory stimuli including ventilator-induced trauma, may further potentiate neonatal hypoxic vasoconstriction, and cause pulmonary circuit vasospasm even after resolution of hypoxia in PPHN.

ACKNOWLEDGEMENTS

This research was funded in part by The Winnipeg Rh Foundation Institute and Manitoba Medical Services Foundation.

REFERENCES

1. **Ay B, Prakash YS, Pabelick CM, and Sieck GC.** Store-operated Ca^{2+} entry in porcine airway smooth muscle. *Am J Physiol Lung Cell Mol Physiol* 286: L909-917, 2004.

2. **Badesch DB, Orton EC, Zapp LM, Westcott JY, Hester J, Voelkel NF, and Stenmark KR.** Decreased arterial wall prostaglandin production in neonatal calves with severe chronic pulmonary hypertension. *Am J Respir Cell Mol Biol* 1: 489-498, 1989.

3. **Bolla M, You D, Loufrani L, Levy BI, Levy-Toledano S, Habib A, and Henrion D.** Cyclooxygenase involvement in thromboxane-dependent contraction in rat mesenteric resistance arteries. *Hypertension* 43: 1264-1269, 2004.

4. **Bonnet S, Belus A, Hyvelin JM, Roux E, Marthan R, and Savineau JP.** Effect of chronic hypoxia on agonist-induced tone and calcium signaling in rat pulmonary artery. *Am J Physiol Lung Cell Mol Physiol* 281: L193-201, 2001.

5. **Bonnet S, Dubuis E, Vandier C, Martin S, Marthan R, and Savineau JP.** Reversal of chronic hypoxia-induced alterations in pulmonary artery smooth muscle electromechanical coupling upon air breathing. *Cardiovasc Res* 53: 1019-1028, 2002.

6. **Bonnet S, Savineau JP, Barillot W, Dubuis E, Vandier C, and Bonnet P.** Role of $Ca^{(2+)}$-sensitive $K^{(+)}$ channels in the remission phase of pulmonary hypertension in chronic obstructive pulmonary diseases. *Cardiovasc Res* 60: 326-336, 2003.

7. **Cogolludo A, Moreno L, Bosca L, Tamargo J, and Perez-Vizcaino F.** Thromboxane A2-induced inhibition of voltage-gated K^+ channels and pulmonary vasoconstriction: role of protein kinase Czeta. *Circ Res* 93: 656-663, 2003.

8. **Coker RK and Laurent GJ.** Pulmonary fibrosis: cytokines in the balance. *Eur Respir J* 11: 1218-1221, 1998.

9. **Dakshinamurti S.** Pathophysiologic mechanisms of persistent pulmonary hypertension of the newborn. *Pediatr Pulmonol* 39: 492-503, 2005.

10. **Dakshinamurti S, Mellow L, and Stephens NL.** Regulation of Pulmonary Arterial Myosin Phosphatase Activity in Neonatal Circulatory Transition and in Hypoxic Pulmonary Hypertension: A Role For CPI-17. *Pediatr Pulmonol* (in press), 2005.

11. **de Beaufort AJ, Bakker AC, van Tol MJ, Poorthuis BJ, Schrama AJ, and Berger HM.** Meconium is a source of pro-inflammatory substances and can induce cytokine production in cultured A549 epithelial cells. *Pediatr Res* 54: 491-495, 2003.

12. **Dipp M, Nye PC, and Evans AM.** Hypoxic release of calcium from the sarcoplasmic reticulum of pulmonary artery smooth muscle. *Am J Physiol Lung Cell Mol Physiol* 281: L318-325, 2001.

13. **Dogan S, Turnbaugh D, Zhang M, Cofie DQ, Fugate RD, and Kem DC.** Thromboxane A2 receptor mediation of calcium and calcium transients in rat cardiomyocytes. *Life Sci* 60: 943-952, 1997.

14. **Dorn GW, 2nd and Becker MW.** Thromboxane A2 stimulated signal transduction in vascular smooth muscle. *J Pharmacol Exp Ther* 265: 447-456, 1993.

15. **Drummond RM and Wadsworth RM.** Contraction of the sheep middle cerebral, pulmonary and coronary arteries initiated by release of intracellular calcium. *J Auton Pharmacol* 14: 109-121, 1994.

16. **Ermert M, Kuttner D, Eisenhardt N, Dierkes C, Seeger W, and Ermert L.** Cyclooxygenase-2-dependent and thromboxane-dependent vascular and bronchial

responses are regulated via p38 mitogen-activated protein kinase in control and endotoxin-primed rat lungs. *Lab Invest* 83: 333-347, 2003.

17. **Fantozzi I, Zhang S, Platoshyn O, Remillard CV, Cowling RT, and Yuan JX.** Hypoxia increases AP-1 binding activity by enhancing capacitative Ca^{2+} entry in human pulmonary artery endothelial cells. *Am J Physiol Lung Cell Mol Physiol* 285: L1233-1245, 2003.

18. **Fike CD and Kaplowitz MR.** Effect of chronic hypoxia on pulmonary vascular pressures in isolated lungs of newborn pigs. *J Appl Physiol* 77: 2853-2862, 1994.

19. **Fike CD, Kaplowitz MR, and Pfister SL.** Arachidonic acid metabolites and an early stage of pulmonary hypertension in chronically hypoxic newborn pigs. *Am J Physiol Lung Cell Mol Physiol* 284: L316-323, 2003.

20. **Fike CD, Pfister SL, Kaplowitz MR, and Madden JA.** Cyclooxygenase contracting factors and altered pulmonary vascular responses in chronically hypoxic newborn pigs. *J Appl Physiol* 92: 67-74, 2002.

21. **Fredberg JJ.** Bronchospasm and its biophysical basis in airway smooth muscle. *Respir Res* 5: 2, 2004.

22. **Fu X, Gong MC, Jia T, Somlyo AV, and Somlyo AP.** The effects of the Rho-kinase inhibitor Y-27632 on arachidonic acid-, GTPgammaS-, and phorbol ester-induced Ca2+-sensitization of smooth muscle. *FEBS Lett* 440: 183-187, 1998.

23. **Goldman AP, Tasker RC, Haworth SG, Sigston PE, and Macrae DJ.** Four patterns of response to inhaled nitric oxide for persistent pulmonary hypertension of the newborn. *Pediatrics* 98: 706-713, 1996.

24. **Grynkiewicz G, Poenie M, and Tsien RY.** A new generation of Ca^{2+} indicators with greatly improved fluorescence properties. *J Biol Chem* 260: 3440-3450, 1985.

25. **Habib A, FitzGerald GA, and Maclouf J.** Phosphorylation of the thromboxane receptor alpha, the predominant isoform expressed in human platelets. *J Biol Chem* 274: 2645-2651, 1999.

26. **Hall SM, Hislop AA, Wu Z, and Haworth SG.** Remodelling of the pulmonary arteries during recovery from pulmonary hypertension induced by neonatal hypoxia. *J Pathol* 203: 575-583, 2004.

27. **Hammerman C, Komar K, and Abu-Khudair H.** Hypoxic vs septic pulmonary hypertension. Selective role of thromboxane mediation. *Am J Dis Child* 142: 319-325, 1988.

28. **Hellstrand P and Nordstrom I.** Cross-bridge kinetics during shortening in early and sustained contraction of intestinal smooth muscle. *Am J Physiol* 265: C695-703, 1993.

29. **Hill PB, Dora KA, Hughes AD, and Garland CJ.** The involvement of intracellular $Ca^{(2+)}$ in 5-HT(1B/1D) receptor-mediated contraction of the rabbit isolated renal artery. *Br J Pharmacol* 130: 835-842, 2000.

30. **Himpens B, Kitazawa T, and Somlyo AP.** Agonist-dependent modulation of Ca^{2+} sensitivity in rabbit pulmonary artery smooth muscle. *Pflugers Arch* 417: 21-28, 1990.

31. **Janiak R, Wilson SM, Montague S, and Hume JR.** Heterogeneity of calcium stores and elementary release events in canine pulmonary arterial smooth muscle cells. *Am J Physiol Cell Physiol* 280: C22-33, 2001.

32. **Jiang MJ, Chan CF, and Chang YL.** Intracellular calcium and myosin light chain phosphorylation during U46619-activated vascular contraction. *Life Sci* 54: 2005-2013, 1994.

33. **Kang TM, Park MK, and Uhm DY.** Characterization of hypoxia-induced $[Ca^{2+}]_i$ rise in rabbit pulmonary arterial smooth muscle cells. *Life Sci* 70: 2321-2333, 2002.

34. **Ko FN.** Low-affinity thromboxane receptor mediates proliferation in cultured vascular smooth muscle cells of rats. *Arterioscler Thromb Vasc Biol* 17: 1274-1282, 1997.

35. **Kurata R, Takayanagi I, and Hisayama T.** Eicosanoid-induced Ca^{2+} release and sustained contraction in $Ca^{(2+)}$-free media are mediated by different signal transduction pathways in rat aorta. *Br J Pharmacol* 110: 875-881, 1993.

36. **Lakshminrusimha S and Steinhorn RH.** Pulmonary vascular biology during neonatal transition. *Clin Perinatol* 26: 601-619, 1999.

37. **Lei Y, Zhen J, Ming XL, and Jian HK.** Induction of higher expression of IL-beta and TNF-alpha, lower expression of IL-10 and cyclic guanosine monophosphate by pulmonary arterial hypertension following cardiopulmonary bypass. *Asian J Surg* 25: 203-208, 2002.

38. **Liu F, Wu JY, Beasley D, and Orr JA.** TxA2-induced pulmonary artery contraction requires extracellular calcium. *Respir Physiol* 109: 155-166, 1997.

39. **McLeod KA, Gerlis LM, and Williams GJ.** Morphology of the elastic pulmonary arteries in pulmonary hypertension: a quantitative study. *Cardiol Young* 9: 364-370, 1999.

40. **Miyagi Y, Kobayashi S, Nishimura J, Fukui M, and Kanaide H.** Resting load regulates cytosolic calcium-force relationship of the contraction of bovine cerebrovascular smooth muscle. *J Physiol* 484 (Pt 1): 123-137, 1995.

41. **Murray R and FitzGerald GA.** Regulation of thromboxane receptor activation in human platelets. *Proc Natl Acad Sci U S A* 86: 124-128, 1989.

42. **Nakayama DK, Motoyama EK, Evans R, and Hannakan C.** Relation between arterial hypoxemia and plasma eicosanoids in neonates with congenital diaphragmatic hernia. *J Surg Res* 53: 615-620, 1992.

43. **Olschewski A, Hong Z, Nelson DP, and Weir EK.** Graded response of K^+ current, membrane potential, and $[Ca^{2+}]_i$ to hypoxia in pulmonary arterial smooth muscle. *Am J Physiol Lung Cell Mol Physiol* 283: L1143-1150, 2002.

44. **Parameswaran K, Janssen LJ, and O'Byrne PM.** Airway hyperresponsiveness and calcium handling by smooth muscle: a "deeper look". *Chest* 121: 621-624, 2002.

45. **Peacock AJ, Scott P, Plevin R, Wadsworth R, and Welsh D.** Hypoxia enhances proliferation and generation of IP3 in pulmonary artery fibroblasts but not in those from the mesenteric circulation. *Chest* 114: 24S, 1998.

46. **Porter VA, Reeve HL, and Cornfield DN.** Fetal rabbit pulmonary artery smooth muscle cell response to ryanodine is developmentally regulated. *Am J Physiol Lung Cell Mol Physiol* 279: L751-757, 2000.

47. **Reynolds PR, Mucenski ML, Le Cras TD, Nichols WC, and Whitsett JA.** Midkine is regulated by hypoxia and causes pulmonary vascular remodeling. *J Biol Chem* 279: 37124-37132, 2004.

48. **Robertson TP, Aaronson PI, and Ward JP.** Ca^{2+} sensitization during sustained hypoxic pulmonary vasoconstriction is endothelium dependent. *Am J Physiol Lung Cell Mol Physiol* 284: L1121-1126, 2003.

49. **Saetre T, Hoiby EA, Aspelin T, Lermark G, and Lyberg T.** Acute serogroup A streptococcal shock: A porcine model. *J Infect Dis* 182: 133-141, 2000.

50. **Shimoda LA, Sham JS, Shimoda TH, and Sylvester JT.** L-type $Ca^{(2+)}$ channels, resting $[Ca^{(2+)}]_{(i)}$, and ET-1-induced responses in chronically hypoxic pulmonary myocytes. *Am J Physiol Lung Cell Mol Physiol* 279: L884-894, 2000.

51. **Soukka H, Viinikka L, and Kaapa P.** Involvement of thromboxane A2 and prostacyclin in the early pulmonary hypertension after porcine meconium aspiration. *Pediatr Res* 44: 838-842, 1998.

52. **Takahashi N, Takeuchi K, Abe T, Sugawara A, and Abe K.** Immunolocalization of rat thromboxane receptor in the kidney. *Endocrinology* 137: 5170-5173, 1996.

53. **Toyofuku K, Nishimura J, Kobayashi S, Nakano H, and Kanaide H.** Effects of U46619 on intracellular Ca^{2+} concentration and tension in human umbilical artery. *Am J Obstet Gynecol* 172: 1414-1421, 1995.

54. **Tozzi CA, Christiansen DL, Poiani GJ, and Riley DJ.** Excess collagen in hypertensive pulmonary arteries decreases vascular distensibility. *Am J Respir Crit Care Med* 149: 1317-1326, 1994.

55. **Tulloh RM, Hislop AA, and Haworth SG.** Role of NO in recovery from neonatal hypoxic pulmonary hypertension. *Thorax* 54: 796-804, 1999.

56. **Vallot O, Combettes L, and Lompre AM.** Functional coupling between the caffeine/ryanodine-sensitive Ca^{2+} store and mitochondria in rat aortic smooth muscle cells. *Biochem J* 357: 363-371, 2001.

57. **Walsh-Sukys MC, Tyson JE, Wright LL, Bauer CR, Korones SB, Stevenson DK, Verter J, Stoll BJ, Lemons JA, Papile LA, Shankaran S, Donovan EF, Oh W, Ehrenkranz RA, and Fanaroff AA.** Persistent pulmonary hypertension of the newborn in the era before nitric oxide: practice variation and outcomes. *Pediatrics* 105: 14-20, 2000.

VI. MANUSCRIPT II

THROMBOXANE HYPERSENSITIVITY IN HYPOXIC PULMONARY ARTERY MYOCYTES: ALTERED TP RECEPTOR LOCALIZATION AND KINETICS

Martha Hinton [1,3], Alex Gutsol [3], Shyamala Dakshinamurti [1,2,3]

Departments of Physiology [1] and Pediatrics [2], University of Manitoba

Biology of Breathing Group [3], Manitoba Institute of Child Health

715 McDermott Ave, Winnipeg, Canada R3E 3P4

Am J Physiol Lung Cell Mol Physiol epub ahead of print, (Nov 3, 2006).doi:10.1152/ ajplung.00229.2006

ABSTRACT

Hypoxia-induced PPHN is characterized by sustained vasospasm and increased thromboxane: prostacyclin ratio. We previously demonstrated that moderate hypoxia induces myocyte thromboxane hypersensitivity. Here, we examined thromboxane prostanoid receptor (TP-R) localization and kinetics following hypoxia to determine the mechanism of hypoxia-induced TxA hypersensitivity. Primary cultured neonatal pulmonary artery myocytes were exposed to 10% O_2 (HM) or 21% O_2 (NM) for 3 days. PPHN was induced in neonatal piglets by *in vivo* exposure to F_iO_2 10% for 3 days. TP-R was studied in whole lung sections from pigs with hypoxic-PPHN and age-matched controls; intracellular localization was studied by immunocytochemistry. TP-R affinity was studied in cultured myocytes by saturation binding kinetics using [H^3]-SQ29548 and competitive binding kinetics by co-incubation with U46619. Phosphorylation and coupling were examined in immunoprecipitated TP-R. We report distal propagation of TP-R expression in PPHN, extending to pulmonary arteries <50μm. In HM, intracellular TP-R moves towards the perinuclear region, mirroring a change in ER morphology. TP-R kinetics also alter in HM membranes, with decreased K_d and B_{max}. Additionally, in hypoxia [H^3]-SQ29548 is displaced at lower concentration of U46619 than in normoxia, suggesting increased agonist affinity. Phosphorylation of serine residues on HM TP-R was significantly decreased compared to NM; this difference correlated with increased Gαq coupling in hypoxia, and was ablated by incubation with PKA. We conclude that the TP-R is normally desensitized in the neonatal pulmonary circuit by PKA-mediated regulatory phosphorylation, decreasing ligand affinity and coupling to Gαq; this protection is lost following hypoxic exposure. Also, the appearance of TP-R in resistance

arteries after development of hypoxic PPHN may contribute to increased pulmonary arterial pressure.

KEY WORDS: smooth muscle, persistent pulmonary hypertension of the newborn, scatchard analysis, thromboxane

INTRODUCTION

At birth, the pulmonary circuit must reduce its high vascular resistance to accommodate an 8-10 fold increase in blood flow. This transition requires pulmonary inflation with oxygen, and active vasodilation by nitric oxide and prostacyclin (39). One of the most rapidly progressive and potentially fatal of the vasculopathies, neonatal persistent pulmonary hypertension (PPHN) has an incidence of up to 6.8 in 1000 live births (46). PPHN is caused in otherwise healthy term infants by interference of normal circulatory transition by perinatal hypoxia, inflammation or direct lung injury such as meconium aspiration (15), and is characterized by sustained vasospasm and chronic vascular remodelling (44). All etiologies of PPHN result in a critical decrease in tissue oxygen delivery (13). Approximately one third of patients meeting treatment criteria do not respond to therapeutic agents including inhaled nitric oxide, and in this subpopulation the disease is lethal, although rescue therapy with extracorporeal membranous oxygenation may limit mortality (8).

Hypoxic pulmonary vasoconstriction may be physiologically advantageous to bypass localized hypoventilated areas of lung. However, chronic alveolar hypoxia acts as a pro-inflammatory stimulus that rapidly induces macrophage recruitment, increases vascular permeability, enhances expression of many inflammatory mediators (24), and induces both proliferation (50) and constriction (34) in vascular smooth muscle. Hypoxic COX-2 upregulation is described in many species (23), as well as in human pulmonary arterial myocytes (52). In the neonatal piglet hypoxia model, altered arachidonic acid metabolism with an increased thromboxane: prostacyclin ratio is described early in the course of PPHN (6); this shift toward the inflammatory arachidonic acid metabolites

mediates increased pulmonary vasoconstriction. Hypoxia has a priming effect on pulmonary vascular smooth muscle agonist response, favouring myocyte contraction by increased inositol tri-phosphate (IP_3) generation to agonist (31).

The major endogenous molecules that regulate pulmonary vascular tone, and are pivotal in the perinatal period, include the nitric oxide (NO) - endothelin (ET-1), and prostacyclin (PGI_2) - thromboxane (TxA) axes (48). A shift in the NO-endothelin ratio away from production of the vasorelaxant NO, due to decreased endothelial NO synthase expression, has been shown to contribute to the development of PPHN (43). In addition, an increased TxA: PGI_2 ratio, due to decreased PGI_2 synthase production, has been described in a hypoxic model of PPHN (6). TxA is a constrictor prostanoid, produced via the arachidonic acid pathway in response to oxidative stress and pro-inflammatory stimuli, and is known to be crucial in mediating septic pulmonary hypertension in the neonate (5, 12). Cyclooxygenase pathway metabolites are implicated in increased pulmonary vascular tone, contributing to the early pulmonary hypertensive response in meconium aspiration (36) and sepsis (12). We have previously shown that neonatal pulmonary artery myocytes exposed to a moderate level of hypoxia have hypersensitive and hyperresponsive peak $[Ca^{2+}]_i$ responses to the thromboxane agonist U46619, despite a reduction in cell surface TxA prostanoid receptor (TP-R) expression (16); this heightened response persists long after removal from hypoxia.

TxA binds to the TP-R, which is a member of the G protein coupled receptor (GPCR) superfamily (19). Differential splicing of the TP-R C-terminal tail gives rise to the two known isoforms of TP-R, α and β. Both isoforms of TP-R couple to Gαq but alternatively regulate adenylate cyclase through activation by TP-Rα or inhibition by TP-

Rβ (17). Signalling through Gαq leads to activation of phospholipase C, which produces diacyl glycerol and IP_3 (28). Altered redox state of the TP-R has been shown to regulate receptor number and affinity in platelet membranes (4) and transfected cells (42). Covalent modification by phosphorylation of the TP-R alters its activity state, with phosphorylation leading to desensitization and dephosphorylation resulting in resensitization (37).

The left-shift in the TxA dose-response curve observed following moderate hypoxic exposure suggests a probable change in TP-R kinetics, involving alteration of either receptor abundance or affinity. While GPCRs are most commonly upregulated by increasing receptor abundance, the mechanism of hypoxia-induced TxA hypersensitivity in the neonatal pulmonary circuit has not been previously studied. In this study, we examine TP-R localization following exposure to moderate hypoxia *in vivo* and *in vitro*, and detailed receptor-ligand kinetics in myocytes after *in vitro* hypoxia. We hypothesize that the hypersensitive TxA response observed following moderate hypoxic exposure is due to an increased affinity of the TP-R for agonist, and that *in vivo* TP-R localization in the pulmonary arterial circuit is altered following development of PPHN.

METHODS

Animal Model and Induction of Neonatal Persistent Pulmonary Hypertension

All primary cell cultures were derived from newborn piglets (< 24hours old; n=13) that were sacrificed on the day of arrival from a pathogen-free farm supplier. Lung tissue for histological analysis was obtained from pigs with hypoxia-induced PPHN (n=4) or from age-matched controls (n=4). The *in vivo* hypoxic model has been previously

described (7). Briefly, newborn piglets were placed in a normobaric hypoxic chamber (FiO_2 0.10, achieved by a mixture of room air with N_2) for 3 days, in accordance with CCAC guidelines. All piglets were euthanized by pentobarbital overdose and exsanguination. Heart and lungs were removed en bloc and placed in oxygenated, cold (4°C) Ca^{2+}-free Krebs-Henseleit physiological buffer (containing in mM: 112.6 NaCl, 25 $NaHCO_3$, 1.38 NaH_2PO_4, 4.7 KCl, 2.46 $MgSO_4 \cdot 7H_2O$, 5.56 Dextrose; pH 7.4). Right ventricular afterloading was determined by relative cardiac weight ratio (blotted tissue weight, right ventricle to left ventricle plus septum) to diagnose development of PPHN (16).

Immunohistochemistry

Lung tissue was paraffin-embedded, and cut into 5μm sections, which were then de-paraffinated in xylene for 20 min followed by stepwise re-hydration in ethanol solutions. Formalin crosslinks were removed by boiling sections in a 5mM sodium citrate and 2mM citric acid solution. Non-specific antibody binding was blocked by pre-incubation with 10% donkey serum in Cyto-TBS+1%BSA (containing in mM; 20 Tris base, 154 NaCl, 2 EGTA, 2 $MgCl_2$; pH 7.4) for 20 min at room temperature in a humidified chamber. Sections were then incubated with rabbit-anti-TP-R antibody (Chemicon International) and mouse-anti-myosin heavy chain antibody (used to visualize small arteries; Abcam, Cambridge, MA) overnight at 4°C, followed by incubation with FITC-conjugated donkey anti-rabbit antibody and Cy3-conjugated donkey anti-mouse antibody. Sections were then mounted with antifade and visualized by fluorescent microscopy. Intensity of TP-R immunohistochemical staining was quantified in all images, employing a constant region of interest radius method. Regions of interest were

chosen randomly, with each region consisting of a constant radius. 20 regions of interest were measured per artery, and the mean intensity was determined. For comparison between treatment groups, the mean TP-R intensity was gathered from at least 10 arteries. The luminal surface of all arteries was excluded from analysis, to avoid interference signal from platelets.

Cell Culture

Pulmonary artery smooth muscle cells (PASMC) were obtained from newborn pigs using a dispersed cell culture method selective for myocytes (35). 3rd to 6th generation pulmonary arteries were obtained by microdissection into Ca^{2+}- free Krebs-Henseleit physiological buffer and were allowed to recover in cold HEPES-buffered saline solution (HBS; composition in mM: 130 NaCl, 5 KCl, 1.2 $MgCl_2$, 1.5 $CaCl_2$, 10 HEPES, 10 glucose; pH 7.4) supplemented with an antibiotic/antimycotic mixture and gentamicin. Arteries were then washed twice with Ca^{2+}-reduced HBS (20μM $CaCl_2$), and finely minced. Arterial tissue was transferred to a digestion solution containing Ca^{2+}-reduced HBS, type I collagenase (1750 U/ml), dithiothreitol (1mM), bovine serum albumin (BSA; 2mg/ml), and papain (9.5 U/ml) for 15 min at 37°C with gentle agitation. Dispersed PASMC were collected by centrifugation at 1200 RPM for 5min, washed in Ca^{2+}-free HBS to remove digestion solution, and then re-suspended in culture medium.

The cells were plated at a density of 4.4 x 10^4 cells/cm^2, in Hams F-12 medium with L-glutamine supplemented with 10% fetal calf serum, 1% penicillin, and 1% streptomycin. Cells were serum-deprived for 2 days once they reached confluence (in Hams F-12 medium with L-glutamine/penicillin/streptomycin and 1% insulin-transferrin-selenium) in order to synchronize cells in a contractile phenotype, then split into two

groups for the final 3 days of culture; (i) control normoxic myocytes (NM), maintained serum-free in 21% O_2, 5% CO_2 and, (ii) hypoxic myocytes (HM), maintained serum-free in 10% O_2, 5% CO_2 for 3 days to mimic the extent and duration of the *in vivo* O_2 exposure.

Immunocytochemistry

PASMCs were fixed with 3% paraformaldehyde for 15 minutes at room temperature followed by permeabilization with 0.3% Triton X-100 for 5 min. Cells were rinsed twice with CB Buffer (containing in mM; 10 MES, 150 NaCl, 5 EGTA, 5 $MgCl_2$, 5 glucose) and stored in Cyto-TBS at 4°C. Non-specific binding was blocked by incubation with 10% normal donkey serum in Cyto-TBS+1%BSA for 20min at room temperature. PASMCs were then incubated with TP-R rabbit polyclonal antibody (Cayman Chemicals, Ann Arbor, MI) overnight at 4°C, followed by incubation with FITC-conjugated donkey anti-rabbit antibody for 2 hours at room temperature. Coverslips were co-incubated with either mouse-anti-Golgin-97 (a golgi-apparatus specific marker; Molecular Probes, Eugene, OR) or mouse-anti-protein disulfide isomerase (PDI; an endoplasmic reticulum specific marker; Stressgen Bioreagents, Victoria, B.C.) which was followed by co-incubation with Cy3-conjugated donkey anti-mouse antibody. Nuclei were counterstained with Hoechst 33342.

Fluorescence immunocytochemistry images were acquired using an Olympus 1X 70 microscope with an UltraPix FSI digital camera and analyzed with UltraView software (PerkinElmer).

RT-PCR

RNA was extracted from frozen PASMCs using TRIzol (Invitrogen) according to the manufacturer's instructions. Briefly, cells were homogenized in TRIzol reagent. Chloroform was added and samples were centrifuged at 12000xg for 15min at 4°C. The resulting aqueous solution was incubated in isopropyl alcohol for 10min at 30°C. The RNA pellet was isolated by centrifuging at 8000xg for 10min at 4°C and washed with 75% ethanol. RNA was redissolved in DEPC-treated water at 55°C for 30min. RNA purity was determined using a spectrophotometer. 2 μg of total RNA was reverse transcribed using the Omniscript RT kit (Qiagen) in a total reaction volume of 20 μl in the presence of 1 μg Oligo(dT)15 primers (Promega) and 10 U RNasin ribonuclease inhibitor (Promega) following the manufacturer's instructions.

TP-R primers were used as previously published (1); sense primer 5'-^{331}CTGGTCCTCACCGACTTCCT^{350}-3', antisense primer 5'-^{525}GATACCCAGG TAGCGCTCTG^{506}-3' for an estimated product size of 200 base pairs. The reaction mixture contained; 10x PCR Buffer (2.5μl), 10mM dNTP (0.5μl), 50mM $MgCl_2$ (0.75μl), 10μM sense primer (0.5μl), 10μM antisense primer (0.5μl), platinum Taq (0.125μl), water (18.125μl), and 2μl sample cDNA. PCR amplifications were carried out using a Techne Genius Unit with the following conditions; denaturation and enzyme activation at 94°C for 5 min, a total of 40 amplification cycles consisting of a 30 sec denaturation at 94°C, 30sec annealing step starting at 60°C then decreasing by 0.5°C increments per cycle until 52°C, followed by a 30 sec extension at 72°C. The final extension was at 72°C for 5 min.

Pig GAPDH primers used were previously published (40); sense primer 5'-TTCCACGGCACAGTCAA-3', antisense primer 5'-GCAGGTCAGGTCCACAA-3', for

an estimated product size of 576 base pairs. The reaction mixture contained; 10x PCR buffer (3.75µl), 10mM dNTP (1µl), 2.5µM sense primer (0.5µl), 2.5µM antisense primer (0.5µl), water (18.125µl), platinum Taq (0.125µl) and 1µl of sample cDNA. PCR amplifications were carried out in the following conditions; denaturation and enzyme activation for 5 min at 95°C, 33 amplification cycles consisting of 30sec denaturation at 94°C, 45 sec annealing phase at 55°C, and 45 sec extension phase at 72°C, with final extension held for 5 min.

PCR products were separated by 1% agarose gel electrophoresis and visualized with GelStar. Bands were analyzed by densitometry, with TP-R normalized to GAPDH.

Thromboxane Receptor Kinetics

PASMCs were rinsed free of culture medium with PBS. Whole cell lysates were obtained by scraping cells in Binding Buffer (containing in mM: 25 Tris, 10 $CaCl_2$, 0.01 indomethacin; pH 7.4) and 75µg/ml PMSF. Unlysed cells and large particulate matter were separated by centrifugation at 1000xg for 5 min and discarded. The supernatant was ultracentrifuged at 75000xg for 60min at 4°C, after which the membrane fraction was resuspended in Binding Buffer. Protein concentration in the membrane fraction was measured using the Biorad method. 100µg membrane protein was used for all radioligand experiments.

Saturation Binding Kinetics. Samples were incubated with [H^3]-SQ29548 ranging from 0nM to 70nM (diluted in Binding Buffer) in 100µl total reaction volume for 1 hour at room temperature. Reactions were terminated by vacuum filtration and membranes were washed twice with ice cold Binding Buffer. Filters were agitated in 500µl ddH_20 to release absorbed radioisotope and were allowed to equilibrate in 5 ml

CytoScint (ICN) for at least 5 hours before counting. Unbound radioisotope was also collected. CPM were analyzed for 10 min per sample.

Competitive Binding Analysis. The molecule used to study TP-R saturation kinetics was an antagonist, but the desired receptor-ligand interaction for study involved the agonist, which may have a different binding site or conformation on the TP receptor than the antagonist, and thus very different kinetics. Accordingly, competitive binding analyses were carried out against both the unlabelled SQ29548 (a TP-R antagonist) and U46619 (a TP-R agonist). Membrane samples were incubated with 10nM [H^3]-SQ29548 and unlabelled ligand ranging in concentration from 0.1nM to 100μM for 1 hour at room temperature.

Immunoprecipitation

Whole cell lysates were collected in RIPA Buffer modified for phospho-protein analysis (containing in mM; 20 MOPS, 2 EGTA, 5 EDTA, 30 sodium fluoride, 40 beta-glycerophosphate, 10 sodium pyrophosphate, 2 sodium orthovanadate , 1 phenyl-methyl-sulfonylfluoride (PMSF), 3 benzamidine, 0.005 pepstatin A, 0.01 leupeptin). A 50% slurry of Protein G Sepharose beads was prepared in lysis buffer (containing in mM; 50 Tris, 150 NaCl, 1 EDTA, 1 PMSF, and 1 %Triton-X; pH 7.4). 500μg of lysate was then pre-cleared by incubation with 35μl of 50% bead slurry in a total volume of 250μl. Beads were isolated by centrifugation at 16000xg for 5 min. The pre-cleared lysate was then added to 2μg rabbit-TP-R antibody (Cayman Chemicals, Ann Arbor, MI) overnight at 4°C. 30μl of 50% bead slurry was then added to pull down the immunoprecipitate. Beads were washed with lysis buffer and boiled in Laemmli Buffer for 10 min; the protein derived was separated by SDS-PAGE and probed with mouse-anti-phospho-

serine antibody (Qiagen) and rabbit-anti-Gαq antibody (Santa Cruz Biotechnology). To determine the signalling pathway involved in hypoxia-induced TP-R desensitization, PASMCs were incubated with 1μM PMA (phorbol 12-myristate 13-acetate; a PKC activator), 10μM forskolin (a PKA activator) for the final 3 days of culture. In a separate experiment, 1μM GTPγS (a stable GTP analog) was added to lysates during antigen-antibody incubation, to maximize receptor active state conformation. TP-R phosphorylation on serine residues was then studied in all groups, as described above.

Live Cell Calcium Mobilization

Live cell calcium imaging was carried out as previously described (16). Control PASMCs or cells treated with 1μM PMA, 10μM forskolin or 1μM GTPγS (as described in *Immunoprecipitation*) were loaded with 5μM fura 2-AM (Molecular Probes)/DMSO in HBSS (containing in mM: 1.26 $CaCl_2$, 0.493 $MgCl_2 \cdot 6H_2O$, 0.407 $MgSO_4 \cdot 7H_2O$, 5.33 KCl, 0.441 KH_2PO_4, 4.17 $NaHCO_3$, 137.93 NaCl, 0.338 $NaHPO_2$, and 0.1% BSA) with 1.0 μg/ml pluronic acid as per manufacturer's instructions. Coverglass plates were secured on an inverted microscope (Olympus) in room air, and studied at 20x magnification. Real-time ratiometric imaging of intracellular calcium concentration used excitation wavelengths of 340 and 380 nm and an emission wavelength of 510 nm; data was captured by a charge-coupled device camera and Perkin Elmer software. Each recording consisted of a stable baseline and a response to 1μM U46619. PMA, forskolin and GTPγS were omitted during fura-2AM loading, but were present at the time of recording.

Statistical Analysis

All data are presented as mean ± SE and analyzed using an unpaired t-test, with $p<0.05$ considered significant.

RESULTS

Development of pulmonary hypertension was diagnosed by increased right ventricle to left ventricle plus septum weight ratio. Newborn piglets had a ratio of 0.709±0.108g, which decreased in control 3 day old pigs with a ratio of 0.573±0.221g. However, this ratio was elevated in 3 day animals with hypoxic PPHN (0.877±0.166g, different from 3 day normoxic controls, $p<0.05$), mainly due to an increase in right ventricular weight.

Immunohistochemical analysis of lung slices from pigs with hypoxic-PPHN and age-matched controls revealed that large arteries expressed similar levels of TP-R (Fig II.1A, B). However, in pulmonary arteries < 50μm in diameter, TP-R was not observed in control animals, while signal was detected in animals with hypoxic-PPHN (Fig II.1C). Quantification of TP-R intensity in the smaller calibre pulmonary arteries showed a statistically significant increase in TP-R intensity in lung slices from pigs with PPHN, with TP-R probe intensity from control arteries composed largely of background signal (Fig II.1D, $p<0.0001$).

We have previously demonstrated decreased cell surface immunostaining for TP-R and intracellular redistribution of TP-R following moderate hypoxic exposure (16). In this study, TP-R colocalization with golgin-97 (a marker for the golgi apparatus; Fig II.2B) was not different between HM and NM. However, the relocation of TP-R in HM to the perinuclear region seemed to mirror a shift in PDI signal (a marker for the

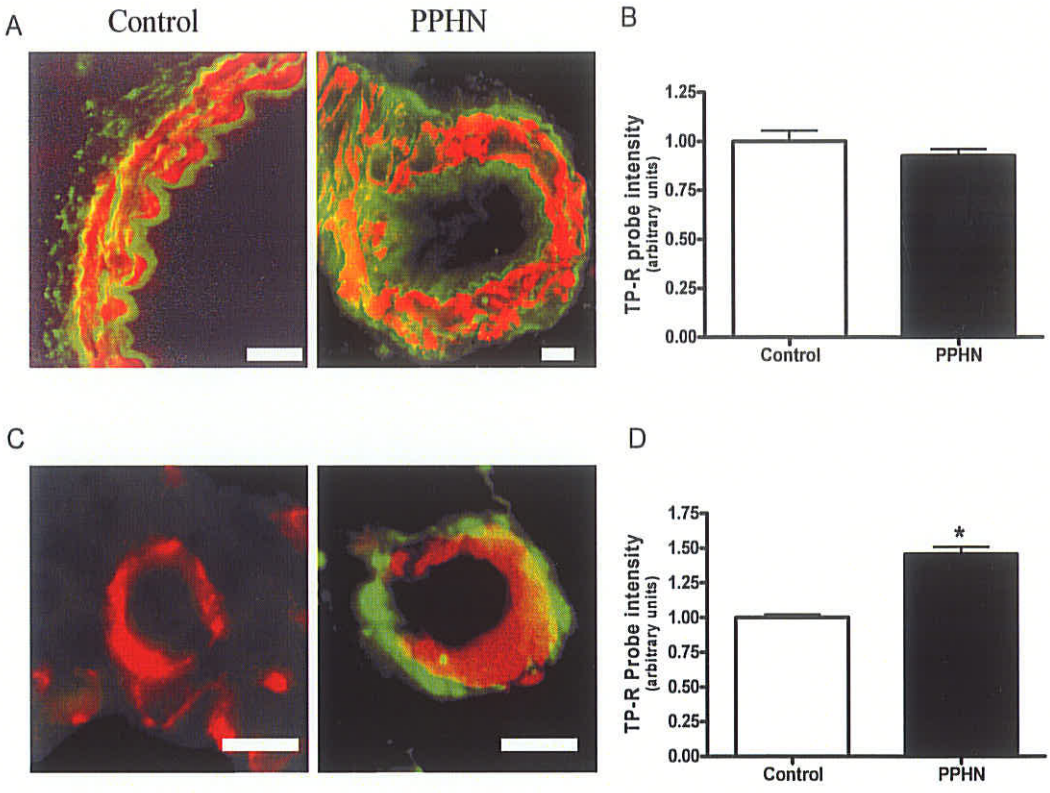

Figure II.1 Thromboxane receptor expression in large and small arteries

Representative pictures of paraffin embedded lung sections showing (A) arteries greater than 80 to 100μm in diameter and (C) arteries between 10 to 50μm in diameter from 3 day old control pigs and 3 day old pigs with hypoxia-induced PPHN co-labelled with mouse-anti-myosin heavy chain to identify arteries (red) and rabbit-anti-thromboxane receptor (green). The white bars represent 10μm for that picture. TP-R probe intensity was quantified in arbitrary units for large (B; n=10, p= not significant) and small pulmonary arteries (D; n=14, *; $p<0.0001$).

endoplasmic reticulum; Fig II.2A). Quantification of PDI signal showed that immunostaining intensity in the perinuclear region was increased in HM compared to NM (Fig II.2C; HM= 1.06 ± 0.01 arbitrary units, NM= 1.00 ± 0.01 arbitrary units, 25 equal regions selected per microscope field image, n=10, $p<0.0001$). Total cell area containing PDI signal, normalized to number of nuclei per image, was slightly, but not significantly, decreased (Fig II.2D; HM= 0.91 ± 0.03 arbitrary units, NM= 1.00 ± 0.07 arbitrary units, n= 10, $p>0.05$).

There was no significant difference in total TP-R expression as measured by RT-PCR in HM compared to NM, after normalization to GAPDH (Fig II.3).

Saturation binding experiments revealed a decrease in TP-R abundance in membrane fractions from HM compared to NM (Table II.1; NM B_{max}= 610.30 ± 270.60 fmol/mg, HM B_{max}= 150.80 ± 32.35 fmol/mg; $p< 0.001$). HM TP-R also had an increased affinity for the TP-R antagonist, SQ29548 (Table II.1; NM K_d= 72.97 ± 46.40 nM, HM K_d= 12.74 ± 7.72 nM; $p<0.03$).

Competitive binding experiments where unlabelled SQ29548 was used to displace [H^3]-SQ29548 binding indicated a significantly right-shifted dose-response curve in HM (Fig II.4A; NM $IC_{50} = 1.13x10^{-7} \pm 0.37$ M, HM $IC_{50} = 1.17x10^{-6} \pm 0.01$ M; $p<0.01$). Membrane fractions co-incubated with [H^3]-SQ29548 and the unlabelled TxA agonist U46619 revealed a significantly left-shifted binding curve for U46619 in HM (Fig II.4B; NM $IC_{50} = 5.47x10^{-9} \pm 0.22$ M, HM $IC_{50} = 4.66x10^{-10} \pm 0.18$ M; $p<0.005$).

We have previously reported that normoxic and hypoxic whole cell lysates have similar TP-R protein abundance (16). Analysis of whole cell TP-R immunoprecipitate with antibody to phospho-serine revealed that HM TP-R was significantly less

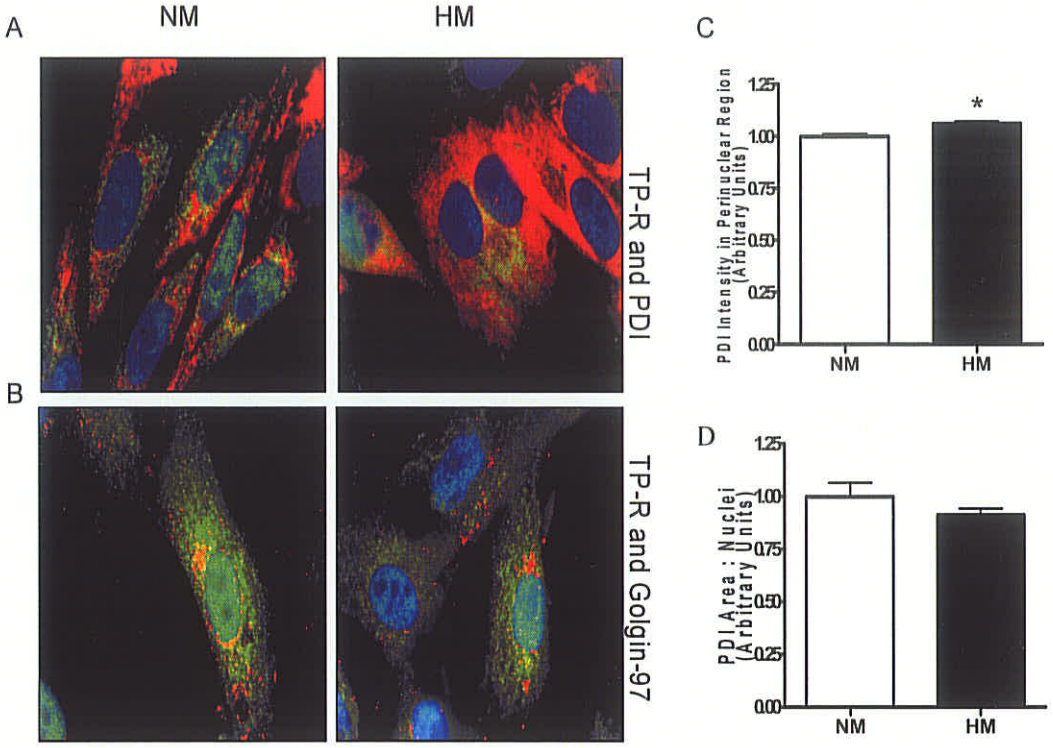

Figure II.2 Subcellular thromboxane receptor localization

Permeabolized PASMCs co-labelled with (A) rabbit-anti-TP-R (green) and mouse-anti-PDI (red) or, (B) rabbit-anti-TP-R (green) and mouse-anti-golgin-97 (red). Nuclei were stained with Hoechst (blue), images captured at 100X magnification. Analysis of peri-nuclear PDI intensity (C) and area normalized to number of nuclei (D) (*; $p<0.0001$, $n=10$ images).

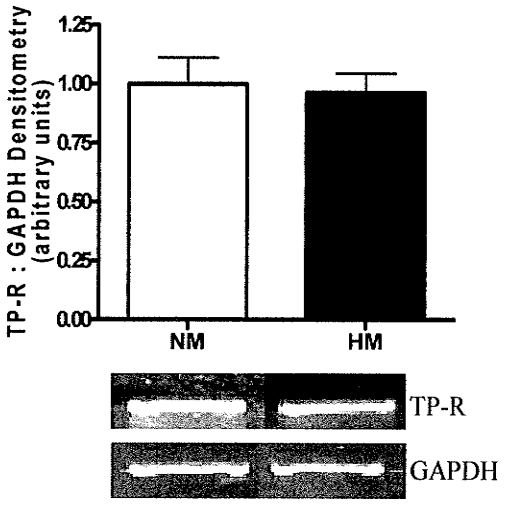

Figure II.3 Thromboxane receptor expression

Primers designed to examine TP-R expression, irrespective of isoform, were used for RT-PCR. Bands obtained were normalized to GAPDH expression. Expression levels were not significantly different between HM (n=5) and NM (n=5, p= not significant).

Table II.1 Thromboxane receptor saturation binding kinetics

[H^3]-SQ29548 dissociation constants (expressed in nM) and maximal binding sites (expressed as fmol/mg) values obtained from 3 different experiments (n=8). Values are represented as mean ± SE.

	K_D	B_{max}
NM	72.97 ± 46.40	610.30 ± 270.60
HM	12.74 ± 7.72 *	150.80 ± 32.35 **

*; $p<0.03$, **; $p<0.002$

A

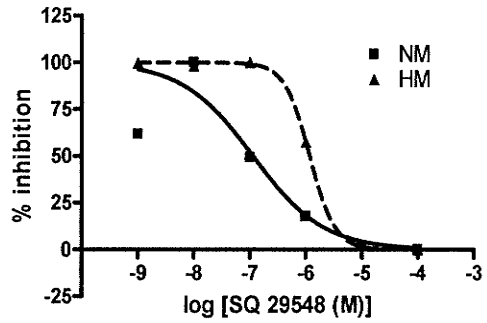

B

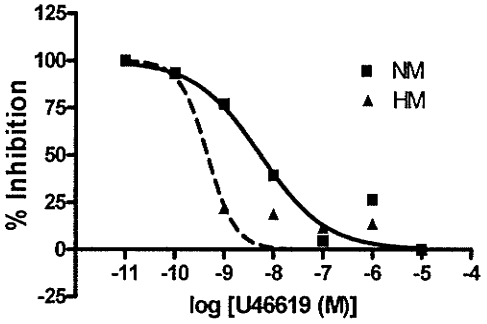

Figure II.4 Competitive binding kinetics

100µg of PASMC membrane was incubated with 10nM [H^3]-SQ29548 and a range of concentrations of (A) unlabelled TP-R antagonist, SQ29548 or (B) unlabelled TP-R agonist, U46619. The IC50 values were significantly different for HM and NM in both cases (A; $p<0.01$, B; $p<0.005$). Data obtained from cell lysates from 13 animals and experiments were performed 3 times.

phosphorylated relative to NM TP-R (Fig II.5A; $p<0.003$, $n=5$). Conversely, immunoblot of the TP-R immunoprecipitate with a Gαq antibody indicated a greater association of HM TP-R with Gαq than was the case for NM TP-R (Fig II.5B; $p<0.03$, $n=3$). The immunoprecipitates contained similar amounts of TP-R (Fig II.5C; $p>0.05$, $n=4$).

The elevated phosphorylation state of the NM TP-R compared to HM TP-R was maintained following immunoprecipitation in the presence of GTPγS, utilized to ensure maximal receptor activation (Fig II.6A, B; $p<0.03$, $n=3$). Incubation with PMA (a PKC activator) increased TP-R serine phosphorylation in the hypoxic group alone (Fig II.6A, B, $p<0.04$, $n=3$). However following incubation with forskolin (a PKA activator), there was a significantly higher level of phosphorylation of both NM and HM TP-R, ablating any difference in receptor phosphorylation between the two groups ($p>0.05$, $n=3$).

As previously observed, PASMC exposed to 10% O_2 for the final 3 days of culture resulted in an elevated peak $[Ca^{2+}]_i$ response to 1μM U46619 (16). Incubation of both HM and NM with GTPγS had no effect on peak calcium response to 1μM U46619 and the hypoxia-induced elevation in agonist response was maintained (Fig II.6C; NM= 1.088±0.224μM, HM= 2.142±0.155μM, $p<0.01$, $n=16$). The hyperresponsivness of the hypoxic myocytes was also maintained following incubation with PMA (Fig II.6C; NM= 1.177±0.185μM, HM= 2.253±0.228, $p<0.01$, $n=16$). In contrast, forskolin markedly inhibited the hypoxia-induced increase in peak calcium response to 1μM U46619 (Fig II. 6C; NM= 0.513±0.099μ, HM= 0.630±0.056μM, $p>0.05$).

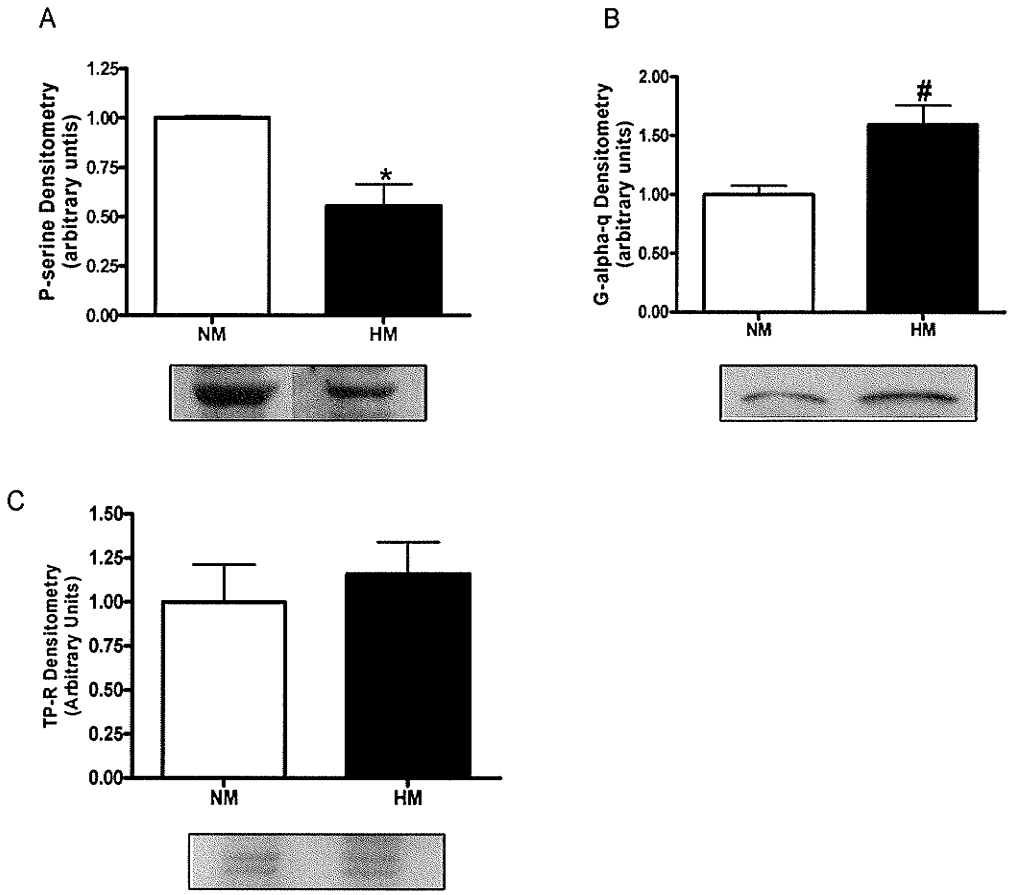

Figure II.5 Thromboxane receptor co-immunoprecipitation

The immunoprecipitate obtained by whole cell lysate incubation with a TP-R antibody was probed with (A) mouse-anti-phospho-serine antibody or (B) rabbit-anti-G-alpha-q antibody. HM had significantly less phosphorylated TP-R than NM (A; *; $p<0.003$, n=5), while HM TP-R associated significantly more with Gαq protein (B; #; $p<0.03$, n=3). (C) The relative amount of TP-R precipitated by whole lysate incubation was not significantly different between NM and HM (p= not significant, n=4).

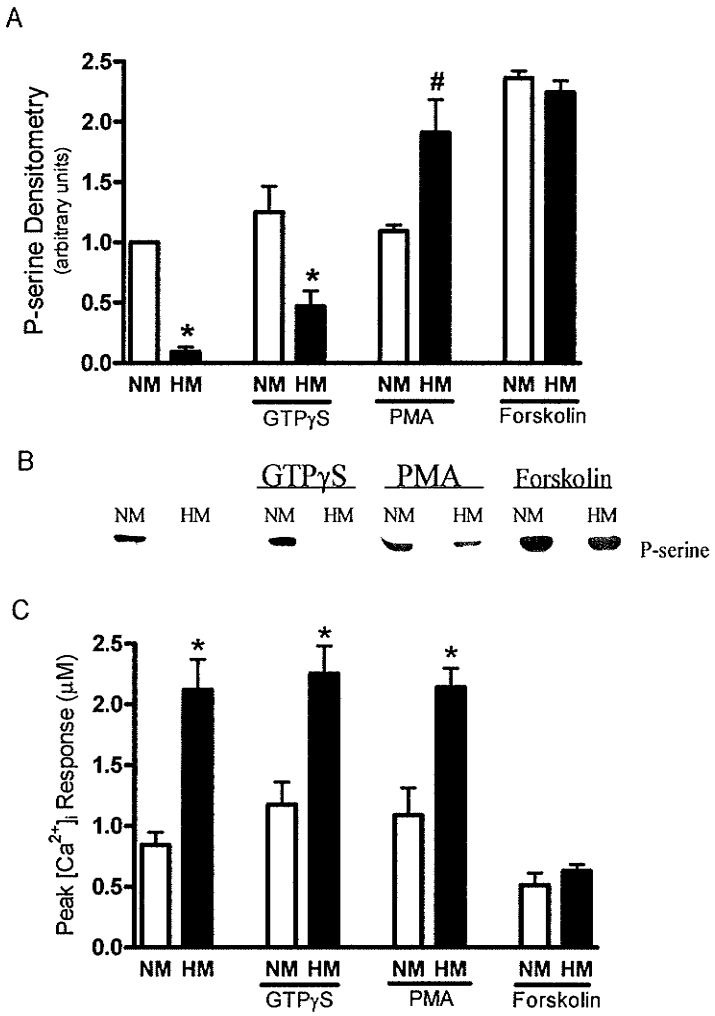

Figure II.6 Maximal G-protein activation, PKC and PKA regulation of thromboxane receptor

PASMCs were incubated with 1μM GTPγS, 1μM PMA or 10μM forskolin to study receptor phosphorylation and signalling. (A) TP-R phosphorylation on serine residues was studied on TP-R immunoprecipitate. HM TP-R was significantly less phosphorylated than NM TP-R under control and GTPγS conditions (*; $p<0.03$, $n=3$). HM TP-R was significantly more phosphorylated after treatment with PMA (#; $p<0.04$, $n=3$), and there was no significant difference following forskolin treatment (p= not significant, $n=3$). (B) Representative TP-R immunoprecipitate probed with mouse-anti-phospho-serine antibody. (C) Peak $[Ca^{2+}]_i$ response to 1μM U46619 measured using fura-2AM remained elevated in PASMC exposed to moderate hypoxia in the presence of GTPγS and PMA, but was ablated when incubated with forskolin (*; $p<0.01$, $n=16$).

DISCUSSION

In this study we examined the effect of moderate hypoxia on TP-R localization and kinetics in a neonatal pulmonary artery smooth muscle cell culture model of hypoxic pulmonary hypertension to determine the mechanism by which these cells become hypersensitive to a TxA agonist. We determined that TP-R localization is altered both in an *in vivo* model of hypoxia-induced PPHN, as well as in pulmonary artery myocytes exposed to moderate hypoxia *in vitro*. After whole animal hypoxia, TP-R appeared in smaller calibre pulmonary arteries where normally TP-R is not expressed. In hypoxic myocytes, there was an intracellular shift in TP-R distribution that followed a change in endoplasmic reticulum distribution. We also observed increased TP-R binding affinity, decreased receptor phosphorylation of serine residues, and an increased coupling to the Gαq protein in pulmonary arterial smooth muscle following hypoxic exposure. Lastly, we found that forskolin treatment increased TP-R phosphorylation in HM and reduced agonist-induced peak $[Ca^{2+}]_i$ response back to control levels.

In discussing these data, we acknowledge certain limitations in application of the *in vitro* hypoxia model to the pathophysiology of hypoxic PPHN *in vivo*. In previous studies, we have established that a comparable degree of TP receptor sensitization occurs under *in vitro* hypoxic exposure as *in vivo*. Our original cellular investigations of TP-R sensitization mechanisms dealt largely with primary cultured pulmonary arterial myocytes using *in vitro* hypoxia, as does the present study. Advantages of this approach include that the hypoxic exposure is proximal to the point of experimentation, while in our *in vivo* model, up to two weeks of normoxic cell culture intervened between exposure and experiment. When examining temporally sensitive effects of hypoxia on cell surface

receptor regulation, the use of serum-starved primary culture myocytes exposed to hypoxia immediately prior to experiment permits more mechanistic investigation, while still fairly representative of the myocyte population of the hypoxic pulmonary vascular wall.

Altered TP-R expression. An increase in TxA production, in conjunction with an increase in COX-2 abundance, has been described in the piglet model of hypoxia-induced PPHN (38). Others have reported an increase in TxA following septic induction of PPHN in the piglet (12). As well, TP-R activation, although not through action of TxA, has been shown to be involved in the increase in endothelin-1 in the rat model of neonatal PPHN (18). Altered receptor abundance for thromboxane has not been previously characterized in hypoxia. In this study, we observed an increase in TP-R expression in small calibre pulmonary arteries. The histology of end-stage pulmonary hypertension is well characterized by thickened vascular media and adventitia, hyperplasia and hypertrophy of the vascular smooth muscle layer and increased extracellular matrix deposition (26), impairing vascular dispensability (41), eventually resulting in a fixed and irreversible increase in pulmonary vascular resistance. *In vivo* hypoxia clearly also results in distal propagation of TP-R expression, such that 10-50μm diameter arteries accrue receptors capable of responding to circulating TxA. Thus whereas under normal conditions only pulmonary arteries 100μm in diameter or larger may be responsible for thromboxane agonist-induced vasoconstriction, after development of PPHN, smaller arteries become capable of contributing to agonist response and overall PA pressure. It should be noted that these immunohistochemistry data indicate whole cell TP-R expression, not cell surface expression, and the latter decreases under *in vitro* hypoxia.

Both control and hypoxic cultured pulmonary artery myocytes expressed TP-R, as indicated by RT-PCR. The pulmonary arteries microdissected for the primary culture preparation contained a mixture of larger and smaller vessels (3^{rd} to 6^{th} generation intrapulmonary branches). As smaller vessels have greater muscular content, the majority of cultured myocytes derive from the smaller arteries. Both control and hypoxic cultured pulmonary artery myocytes abundantly expressed TP-R, as shown by RT-PCR. Expression of TP-R in normoxia may have been simply induced under cell culture conditions, or may reflect contribution from smooth muscle cells from larger arteries, as vessel size had an important impact on TP-R expression in our study. Therefore a limitation in interpretation of this study is that altered regulation of TP-R observed in cultured myocytes may not be entirely representative of TP-R alterations *in vivo*, depending on the original location of the studied TP-R within the arterial tree.

TP-R intracellular localization. We have previously shown that moderate hypoxic exposure alters TP-R localization following *in vitro* hypoxia for 3 days, with decreased cell surface expression and a translocation of the intracellular receptor to the perinuclear region (16). Cell surface receptor abundance is known to be modulated by internalization and endoplasmic reticulum-associated degradation (42). Agonist-induced internalization of the TP receptor is mediated by Gαq signalling (33). In the context of an increased thromboxane: prostacyclin milieu and increased receptor affinity, TP-R internalization in hypoxia may constitute a negative feedback mechanism attenuating vasoconstrictor response. In this study, we also observed that the endoplasmic reticulum relocates to a perinuclear position in hypoxic myocytes, although this change was numerically small. There is precedent for this observation; a reduction in smooth

endoplasmic reticulum has been described in rat hepatocytes following exposure to 5% environmental O_2 (49). The admittedly minor (albeit statistically significant) change in the ER morphology of hypoxic myocytes may explain the observed shift in intracellular TP-R distribution, which may impact upon receptor internalization and cycling. Observations reported elsewhere of altered TP-R localization following oxidative stress, involving stabilization of the TP-R and translocation from the ER to the golgi apparatus following exposure to H_2O_2 (42), describe a change in cell surface receptor immunostaining within this range. A 3-dimensional analysis of ER distribution ascribes functional specialization of protein import machinery to ER lamellae organized a few nanometers apart (10), suggesting small differences in ER distribution may confer significant changes of function. Luminal ER protein chaperones such as protein disulfide isomerase (utilized in this study as an ER marker) function as protein escorts, hence minor alterations in localization of this protein may have functional significance (22, 27). The slight shift in ER distribution we observe in hypoxic myocytes may alter receptor cycling, post-transcriptional modification and/or compartmentalization, which would impact upon cell surface abundance and activity of the TP-R, as we report is the case in hypoxic myocytes.

TP-R binding kinetics. Published values of SQ29548 binding to TP-R range from a K_d of 6.3nM (42) to 1.72nM (14). The K_d value we obtained for HM was comparable to previously reported values, while the NM K_d was relatively elevated, suggesting that the NM TP-R is relatively desensitized. The B_{max} was also decreased in HM TP-R compared to normoxic myocytes, supporting our previous observation by immunocytochemistry (16). After observing an alteration in both TP-R abundance and

binding affinity following hypoxic exposure, it was necessary to examine competitive binding kinetics. As the desired receptor-ligand interaction involved the agonist rather than the available radiolabeled antagonist, the competitive binding analysis was carried out against both unlabelled SQ29548 (a TP-R antagonist) and unlabelled U46619 (a TP-R agonist). Published values of SQ29548 binding to TP-R range from a K_d of 6.3nM (42) to 1.72nM (14). In normoxic myocytes, unlabelled SQ29548 had a lower IC50, suggesting increased affinity for antagonist in the normal condition compared to hypoxic cells, a finding inconsistent with that observed in saturation binding experiments; this may have been an artefact of the greater cell surface receptor abundance (B_{max}) in normoxic myocytes, leading to increased availability of open receptor for binding. However unlabelled U46619 displaced the [H^3]-SQ29548 in hypoxic myocytes at significantly lower concentrations, suggesting that the hypoxic receptor has increased affinity for the agonist; this observation supports the saturation binding kinetics. The difference in agonist/antagonist displacement of the labelled antagonist may be due to the consistently lower K_d of SQ29548 compared to the K_d for U46619 (25). Since it is only activation of the TP-R by U46619 that leads to increased $[Ca^{2+}]_i$ and subsequent smooth muscle contraction, the significance of the competitive binding data lies in the clear indication that the hypoxic TP-R has an increased affinity for the agonist.

TP-R phosphorylation. The two known isoforms of mammalian TP receptor share the first 328 residues, but differ at the C-terminal end (29); TP isoform may determine specificity of interaction with Gα protein subunits, but both couple to PLC similarly, and no major differences in ligand affinity have been identified (2). Both thromboxane receptor isoforms are regulated by C-terminal serine phosphorylation (11). TPα is

phosphorylated and desensitized by pulmonary circuit relaxants (32). Upon agonist-induced C-terminal phosphorylation, the TPβ isoform is amenable to β-arrestin binding (30), which results in desensitization, uncoupling from heterotrimeric G-protein and actin-dependent receptor endocytosis (21). When oligomerized with TPβ, TPα will also undergo endocytosis (20). In this study, phosphorylation state of the normoxic TP-R was elevated compared to hypoxic TP-R. The hypoxic TP-R had increased association with Gαq compared to normoxic TP-R, suggesting that downstream contractile signalling in hypoxic TP-R may be augmented compared to the relatively desensitized normoxic TP-R. As this dephosphorylation of hypoxic TP-R occurred in the context of increased receptor internalization, we speculate that TP-R internalization may represent receptor cycling as a consequence of increased TxA production, receptor sensitization and/or downstream signalling in hypoxia, while decreased TP-R phosphorylation state may be mediated by the contrary loss of vasorelaxant stimulation in hypoxic myocytes.

Regulation of TP-R phosphorylation. Covalent modification of various GPCRs has been shown to regulate their activity, due to alterations in active state conformation or to regulatory phosphorylation. Activity of smooth muscle TP-R is primarily regulated by serine phosphorylation. Serine-331 on the C-terminal TP-R tail is known to be phosphorylated by PKC, resulting in desensitization (51). There is evidence that TPα, but not TPβ, may be subject to DP-prostanoid receptor-mediated cross desensitization, occurring via direct PKA-mediated phosphorylation of TPα at Serine-329 after DP stimulation (9). Signalling by TPα, but not TPβ, is also subject to prostacyclin-induced desensitization (via IP-prostanoid receptor stimulation) mediated by PKA phosphorylation of Serine-329 (45). An independent mechanism of TP-R desensitization

involves direct PKG phosphorylation of Serine-331, in response to NO (32). Hypoxia causes sensitization of the TP-R in neonatal pulmonary artery myocytes, but under control conditions the TP-R is relatively desensitized due to regulatory phosphorylation. TP-R phosphorylation and peak $[Ca^{2+}]_i$ response to agonist is unaffected by GTP-induced increase in active state conformation, as maximal activation of the TP-R had no effect on phosphorylation state of the receptor, and peak $[Ca^{2+}]_i$ response to TxA agonist remained significantly elevated in HM. PKC activation increases hypoxic myocytes TP-R phosphorylation, however the $[Ca^{2+}]_i$ response to U46619 remained elevated compared to normoxic controls, suggesting that in neonatal pulmonary artery myocytes, PKC may target residues with no direct effect on receptor-induced Ca^{2+} signalling. Incubation with a direct activator of PKA resulted in markedly increased TP-R phosphorylation, ablating the difference between hypoxia and normoxia. PKA activation also inhibited the hypoxia-induced increase in peak $[Ca^{2+}]_i$ response to U46619, suggesting that PKA-targeted serine residues on TP-R are involved in normoxic desensitization of TP-R.

Protein phosphatases PP1 and PP2A are implicated in TP-R dephosphorylation (38). We have previously reported a decrease in PP1M (myosin phosphatase) activity in hypoxic neonatal pulmonary artery; PP2 activity was not altered (3). This has also been reported in hypoxic PA myocytes (47). The mechanism by which TP-R is dephosphorylated in hypoxia falls outside the scope of this paper, but deserves further study.

We conclude that hypoxia in the perinatal pulmonary circuit causes distal propagation of thromboxane receptor expression; increased TP-R agonist affinity despite a decrease in B_{max} resulting from increased receptor internalization; and a loss of basal

TP-R phosphorylation, resulting in increased coupling of the receptor complex to vasoconstrictor signalling intermediates. We speculate that under normal conditions in the pulmonary circuit, the neonatal TP-R is relatively desensitized compared to the adult TP-R, due to increased serine residue phosphorylation. This may be physiologically advantageous, as pulmonary arteries would be less able to constrict in response to circulating TxA, and therefore would not hinder normal circulatory transition. However after exposure to hypoxia, TP-R appears in smaller pulmonary arteries and becomes dephosphorylated, which increases its affinity for thromboxane agonist U46619, and increases coupling to Gαq. Regulatory phosphorylation of TP-R in the neonatal pulmonary circuit may be mediated via the PKA pathway; PKA activation results in TP-R phosphorylation and can inhibit development of hypoxia-induced TP-R hypersensitivity. Altered TP-R localization and kinetics in hypoxic myocytes may result in inflammatory agonist hypersensitivity in resistance level pulmonary arteries, which would contribute to the increased pulmonary arterial pressure observed in PPHN, and could interfere with current PPHN therapies.

ACKNOWLEDGEMENTS

We thank Dr. Andrew Halayko for the generous donation of Gαq antibody. Research was funded by grants from Manitoba Medical Services Foundation and Manitoba Institute of Child Health. MH is supported by a Canadian Institute for Health Research graduate studentship, and SD by New Investigator funding from Winnipeg Rh Institute Foundation.

REFERENCES

1. **Alzoghaibi MA, Walsh SW, Willey A, Yager DR, Fowler AA, 3rd, and Graham MF.** Linoleic acid induces interleukin-8 production by Crohn's human intestinal smooth muscle cells via arachidonic acid metabolites. *Am J Physiol Gastrointest Liver Physiol* 286: G528-537, 2004.

2. **Becker KP, Garnovskaya M, Gettys T, and Halushka PV.** Coupling of thromboxane A2 receptor isoforms to Galpha13: effects on ligand binding and signalling. *Biochim Biophys Acta* 1450: 288-296, 1999.

3. **Dakshinamurti S, Mellow L, and Stephens NL.** Regulation of pulmonary arterial myosin phosphatase activity in neonatal circulatory transition and in hypoxic pulmonary hypertension: a role for CPI-17. *Pediatr Pulmonol* 40: 398-407, 2005.

4. **Dorn GW, 2nd.** Cyclic oxidation-reduction reactions regulate thromboxane A2/prostaglandin H2 receptor number and affinity in human platelet membranes. *J Biol Chem* 265: 4240-4246, 1990.

5. **Ermert M, Kuttner D, Eisenhardt N, Dierkes C, Seeger W, and Ermert L.** Cyclooxygenase-2-dependent and thromboxane-dependent vascular and bronchial responses are regulated via p38 mitogen-activated protein kinase in control and endotoxin-primed rat lungs. *Lab Invest* 83: 333-347, 2003.

6. **Fike CD, Kaplowitz MR, and Pfister SL.** Arachidonic acid metabolites and an early stage of pulmonary hypertension in chronically hypoxic newborn pigs. *Am J Physiol Lung Cell Mol Physiol* 284: L316-323, 2003.

7. **Fike CD, Pfister SL, Kaplowitz MR, and Madden JA.** Cyclooxygenase contracting factors and altered pulmonary vascular responses in chronically hypoxic newborn pigs. *J Appl Physiol* 92: 67-74, 2002.

8. **Finer NN and Barrington KJ.** Nitric oxide for respiratory failure in infants born at or near term. *Cochrane Database Syst Rev*: CD000399, 2001.

9. **Foley JF, Kelley LP, and Kinsella BT.** Prostaglandin D(2) receptor-mediated desensitization of the alpha isoform of the human thromboxane A(2) receptor. *Biochem Pharmacol* 62: 229-239, 2001.

10. **Geuze HJ, Murk JL, Stroobants AK, Griffith JM, Kleijmeer MJ, Koster AJ, Verkleij AJ, Distel B, and Tabak HF.** Involvement of the endoplasmic reticulum in peroxisome formation. *Mol Biol Cell* 14: 2900-2907, 2003.

11. **Habib A, Vezza R, Creminon C, Maclouf J, and FitzGerald GA.** Rapid, agonist-dependent phosphorylation in vivo of human thromboxane receptor isoforms. Minimal involvement of protein kinase C. *J Biol Chem* 272: 7191-7200, 1997.

12. **Hammerman C, Komar K, and Abu-Khudair H.** Hypoxic vs septic pulmonary hypertension. Selective role of thromboxane mediation. *Am J Dis Child* 142: 319-325, 1988.

13. **Hammerman C, Komar K, Abu-Khudair H, and Olsen T.** Oxygen transport in newborn piglets with pulmonary hypertension. *Crit Care Med* 16: 773-778, 1988.

14. **Hanasaki K and Arita H.** A common binding site for primary prostanoids in vascular smooth muscles: a definitive discrimination of the binding for thromboxane A2/prostaglandin H2 receptor agonist from its antagonist. *Biochim Biophys Acta* 1013: 28-35, 1989.

15. **Haworth SG.** Development of the normal and hypertensive pulmonary vasculature. *Exp Physiol* 80: 843-853, 1995.

16. **Hinton M, Mellow L, Halayko AJ, Gutsol A, and Dakshinamurti S.** Hypoxia induces hypersensitivity and hyperreactivity to thromboxane receptor agonist in neonatal pulmonary arterial myocytes. *Am J Physiol Lung Cell Mol Physiol* 290: L375-384, 2006.

17. **Huang JS, Ramamurthy SK, Lin X, and Le Breton GC.** Cell signalling through thromboxane A2 receptors. *Cell Signal* 16: 521-533, 2004.

18. **Jankov RP, Belcastro R, Ovcina E, Lee J, Massaeli H, Lye SJ, and Tanswell AK.** Thromboxane A(2) receptors mediate pulmonary hypertension in 60% oxygen-exposed newborn rats by a cyclooxygenase-independent mechanism. *Am J Respir Crit Care Med* 166: 208-214, 2002.

19. **Kinsella BT.** Thromboxane A2 signalling in humans: a 'Tail' of two receptors. *Biochem Soc Trans* 29: 641-654, 2001.

20. **Laroche G, Lepine MC, Theriault C, Giguere P, Giguere V, Gallant MA, de Brum-Fernandes A, and Parent JL.** Oligomerization of the alpha and beta isoforms of the thromboxane A2 receptor: relevance to receptor signaling and endocytosis. *Cell Signal* 17: 1373-1383, 2005.

21. **Laroche G, Rochdi MD, Laporte SA, and Parent JL.** Involvement of actin in agonist-induced endocytosis of the G protein-coupled receptor for thromboxane A2: overcoming of actin disruption by arrestin-3 but not arrestin-2. *J Biol Chem* 280: 23215-23224, 2005.

22. **Liepinsh E, Baryshev M, Sharipo A, Ingelman-Sundberg M, Otting G, and Mkrtchian S.** Thioredoxin fold as homodimerization module in the putative chaperone

ERp29: NMR structures of the domains and experimental model of the 51 kDa dimer. *Structure* 9: 457-471, 2001.

23. **MacEachern KE, Smith GL, and Nolan AM.** Characteristics of the in vitro hypoxic pulmonary vasoconstrictor response in isolated equine and bovine pulmonary arterial rings. *Vet Anaesth Analg* 31: 239-249, 2004.

24. **Madjdpour C, Jewell UR, Kneller S, Ziegler U, Schwendener R, Booy C, Klausli L, Pasch T, Schimmer RC, and Beck-Schimmer B.** Decreased alveolar oxygen induces lung inflammation. *Am J Physiol Lung Cell Mol Physiol* 284: L360-367, 2003.

25. **Mayeux PR, Morinelli TA, Williams TC, Hazard ES, Mais DE, Oatis JE, Baron DA, and Halushka PV.** Differential effect of pH on thromboxane A2/prostaglandin H2 receptor agonist and antagonist binding in human platelets. *J Biol Chem* 266: 13752-13758, 1991.

26. **McLeod KA, Gerlis LM, and Williams GJ.** Morphology of the elastic pulmonary arteries in pulmonary hypertension: a quantitative study. *Cardiol Young* 9: 364-370, 1999.

27. **Mezghrani A, Courageot J, Mani JC, Pugniere M, Bastiani P, and Miquelis R.** Protein-disulfide isomerase (PDI) in FRTL5 cells. pH-dependent thyroglobulin/PDI interactions determine a novel PDI function in the post-endoplasmic reticulum of thyrocytes. *J Biol Chem* 275: 1920-1929, 2000.

28. **Noh DY, Shin SH, and Rhee SG.** Phosphoinositide-specific phospholipase C and mitogenic signaling. *Biochim Biophys Acta* 1242: 99-113, 1995.

29. **Parent JL, Labrecque P, Driss Rochdi M, and Benovic JL.** Role of the differentially spliced carboxyl terminus in thromboxane A2 receptor trafficking:

identification of a distinct motif for tonic internalization. *J Biol Chem* 276: 7079-7085, 2001.

30. **Parent JL, Labrecque P, Orsini MJ, and Benovic JL.** Internalization of the TXA2 receptor alpha and beta isoforms. Role of the differentially spliced cooh terminus in agonist-promoted receptor internalization. *J Biol Chem* 274: 8941-8948, 1999.

31. **Peacock AJ, Scott P, Plevin R, Wadsworth R, and Welsh D.** Hypoxia enhances proliferation and generation of IP3 in pulmonary artery fibroblasts but not in those from the mesenteric circulation. *Chest* 114: 24S, 1998.

32. **Reid HM and Kinsella BT.** The alpha, but not the beta, isoform of the human thromboxane A2 receptor is a target for nitric oxide-mediated desensitization. Independent modulation of Tp alpha signaling by nitric oxide and prostacyclin. *J Biol Chem* 278: 51190-51202, 2003.

33. **Rochdi MD and Parent JL.** Galphaq-coupled receptor internalization specifically induced by Galphaq signaling. Regulation by EBP50. *J Biol Chem* 278: 17827-17837, 2003.

34. **Rodman DM, Yamaguchi T, O'Brien RF, and McMurtry IF.** Hypoxic contraction of isolated rat pulmonary artery. *J Pharmacol Exp Ther* 248: 952-959, 1989.

35. **Shimoda LA, Sham JS, Shimoda TH, and Sylvester JT.** L-type $Ca^{(2+)}$ channels, resting $[Ca^{(2+)}]_{(i)}$, and ET-1-induced responses in chronically hypoxic pulmonary myocytes. *Am J Physiol Lung Cell Mol Physiol* 279: L884-894, 2000.

36. **Soukka H, Viinikka L, and Kaapa P.** Involvement of thromboxane A2 and prostacyclin in the early pulmonary hypertension after porcine meconium aspiration. *Pediatr Res* 44: 838-842, 1998.

37. **Spurney RF.** Regulation of thromboxane receptor (TP) phosphorylation by protein phosphatase 1 (PP1) and PP2A. *J Pharmacol Exp Ther* 296: 592-599, 2001.

38. **Spurney RF.** Regulation of thromboxane receptor (TP) phosphorylation by protein phosphatase 1 (PP1) and PP2A. In: *J Pharmacol Exp Ther*, 2001, p. 592-599.

39. **Steinhorn RH.** Persistent pulmonary hypertension of the newborn. *Acta Anaesthesiol Scand Suppl* 111: 135-140, 1997.

40. **Suradhat S, Thanawongnuwech R, and Poovorawan Y.** Upregulation of IL-10 gene expression in porcine peripheral blood mononuclear cells by porcine reproductive and respiratory syndrome virus. *J Gen Virol* 84: 453-459, 2003.

41. **Tozzi CA, Christiansen DL, Poiani GJ, and Riley DJ.** Excess collagen in hypertensive pulmonary arteries decreases vascular distensibility. *Am J Respir Crit Care Med* 149: 1317-1326, 1994.

42. **Valentin F, Field MC, and Tippins JR.** The mechanism of oxidative stress stabilization of the thromboxane receptor in COS-7 cells. *J Biol Chem* 279: 8316-8324, 2004.

43. **Villanueva ME, Zaher FM, Svinarich DM, and Konduri GG.** Decreased gene expression of endothelial nitric oxide synthase in newborns with persistent pulmonary hypertension. *Pediatr Res* 44: 338-343, 1998.

44. **Walsh MC and Stork EK.** Persistent pulmonary hypertension of the newborn. Rational therapy based on pathophysiology. *Clin Perinatol* 28: 609-627, vii, 2001.

45. **Walsh MT, Foley JF, and Kinsella BT.** The alpha, but not the beta, isoform of the human thromboxane A2 receptor is a target for prostacyclin-mediated desensitization. *J Biol Chem* 275: 20412-20423, 2000.

46. **Walsh-Sukys MC, Tyson JE, Wright LL, Bauer CR, Korones SB, Stevenson DK, Verter J, Stoll BJ, Lemons JA, Papile LA, Shankaran S, Donovan EF, Oh W, Ehrenkranz RA, and Fanaroff AA.** Persistent pulmonary hypertension of the newborn in the era before nitric oxide: practice variation and outcomes. *Pediatrics* 105: 14-20, 2000.

47. **Wang Z, Lanner MC, Jin N, Swartz D, Li L, and Rhoades RA.** Hypoxia inhibits myosin phosphatase in pulmonary arterial smooth muscle cells: role of Rho-kinase. *Am J Respir Cell Mol Biol* 29: 465-471, 2003.

48. **Weinberger B, Weiss K, Heck DE, Laskin DL, and Laskin JD.** Pharmacologic therapy of persistent pulmonary hypertension of the newborn. *Pharmacol Ther* 89: 67-79, 2001.

49. **Welt K, Weiss J, Martin R, Dettmer D, Hermsdorf T, Asayama K, Meister S, and Fitzl G.** Ultrastructural, immunohistochemical and biochemical investigations of the rat liver exposed to experimental diabetes und acute hypoxia with and without application of Ginkgo extract. *Exp Toxicol Pathol* 55: 331-345, 2004.

50. **Wohrley JD, Frid MG, Moiseeva EP, Orton EC, Belknap JK, and Stenmark KR.** Hypoxia selectively induces proliferation in a specific subpopulation of smooth muscle cells in the bovine neonatal pulmonary arterial media. *J Clin Invest* 96: 273-281, 1995.

51. **Yan FX, Yamamoto S, Zhou HP, Tai HH, and Liao DF.** Serine 331 is major site of phosphorylation and desensitization induced by protein kinase C in thromboxane receptor alpha. *Acta Pharmacol Sin* 23: 952-960, 2002.

52. **Yang X, Sheares KK, Davie N, Upton PD, Taylor GW, Horsley J, Wharton J, and Morrell NW.** Hypoxic induction of cox-2 regulates proliferation of human pulmonary artery smooth muscle cells. *Am J Respir Cell Mol Biol* 27: 688-696, 2002.

VII. SUMMARY

To date, the major focus in neonatal pulmonary hypertension research has focused on vascular remodelling and altered generation of vasoactive molecules such as decreased production of NO and prostacyclin, or increased production of endothelin-1 and thromboxane. TxA levels have been shown to be altered in hypoxic-induced PPHN, however mainly tissue contractile studies have been done, demonstrating increased vascular contraction to TxA in hypertensive animals. However, the mechanisms behind such changes are unknown because very little research has been done on TxA responsiveness and the TP-R in the neonatal pulmonary circuit.

TxA responsiveness. We found that pulmonary artery smooth muscle cells became hyperresponsive and hypersensitive to a thromboxane agonist after exposure to moderate hypoxia. The heightened Ca^{2+} responses to TxA observed were maintained long after removal from hypoxia, suggesting altered expression or sustained alteration of the TP-R or part of its downstream signalling pathway. The increased Ca^{2+} response to TxA following hypoxia was unaffected by inhibition of Ca^{2+} entry or store re-filling during stimulation, but could be inhibited by blocking Ca^{2+} mobilization from internal stores. Stimulation of SR Ca^{2+} pool Ca^{2+} release, particularly from the IP3-gated Ca^{2+} pool, did not affect PASMC responsiveness to all GPCR agonists following hypoxia; P2Y activation was unaltered in hypoxic myocytes. Therefore, the Ca^{2+} pool itself was not increased.

The TP-R is known to signal through the IP3 pathway; the IP3 gated Ca^{2+} pools contributed to the hypoxia-induced increase in TxA responsiveness but do not exhibit increased Ca^{2+} release to all agonists. Therefore, there must have been some alteration

either with receptor-ligand interaction or in the downstream signal transduction cascade. We chose in this study to focus on the TP-R. With controlled administration of agonist concentration, receptor- ligand interaction can be altered in two ways; localization and kinetics.

TP-R localization. In lung tissue slices, TP-R localization was unaltered in large pulmonary arteries. In vessels less than 50μM in diameter, from control animals, the TP-R was non-existent. However, following induction of PPHN, the TP-R was expressed in these arteries, therefore allowing them to respond to the circulating vasoconstrictor and contribute to the increased PA pressure characteristic of neonatal hypertension. Cultured PASMC also have altered TP-R localization. Intracellular TP-R colocalizes with the ER marker, PDI. In hypoxic myocytes, intracellular TP-R translocates to the perinuclear region, seeming to follow the change in ER distribution. Cell surface TP-R abundance is decreased following hypoxic exposure; a phenomenon which is opposite of what would be expected in the face of increased TxA responsiveness.

TP-R kinetics. With decreased TP-R on the cell surface available for interaction with ligand, the observed increase in Ca^{2+} response in hypoxia must come from an increased TP-R affinity. Saturation binding kinetics did reveal a decreased Kd. TP-R kinetics can be regulated by covalent modification of the receptor. Specifically, phosphorylation on serine residues has been shown to be inhibitory. We found that phosphorylation of normoxic TP-R was increased, suggesting that the receptor is normally in a desensitized state. The decreased phosphorylation state of the TP-R in hypoxic myocytes correlated with increased TP-R coupling to Gαq, the protein that links receptor-ligand interaction to Ca^{2+} mobilization. The relatively desensitized state of the

normoxic TP-R could be mimicked following hypoxic exposure only by TP-R-independent activation of PKA, which resulted in both increased TP-R serine-phosphorylation and decreased Ca^{2+} response to TxA.

We speculate that under normal conditions the TP-R is relatively desensitized so as to not hinder normal circulatory transition. This desensitization is achieved by phosphorylation of serine residues via a PKA-dependent pathway. We infer that this PKA-mediated desensitization is lost in hypoxia. Hypoxia may also result in activation of a specific phosphatase, however non-specificity of phosphatase inhibitors hindered exploration of the precise enzyme involved. If the TP-R is resensitized in the pulmonary circuit because of a hypoxic episode, a state which persists after removal from hypoxia, *and* there is TP-R present in smaller arteries, this may make the pulmonary circuit more vasospastic. Also, it has been documented that there are elevated levels of TxA in the serum following hypoxia. Therefore the combination of increased agonist with increased *responsive* receptor elevates the chance of heightened pulmonary artery pressure. This is an important consideration when attempting to treat an infant with PPHN.

VIII. Future Directions

PASMC prostanoid production in hypoxia. We observed altered TP-R signalling in hypoxia. This may have been due to endogenous ligand produced by the cultured myocytes, and this prostanoid production may be altered following moderate hypoxia. An ELISA or radioimmunoassay can be done to determine relative amounts of prostacyclin and thromboxane. If TxA and PGI_2 levels are altered by hypoxia, then this may lead to altered receptor (TP-R or IP-R) activation which could, in part, explain the TP-R changes that we observed. To study this, we could incubate the PASMC with TP-R

and IP-R antagonists for the final 3 days of culture when they are split into either normoxic or hypoxic groups, and then see if the same hypoxia-induced changes in TP-R signalling occur.

IP-R study following in vivo and in vitro hypoxia. Because such dramatic changes were observed in hypoxic myocyte TP-R, analogous changes could be observed with the prostacyclin receptor (IP-R), in a way that would hinder relaxation in hypoxic cells. IP-R localization, kinetics and cAMP production could be studied to determine if moderate hypoxia also affects this prostanoid receptor.

GPCR crosstalk. It is known that GPCR signalling leads to activation of signalling pathways that result in regulation of other receptors. For example, it is known that IP-R couples to Gαs/(adenylate cyclase) to result in PKA activation. We found that the PKA pathway is involved in TP-R phosphorylation and subsequent desensitization. It is known that there are normally higher levels of prostacyclin, relative to TxA, in the perinatal period. In hypoxia-induced PPHN, the arachidonic acid metabolites shift away from the vasodilator, towards the vasoconstrictor, thromboxane. It is plausible that IP-R-induced PKA activation is involved in the normal desensitization of the TP-R at the time of perinatal circulatory transition. It is not known if IP-R signalling is decreased in hypoxia or if IP-R signalling results in phosphorylation of the TP-R. If hypoxia alters IP-R signalling, either through regulation of PGI_2 production or through regulation of the IP-R, it is unknown how this would affect the TP-R (Figure **2A**). If IP-R signal is reduced in hypoxia and this alters phosphorylation state of the TP-R, it is unknown if this could be rescued by exogenous addition of the IP-R agonist, iloprost (Figure 2**B**). How IP-R signalling affects TP-R signalling, cycling or degradation is unknown in the perinatal

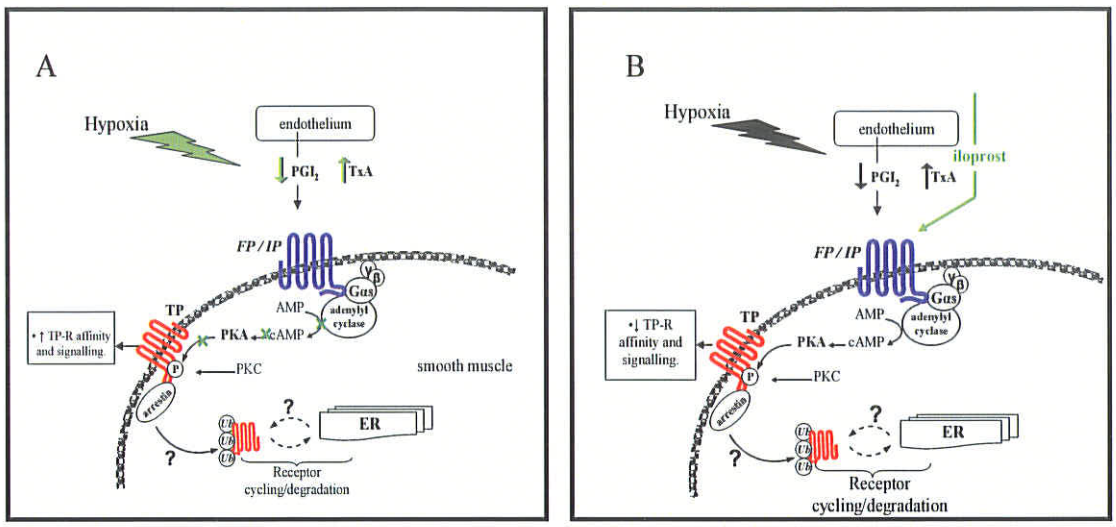

Figure 2. GPCR cross-talk and regulation of IP-R signalling in hypoxia.

Schematic of hypoxic effects on IP-R signalling might effect the TP-R. (A) Hypoxia is known to decrease prostacyclin (PGI_2) production relative to thromboxane (TxA). This would reduce downstream signalling pathways of the IP-R, which involves adenlyate cyclase regulation of PKA activity. Less IP-R signalling would lead to less (X) PKA activity and therefore less TP-R phosphorylation. (B) Exogenous addition of the IP-R agonist, iloprost, may lead to increased IP-R function, therefore leading to increased TP-R phosphorylation. How this effects TP-R cycling and degradation in PASMC is unknown.

pulmonary circuit, but would be a potentially beneficial therapeutic area of study regarding PPHN.

Extinction of hypoxic effects on TP-R responsiveness. Our *in vivo* data suggest that the hypoxic effects on TxA signalling are not resolved simply by removal from hypoxia. The longevity of such changes should be determined as well as the mechanisms by which they are maintained. The exposure to hypoxia *in vitro* and points of measurement are detailed in Figure **3**. If the pulmonary circuit remains hypersensitive to TxA, treatment with vasodilators without acknowledging the persistent change in TP-R signalling may hinder positive outcomes.

Functional change in TP-R (contractility/IP3). An increase in TxA-induced Ca^{2+} response does not necessarily imply increased contraction. Therefore, contractile responses to TxA should be studied. As well, a different endpoint of receptor-ligand interaction, such as IP3, could be measured to verify increased Gαq coupling in hypoxia. TP-R does not only signal through the PLC pathway, but also through the Rho pathway which leads to Ca^{2+} sensitization. Therefore, measurement of MLCP activity may be altered in the hypoxic state (Figure **4**).

Hypoxic regulation of ROS. The oxygen sensor in smooth muscle cells is unknown. It has been speculated that ROS increase and even decrease in some cases in response to hypoxia. The connection between such a change and TP-R phosphorylation and responsiveness would assist in determining a point in the cellular signalling at which therapeutic intervention should be administered to be most effective.

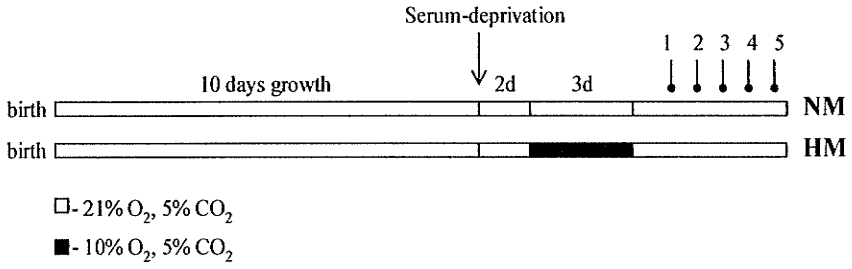

Figure 3. Extinction of hypoxic effects on TP-R responsiveness.

Similar culture conditions as used throughout the previous experiments with PASMCs obtained from newborn animals, cultured to confluence and the serum-deprived to synchronize in a contractile phenotype. Cultures would then be randomized into normoxic (NM) or hypoxic (HM) environments for 3 days. Experimental time points would then be taken daily (•) to look at change in receptor function or signalling.

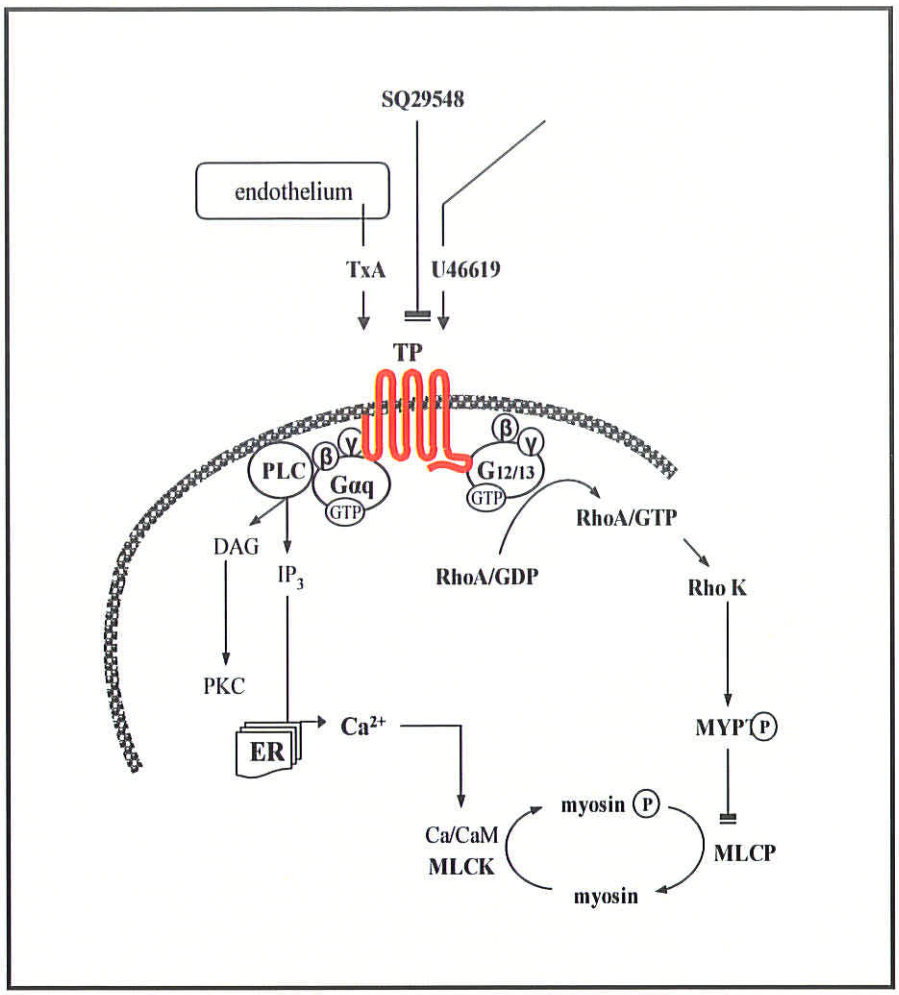

Figure 4. TP-R signalling and PASMC contraction.

The thromboxane receptor is known to couple to both Gαq and Gα12/13, which can lead to smooth muscle cell contraction in a Ca^{2+}-dependent and Ca^{2+}-independent manner. We have demonstrated increased Ca^{2+} response to U46619 in hypoxia, however it is unknown if the Gα12/13 signal transduction cascade is altered. Therefore, measurement of MYPT phosphorylation, myosin light chain phosphatase activity or smooth muscle contraction should be measured in hypoxic and normoxic PASMC.

IX. REFERENCES

1. **Ambalavanan N, Bulger A, Murphy-Ullrich J, Oparil S, and Chen YF.** Endothelin-A receptor blockade prevents and partially reverses neonatal hypoxic pulmonary vascular remodeling. *Pediatr Res* 57: 631-636, 2005.

2. **Balsinde J, Winstead MV, and Dennis EA.** Phospholipase A(2) regulation of arachidonic acid mobilization. *FEBS Lett* 531: 2-6, 2002.

3. **Becker KP, Garnovskaya M, Gettys T, and Halushka PV.** Coupling of thromboxane A2 receptor isoforms to Galpha13: effects on ligand binding and signalling. *Biochim Biophys Acta* 1450: 288-296, 1999.

4. **Blatter LA and Wier WG.** Agonist-induced $[Ca^{2+}]_i$ waves and $Ca^{(2+)}$-induced Ca^{2+} release in mammalian vascular smooth muscle cells. *Am J Physiol* 263: H576-586, 1992.

5. **Chen CA and Manning DR.** Regulation of G proteins by covalent modification. *Oncogene* 20: 1643-1652, 2001.

6. **Dakshinamurti S.** Pathophysiologic mechanisms of persistent pulmonary hypertension of the newborn. *Pediatr Pulmonol* 39: 492-503, 2005.

7. **Dorn GW, 2nd.** Cyclic oxidation-reduction reactions regulate thromboxane A2/prostaglandin H2 receptor number and affinity in human platelet membranes. *J Biol Chem* 265: 4240-4246, 1990.

8. **Fike CD, Kaplowitz MR, and Pfister SL.** Arachidonic acid metabolites and an early stage of pulmonary hypertension in chronically hypoxic newborn pigs. *Am J Physiol Lung Cell Mol Physiol* 284: L316-323, 2003.

9. **Ganitkevich V, Hasse V, and Pfitzer G.** Ca^{2+}-dependent and Ca^{2+}-independent regulation of smooth muscle contraction. *J Muscle Res Cell Motil* 23: 47-52, 2002.

10. **Ghanayem NS and Gordon JB.** Modulation of pulmonary vasomotor tone in the fetus and neonate. *Respir Res* 2: 139-144, 2001.

11. **Granstrom E.** The arachidonic acid cascade. The prostaglandins, thromboxanes and leukotrienes. *Inflammation* 8 Suppl: S15-25, 1984.

12. **Hakonarson H and Grunstein MM.** Regulation of second messengers associated with airway smooth muscle contraction and relaxation. *Am J Respir Crit Care Med* 158: S115-122, 1998.

13. **Hamm HE.** How activated receptors couple to G proteins. *Proc Natl Acad Sci U S A* 98: 4819-4821, 2001.

14. **Han RN and Stewart DJ.** Defective lung vascular development in endothelial nitric oxide synthase-deficient mice. *Trends Cardiovasc Med* 16: 29-34, 2006.

15. **Hanasaki K and Arita H.** A common binding site for primary prostanoids in vascular smooth muscles: a definitive discrimination of the binding for thromboxane A2/prostaglandin H2 receptor agonist from its antagonist. *Biochim Biophys Acta* 1013: 28-35, 1989.

16. **Heymann MA.** Control of the pulmonary circulation in the fetus and during the transitional period to air breathing. *Eur J Obstet Gynecol Reprod Biol* 84: 127-132, 1999.

17. **Hislop A.** Developmental biology of the pulmonary circulation. *Paediatr Respir Rev* 6: 35-43, 2005.

18. **Hoshi T and Lahiri S.** Cell biology. Oxygen sensing: it's a gas! *Science* 306: 2050-2051, 2004.

19. **Huang JS, Ramamurthy SK, Lin X, and Le Breton GC.** Cell signalling through thromboxane A2 receptors. *Cell Signal* 16: 521-533, 2004.

20. **Janiak R, Wilson SM, Montague S, and Hume JR.** Heterogeneity of calcium stores and elementary release events in canine pulmonary arterial smooth muscle cells. *Am J Physiol Cell Physiol* 280: C22-33, 2001.

21. **Jiang H and Stephens NL.** Calcium and smooth muscle contraction. *Mol Cell Biochem* 135: 1-9, 1994.

22. **Kinsella BT.** Thromboxane A2 signalling in humans: a 'Tail' of two receptors. *Biochem Soc Trans* 29: 641-654, 2001.

23. **Kinsella JP and Abman SH.** Recent developments in the pathophysiology and treatment of persistent pulmonary hypertension of the newborn. *J Pediatr* 126: 853-864, 1995.

24. **Kiserud T.** Physiology of the fetal circulation. *Semin Fetal Neonatal Med* 10: 493-503, 2005.

25. **Kourembanas S, Morita T, Christou H, Liu Y, Koike H, Brodsky D, Arthur V, and Mitsial SA.** Hypoxic responses of vascular cells. *Chest* 114: 25S-28S, 1998.

26. **Lettino M, Cantu F, and Mariani M.** Cyclo-oxygenase-1 and cyclo-oxygenase-2 and cardiovascular system. *Dig Liver Dis* 33 Suppl 2: S12-20, 2001.

27. **Liel N, Mais DE, and Halushka PV.** Binding of a thromboxane A2/prostaglandin H2 agonist [3H]U46619 to washed human platelets. *Prostaglandins* 33: 789-797, 1987.

28. **Marks AR.** Calcium channels expressed in vascular smooth muscle. *Circulation* 86: III61-67, 1992.

29. **Matthew A, Shmygol A, and Wray S.** Ca^{2+} entry, efflux and release in smooth muscle. *Biol Res* 37: 617-624, 2004.

30. **Mercer JS and Skovgaard RL.** Neonatal transitional physiology: a new paradigm. *J Perinat Neonatal Nurs* 15: 56-75, 2002.

31. **Mihara S, Doteuchi M, Hara S, Ueda M, Ide M, Fujimoto M, and Okabayashi T.** Characterization of [3H]U46619 binding in pig aorta smooth muscle membranes. *Eur J Pharmacol* 151: 59-65, 1988.

32. **Milas L.** Cyclooxygenase-2 (COX-2) enzyme inhibitors and radiotherapy: preclinical basis. *Am J Clin Oncol* 26: S66-69, 2003.

33. **Moudgil R, Michelakis ED, and Archer SL.** Hypoxic pulmonary vasoconstriction. *J Appl Physiol* 98: 390-403, 2005.

34. **Noh DY, Shin SH, and Rhee SG.** Phosphoinositide-specific phospholipase C and mitogenic signaling. *Biochim Biophys Acta* 1242: 99-113, 1995.

35. **Perez-Vizcaino F, Cogolludo AL, Ibarra M, Fajardo S, and Tamargo J.** Pulmonary artery vasoconstriction but not $[Ca^{2+}]_i$ signal stimulated by thromboxane A2 is partially resistant to NO. *Pediatr Res* 50: 508-514, 2001.

36. **Perreault T and Coceani F.** Endothelin in the perinatal circulation. *Can J Physiol Pharmacol* 81: 644-653, 2003.

37. **Pfitzer G.** Invited review: regulation of myosin phosphorylation in smooth muscle. *J Appl Physiol* 91: 497-503, 2001.

38. **Raj U and Shimoda L.** Oxygen-dependent signaling in pulmonary vascular smooth muscle. *Am J Physiol Lung Cell Mol Physiol* 283: L671-677, 2002.

39. **Reid HM and Kinsella BT.** The alpha, but not the beta, isoform of the human thromboxane A2 receptor is a target for nitric oxide-mediated desensitization. Independent modulation of Tp alpha signaling by nitric oxide and prostacyclin. *J Biol Chem* 278: 51190-51202, 2003.

40. **Rodman DM, Yamaguchi T, O'Brien RF, and McMurtry IF.** Hypoxic contraction of isolated rat pulmonary artery. *J Pharmacol Exp Ther* 248: 952-959, 1989.

41. **Schumacker PT.** Hypoxia-inducible factor-1 (HIF-1). *Crit Care Med* 33: S423-425, 2005.

42. **Semenza GL.** Involvement of hypoxia-inducible factor 1 in pulmonary pathophysiology. *Chest* 128: 592S-594S, 2005.

43. **Spurney RF.** Regulation of thromboxane receptor (TP) phosphorylation by protein phosphatase 1 (PP1) and PP2A. *J Pharmacol Exp Ther* 296: 592-599, 2001.

44. **Steinhorn RH.** Persistent pulmonary hypertension of the newborn. *Acta Anaesthesiol Scand Suppl* 111: 135-140, 1997.

45. **Valentin F, Field MC, and Tippins JR.** The mechanism of oxidative stress stabilization of the thromboxane receptor in COS-7 cells. *J Biol Chem* 279: 8316-8324, 2004.

46. **Walsh MC and Stork EK.** Persistent pulmonary hypertension of the newborn. Rational therapy based on pathophysiology. *Clin Perinatol* 28: 609-627, vii, 2001.

47. **Ward JP, Snetkov VA, and Aaronson PI.** Calcium, mitochondria and oxygen sensing in the pulmonary circulation. *Cell Calcium* 36: 209-220, 2004.

48. **Warshaw DM, Rees DD, and Fay FS.** Characterization of cross-bridge elasticity and kinetics of cross-bridge cycling during force development in single smooth muscle cells. *J Gen Physiol* 91: 761-779, 1988.

49. **Webb RC.** Smooth muscle contraction and relaxation. *Adv Physiol Educ* 27: 201-206, 2003.

50. **Weinberger B, Weiss K, Heck DE, Laskin DL, and Laskin JD.** Pharmacologic therapy of persistent pulmonary hypertension of the newborn. *Pharmacol Ther* 89: 67-79, 2001.

51. **Wilson DP, Susnjar M, Kiss E, Sutherland C, and Walsh MP.** Thromboxane A2-induced contraction of rat caudal arterial smooth muscle involves activation of Ca^{2+} entry and Ca^{2+} sensitization: Rho-associated kinase-mediated phosphorylation of MYPT1 at Thr-855, but not Thr-697. *Biochem J* 389: 763-774, 2005.

52. **Wohrley JD, Frid MG, Moiseeva EP, Orton EC, Belknap JK, and Stenmark KR.** Hypoxia selectively induces proliferation in a specific subpopulation of smooth muscle cells in the bovine neonatal pulmonary arterial media. *J Clin Invest* 96: 273-281, 1995.

53. **Wolin MS, Ahmad M, and Gupte SA.** The sources of oxidative stress in the vessel wall. *Kidney Int* 67: 1659-1661, 2005.

54. **Wray S, Burdyga T, and Noble K.** Calcium signalling in smooth muscle. *Cell Calcium* 38: 397-407, 2005.

55. **Yamataka T and Puri P.** Pulmonary artery structural changes in pulmonary hypertension complicating congenital diaphragmatic hernia. *J Pediatr Surg* 32: 387-390, 1997.